2016

Dna Disentangled: Roles For Sgs1 And Top3 In Rec-X Resolution And Replication Fork Restart

Mary Rebecca Glineburg
University of Pennsylvania, billmire@mail.med.upenn.edu

Dna Disentangled: Roles For Sgs1 And Top3 In Rec-X Resolution And Replication Fork Restart

Abstract
Homologous recombination (HR), becomes important for repair during replication where completion of DNA synthesis relies on recombination intermediate-mediated lesion bypass. For decades, Holliday Junctions (HJs) were considered the primary recombination intermediate utilized during this repair process, but increasing evidence points out two strong discrepancies: 1) X-structures, when present, are often biochemically inconsistent with being HJs, and 2) despite HR mutants being sensitive to numerous DNA damaging agents, most insults don't result in X-structure accumulation, suggesting alternative HR pathways are at play. The Sgs1-Top3-Rmi1 (STR) complex, in Saccharomyces cerevisiae, is vital for maintaining genome integrity, and is known to resolve recombination intermediates. We took advantage of this function to identify the recombination intermediates employed, and consequently, the distinct HR pathways at play in response to damage induced by methyl methanesulfonate (MMS), and the ribonucleotide reductase inhibitor, hydroxyurea.

Using genetic manipulation, 2D-gel electrophoresis and in vitro biochemical and enzymatic assays, we find that Top3, unassisted by Sgs1 and Rmi1, is able to function through two distinct HR-dependent mechanisms. In the presence of MMS, Top3 is able to provide rescue and reduce recombination-dependent X-structures in sgs1Δ mutants. We find that these X-structures are biochemically consistent with being hemicatenane-related template switch recombination intermediates (Rec-Xs) and not HJs. Furthermore, Top3 and the entire STR complex are capable of resolving Rec-Xs but not equivalent dHJs in vitro. We also find that in the absence of the sumo-targeted ubiquitin ligase, Uls1, Top3 provides rescue to sgs1Δ mutants on HU through a mechanism entirely distinct from Rec-X resolution. We show that in the absence of Sgs1 and Uls1, Top3 is required to promote site specific breaks, and subsequent Rad51-dependent D-loop-mediated fork restart, distinct from a Rad51-independent mechanism in sgs1Δ mutants, and indicative of a Uls1-mediated repair pathway switch. These activities point to the use of template-switch recombination (via gap repair) as a primary mechanism for bypassing MMS-induced damage and coordinated break and D-loop-meditated fork reestablishment in response to HU-induced fork stalling. Importantly, this work highlights novel differences between primary HR repair mechanisms in response to different types of DNA damage, and provides evidence for context-dependent repair pathway choice.

Degree Type
Dissertation

Degree Name
Doctor of Philosophy (PhD)

Graduate Group
Cell & Molecular Biology

First Advisor
Frederick B. Johnson

Keywords
D-loop, DNA repair, Holliday junction, Rec-X, Sgs1, Top3

Subject Categories
Genetics | Molecular Biology

DNA DISENTANGLED: ROLES FOR SGS1 AND TOP3 IN REC-X RESOLUTION AND REPLICATION FORK RESTART

M. Rebecca Glineburg

A DISSERTATION

in

Cell and Molecular Biology

Presented to the Faculties of the University of Pennsylvania

in

Partial Fulfillment of the Requirements for the

Degree of Doctor of Philosophy

2016

Supervisor of Dissertation

_____

F. Brad Johnson
Associate Professor of Pathology and Laboratory Medicine

Graduate Group Chairperson

_____

Daniel S. Kessler
Associate Professor of Cell and Developmental Biology

Dissertation Committee:

Eric Brown, Associate Professor of Cancer Biology
Eishi Noguchi, Associate Professor; Director, Graduate Program in Molecular & Cellular Biology & Genetics
Paul Lieberman, Professor and program leader, Gene Expression and Regulation Program; Director, Center for Chemical Biology and Translational Medicine
Roger Greenberg, Associate Professor of Cancer Biology

ACKNOWLEDGMENT

I came into grad school thinking I knew what I wanted to study, and how I wanted to impact the world, and ended up with a completely different perspective on my life goals and science entirely. None of this would have happened had I not taken a chance by joining Brad Johnson's lab, and agreed to be mentored by Alex Chavez. I want to thank Alex, for introducing me to the fascinating world of basic science, and for pushing me to think critically, for constantly challenging me, and for making me excited to come to lab. Although I was only under his wing for a few months, his mentorship was critical in shaping me into the scientist that I am today, and giving me the realization that my interest in science is strictly in the details. I will be forever grateful for his time and devotion to teaching me, not simply how to do experiments, but how to think about them from every angle, and how to ask the right questions.

I want to thank Brad, for his undying support and sincerity these past six years. For never having a temper, and for always having my back. For giving me the freedom to work independently, but always willing to provide advice when needed. For being not just a mentor, but also a life coach and universal handyman (incidentally, for teaching me how to fix every single piece of lab equipment). For supplying me with chocolate, my number one motivator, and for keeping me company in lab on weekends, even if that meant I had to listen to Laurie Anderson performance art. You are one of a kind.

I'd like to thank my lab members, particularly Ting Yang and Sophie Song-Mouster, who have made working in the Johnson lab so enjoyable these past years. Your constant support and friendship has meant so much to me and I can only hope to find a similar duo in the next phase of my career. My undergraduate, Eleanor Johns, who stuck with me, even when my project temporarily imploded, and willingly continued experiments during my absence, thank you.

I want to thank my parents for never doubting my potential or the choices I've made, and for supporting me through all my endeavors even if they didn't understand what I was doing. To my dad, for setting me up with my first research positions, and providing the catalyst that got me to where I am today, thank you. To my brothers, Matt and Mike, thank you for being the best role models growing up. Your academic achievements always pushed me to try harder. To my husband Paul, thank you for never making me choose, for letting me know that my goals and career dreams matter, and for assuring me that the long distance was worth it as long as I was still learning something new. To my dogs, Kirby and Eppie, thank you for (literally) being right by my side as I write this, for still loving me after months of neglect, and for giving me a tummy to rub in between paragraphs.

ABSTRACT

DNA DISENTANGLED: ROLES FOR SGS1 AND TOP3 IN REC-X RESOLUTION AND REPLICATION FORK RESTART

M. Rebecca Glineburg

F. Brad Johnson

Homologous recombination (HR), becomes important for repair during replication where completion of DNA synthesis relies on recombination intermediate-mediated lesion bypass. For decades, Holliday Junctions (HJs) were considered the primary recombination intermediate utilized during this repair process, but increasing evidence points out two strong discrepancies: 1) X-structures, when present, are often biochemically inconsistent with being HJs, and 2) despite HR mutants being sensitive to numerous DNA damaging agents, most insults don't result in X-structure accumulation, suggesting alternative HR pathways are at play. The Sgs1-Top3-Rmi1 (STR) complex, in Saccharomyces cerevisiae, is vital for maintaining genome integrity, and is known to resolve recombination intermediates. We took advantage of this function to identify the recombination intermediates employed, and consequently, the distinct HR pathways at play in response to damage induced by methyl methanesulfonate (MMS), and the ribonucleotide reductase inhibitor, hydroxyurea.

Using genetic manipulation, 2D-gel electrophoresis and in vitro biochemical and enzymatic assays, we find that Top3, unassisted by Sgs1 and Rmi1, is able to function through two distinct HR-dependent mechanisms. In the presence of MMS, Top3 is able to

provide rescue and reduce recombination-dependent X-structures in sgs1Δ mutants. We find that these X-structures are biochemically consistent with being hemicatenane-related template switch recombination intermediates (Rec-Xs) and not HJs. Furthermore, Top3 and the entire STR complex are capable of resolving Rec-Xs but not equivalent dHJs in vitro. We also find that in the absence of the sumo-targeted ubiquitin ligase, Uls1, Top3 provides rescue to sgs1Δ mutants on HU through a mechanism entirely distinct from Rec-X resolution. We show that in the absence of Sgs1 and Uls1, Top3 is required to promote site specific breaks, and subsequent Rad51-dependent D-loop-mediated fork restart, distinct from a Rad51-independent mechanism in sgs1Δ mutants, and indicative of a Uls1-mediated repair pathway switch. These activities point to the use of template-switch recombination (via gap repair) as a primary mechanism for bypassing MMS-induced damage and coordinated break and D-loop-meditated fork reestablishment in response to HU-induced fork stalling. Importantly, this work highlights novel differences between primary HR repair mechanisms in response to different types of DNA damage, and provides evidence for context-dependent repair pathway choice.

TABLE OF CONTENTS

LIST OF TABLES

LIST OF FIGURES

1. Introduction

DNA damage in the context of replication poses unique challenges to genome integrity; and the choice of whether to complete replication or repair the lesion first is mediated by intimate crosstalk between the replisome and a complex network of DNA repair machinery. What is becoming increasingly evident, regardless of the DNA lesion encountered, is that homologous recombination (HR) plays a crucial role in this process. Unless otherwise noted, the events and factors discussed below are from studies in *S. cerevisiae.*

1.1 DNA Lesions

There are 3 broad categories of DNA damage in the context of replication: double template lesions (DTLs), single template lesions (STLs), and replication uncoupling. DTLs are arguably the most deleterious of lesions as they affect both template strands. Agents that cause this type of damage include double strand break (DSB)-inducing agents like IR, and topoisomerase II inhibitors, as well as interstrand crosslinking agents. STLs only affect one template strand, but can be caused by a variety of insults including methylating agents (e.g. methylmethane sulfonate (MMS), UV, topoisomerase I inhibitors (e.g. camptothecin (CPT)), and even secondary structure (e.g. G-quadruplexes) in the DNA itself. Lastly, replication uncoupling—i.e. when the replicative helicase dissociates from the DNA polymerase—can also pose serious problems to the genome, as it results in extensive stretches of single stranded DNA (ssDNA), which are more prone to accumulating DNA damage and have the potential to break. Uncoupling of replication

machinery can occur from treatment with the polymerase inhibitor, aphidicolin, and the ribonucleotide reductase inhibitor, hydroxyurea (HU).

HR is the primary response to a DSB during replication; consequently, repair of DTLs during replication is entirely dependent on HR pathways, and mutants in HR pathways are hypersensitive to DSB-inducing agents. It has also been known for some time that HR repair mutants are similarly sensitive to DNA damaging agents that cause STLs and uncouple replication; however, how these lesions trigger an HR response was not immediately obvious. What has only recently come to light is that all types of DNA damaging agents induce two universal phenomenon during replication: fork stalling and accumulation of ssDNA gaps behind the fork [1-3]. This review will cover the evidence for various HR repair pathways utilized during replication to overcome these two DNA lesion-causing events, including the steps and players involved in sensing lesions, lesion bypass mechanisms, and recombination intermediate resolution.

1.2 Lesion Sensing: PCNA and Pathway Choice

The coordination of the replisome and DNA repair machinery is carried out primarily *via* interactions with the sliding clamp PCNA. Upon DNA damage, PCNA gets both monoubiquitinated, by Rad6 and Rad18, and polyubiquitinated by Ubc13-Mms2 and Rad5 on Lys164 [4]. Whereas monoubiquitination triggers lesion bypass by translesion synthesis (TLS), polyubiquitination triggers lesion bypass by a Rad51-dependent template switch mechanism [4, 5]. In addition to these modifications, PCNA can also get sumoylated at the same Lys164, primarily by Siz1[5]. This sumoylation has been shown to prevent Rad18-independent HR, as evidenced by MMS-exposed PCNA sumo defective mutants having increased recombination intermediates (visualized as X-shaped

structures on two-dimensional electrophoretic gels (2DGE)), and this activity is thought to be through the recruitment of Srs2 to inhibit Rad51 filament formation [5, 6]. Interestingly sumoylation of PCNA is primarily restricted to S-phase whereas ubiquitination of PCNA persists into G2 [7]. This biphasic control is likely to influence repair pathway choice, restricting utilization of HR pathways to G2/M, where a sister chromatid is available to provide a template for repair.

1.3 HR-dependent Lesion Bypass

The notion that HR had to be triggered by a DSB coupled with the observation that many genotoxins cause DSBs either through a direct mechanism, or indirectly as a result of replication runoff (e.g. replication through a nicked template leading to a one ended DSB), led to the long standing model in which replication forks regularly collapsed into DSBs that were repaired *via* HR mechanisms to reestablish the fork. However, it has been noted that eliminating both HR and NHEJ pathways in yeast (e.g. a *rad52 lig4* double mutant) does not impede replication any more so than a single *rad52* mutation, suggesting that DSBs are not a prominent lesions during replication [8]. And while it is true that some forms of DNA damage, like IR and topoisomerase inhibitors can directly result in DNA breaks, a larger subset, including UV, oxidizing agents, and agents that uncouple replication (HU and aphidicolin), create breaks only as a secondary lesion through enzymatic cleavage (e.g. incomplete NER) [3, 9, 10]. Furthermore, it has been shown that eliminating DNA cleavage enzymes involved in DNA repair (e.g. Rad14, Mus81), does not reduce Rad51 foci formation or Rad51/Rad52 X-structures, and further eliminating HR renders these mutants even more sensitive to DNA damaging agents, strongly suggesting that induction of HR is not dependent on a DSB [3, 11, 12]. The most

obvious challenge to this DSB model is the fact that DNA alkylating agents (e.g. MMS), induce Rad51-dependent X-structures to a much larger extent than any other type of DNA damage, and have pronounced toxicity to HR mutants, yet cause significantly fewer breaks than other types of damage, strongly suggesting that the mechanisms of HR repair are not restricted to the context of a DSB [5, 13, 14].

Recent studies using electron microscopy (EM) to observe replication intermediates in human cells exposed to a variety of DNA damaging agents revealed quite surprisingly that all types of DNA damaging agents tested cause increases in 1) stalled forks and 2) ssDNA gaps [1]. The appearance of ssDNA gaps is strongly indicative of a lesion bypass mechanism, and evidence for post replicative repair of these gaps supports two pathways: the error-prone TLS pathway, and the error-free gap repair (GR) template switch pathway—the latter of which will be described below. What happens at stalled forks appears to be more species dependent. Herein we describe both break-dependent and break-independent models, and the evidence that supports them, for lesion bypass by HR repair during replication.

1.3.1 Break-Dependent Lesion Bypass

A number of HR mechanisms are in place to repair DNA that is broken either directly from exposure to a DSB-inducing agent, or indirectly following enzymatic processing of a stalled fork (Figure 1.1A-G). In the first scenario, a break occurs behind a replication fork, and can be repaired off of the intact sister chromatid (Figure 1.1D-G). In the latter scenario, the break occurs at the replication fork and repair of this break aids in fork restart *via* HR-induced invasion of the broken end into the intact sister to reestablish the fork (Figure 1.1A-E). Depending on the location of the break, the type of break, and

the nature of the surrounding sequence, one of three different HR pathways can be utilized to repair a break following lesion encounter: gene conversion (GC), break-induced replication (BIR), or single strand annealing (SSA).

GC will occur if the break is double ended and if homology exists on either side of the break, which is often the case during repair of a DSB behind a fork (Figure 1.1F). Following a break in this context, the exposed ends are quickly bound by the MRX complex and undergo 5'-3' end resection *via* Exo1 and Sgs1-Dna2 nuclease activity, producing 3' tails [15, 16]. Rad51 then binds these tails and mediates strand invasion of one of the tails into the intact sister chromatid, displacing the identical strand thereby creating a displacement loop (D-loop) structure (Figure 1.1C right) [17, 18]. This D-loop will then be extended past the site of the DSB *via* Pol δ, and can be resolved by one of two ways: either the D-loop will be displaced by Srs2, allowing the broken sister chromatid to anneal and religate to its other half (i.e. synthesis dependent strand annealing (SDSA) (Figure 1.1E), or following a second end capture *via* Rad52 mediated strand annealing and ligation of the second 3' tail, a double Holliday junction (dHJ) is formed, which then gets resolved through the resolution of the STR complex or HJ resolvases (see *Part 5: Resolution*) (Figure 1.1D) [19-22].

GC can also occur at a replication fork if the break does not occur directly at a fork junction, and instead results in gaps or flaps that require further processing (Figure 1.1A). In this pathway, a DSB leads to two exposed ends: the fully broken sister chromatid, as well as the flap or gap within the nicked chromatid. 5' end resection and 3' invasion occur similarly as described above, and either SDSA or dHJ formation can be

utilized as forks can be reestablished following resolution of either the D-loop or dHJ respectively (Figure 1.1C-E).

If the break occurs directly at the fork junction, it will produce a one-ended DSB on one sister chromatid while the other sister chromatid will contain a single stranded nick that can be readily ligated to the parental duplex. If this scenario occurs, as is often the case following replication through a nicked template, BIR is utilized (Figure 1.1B). The first steps of BIR are similar to GC, and involve resection of the 5' strand, and invasion of the 3' tail into a homologous sequence [23]. Following strand invasion, the D-loop, instead of being displaced, acts as a "migrating bubble" replication fork, with the leading strand synthesizing off the intact template strand, and the lagging strand synthesizing off the nascent leading strand [24]. In contrast to GC, DNA synthesis during BIR is dependent on the nonessential Pol δ subunit, Pol32 [25, 26]. Interestingly, despite similarities in the initiation events of BIR and GC, Rad51 is dispensable in some types of BIR [23, 25, 27]. One mechanism by which BIR can initiate in the absence of Rad51, is if ssDNA homologous to the extruding 3' tail is available. In this setting, strand invasion is not necessary, as the exposed ssDNA provides an ideal substrate for Rad52 to assist in annealing.

Lastly, SSA, arguably the most deleterious and least common pathway, may occur during repair of a DSB behind (or ahead of) the fork in regions of direct repeats (e.g. rDNA) [28]. SSA does not utilize a strand invasion step and thus is not dependent on Rad51. Instead, extensive 5'-3' end resection occurs on two ends of a DSB, until enough homology (between 29 and 415 bp) is found for Rad52 to anneal the 3' tails to each other [29]. Annealing of these ssDNA segments together leads to protrusion of

nonhomologous 3' flaps which are then processed by the flap endonuclease, Rad1-Rad10, followed by ligation of the nicked strands (Figure 1.1F-G) [30]. In the rDNA, a region comprising 100-200 copies of rDNA repeats, this process can even occur in the absence of Rad52, resulting in a loss of repeats [31].

Break-dependent Pathway Choice during Replication

Although the biochemical nature of a collapsed fork should favor the BIR repair pathway, this process can be deleterious, particularly in repetitive regions, where BIR could initiate at a downstream repeat, leading to loss of copy number, or in diploid cells where it could lead to loss of heterozygosity. Furthermore, the reliance of BIR on the error-prone subunit, Pol32, results in increased mutagenesis and chromosomal rearrangements ([32, 33]. Consequently, having mechanisms in place to promote GC over BIR could help prevent these potential losses. There are clues that pathway choice is regulated at a number of steps to channel repair into GC over BIR, including downstream of strand invasion, during end resection, and even earlier on at induction of the break.

While BIR might initiate HR repair of a collapsed replication fork, there is evidence that repair can be switched to the less deleterious GC pathway. Most notably, strand invasion occurs at similar kinetics for both BIR and GC repair events, but initiation of DNA synthesis is considerably delayed during BIR compared to GC [28]. A likely explanation is that this delay allows for more extensive homology search to occur, thereby displacing BIR machinery with GC synthesis machinery. There is also evidence that after a short round of DNA synthesis by BIR, Mus81 cleaves the "migrating bubble" replication fork, displacing Pol32-dependent replication machinery, and allowing structural reorganization of the replication fork and continued synthesis *via* Pol32-

independent replication [34]. While both of these scenarios help reduce mutagenic effects of Pol32 away from a break site, they do not fully protect cells from these events.

An earlier step that seems to regulate this choice is the extent of end resection. GC requires end resection and homology of at least 100 nts to promote Rad51 binding and strand invasion, while Rad51-independent HR can occur efficiently with as little as 30 nts of homology [35, 36]. Interestingly, the frequency of BIR, which can occur by both Rad51-dependent and Rad51-independent mechanisms, to repair a DSB, increases dramatically in the absence of Sgs1 or Exo1, where end resection is inhibited [37, 38]. Furthermore, microhomology mediated BIR, involving as little as 0-6nts, has been shown to occur following homology-driven BIR, through the action of translesion polymerases, substantiating this idea that BIR, particularly when Rad51-independent, does not require extensive end resection [39].

Lastly, the manner in which a replication fork is broken could influence repair pathway choice. During replication, BIR is thought to occur when a fork collapses directly at the junction, leading to a one-ended DSB on the leading strand duplex, and an intact lagging strand duplex with a ligatable nick at the fork junction. While this would be the expected result of replication runoff (e.g. in the context of CPT-induced damage), it is distinguishable from another scenario in which the stalled replication fork is specifically cleaved enzymatically, the consequence of which could leave an overhang or gap at the break point which would not be immediately ligatable without further processing. Intriguingly, Mus81-Mms4, with known roles in inducing DSBs following fork stalling, has been shown *in vitro* to cleave a few basepairs away from a junction, a mechanism that could influence whether repair occurs *via* GC or BIR [11, 40].

1.3.2 Break-Independent HR Lesion Bypass

While a number of DNA damaging agents, either directly or indirectly, cause DSBs, and consequently would require the utilization of one of the previously mentioned repair pathways, others induce damage that does not result in a DSB, but still require HR [13]. In these scenarios, fork reversal and Rec-X mediated template switch recombination are utilized.

Lesion Bypass via Fork Regression

Fork reversal has been proposed as the primary mechanism by which stalled forks are stabilized following an encounter with a replication block. Evidence supports two mechanistic arms of this pathway: in the first, the stalled fork gets reversed, stabilizing the fork until the lesion can be removed, and eventually gets regressed back to a fork structure following lesion removal [41]; in the second, the lagging strand replication is uncoupled from the leading strand replication, allowing for replication of the lagging strand beyond the lesion on the leading strand template. This newly synthesized lagging strand is then peeled back and used as a template for the stalled leading strand [42]. These two strands together then can either be branch migrated back into an intact replication fork bypassing the lesion, or can reinvade over the lesion, forming a dHJ (Figure 1.1I left and right respectively) [43-45].While 2DGE studies in yeast rarely detect these types of events, and EM studies have only observed fork reversal in check-point deficient yeast or in WT yeast treated with the topoisomerase inhibitor, CPT, recent studies using EM to observe replication intermediates in human cells found fork reversal to be the most common response to any type of genotoxin, even those known to cause

breaks, suggesting that primary DNA repair pathways may differ across species [1, 46, 47].

Gap Repair via Template Switch Recombination (GR-TSR)

In the absence of a fork reversal mechanism, lesion bypass can occur by template switch *via* a Rec-X recombination intermediate, 1) at a stalled replication fork, or 2) at a gap left behind the replication fork (GR) (Figure1.1J & K respectively) [48-51]. The primary distinction between these two models is the timing of Rec-X formation, with the first assuming a role for HR directly at the replication fork during S-phase. In this model, the leading strand stalls when it encounters a lesion, but the lagging strand replicates past the block, providing a template for the leading strand to invade and replicate off and over the lesion, coming back down during a second end capture event to form a Rec-X structure (Figure1.1J). This structure, much like a HJ, is a fully replicated, joint molecule, but unlike a HJ, which comprises fully base paired strands that are plectonemically coiled, the Rec-X possesses outer strands that are single stranded or base paired *via* paranemic coiling, a distinction that will be addressed below. Alternatively, in the GR model, upon encountering a lesion, the entire replication machinery reprimes downstream of the lesion, leaving a gap in the newly synthesized DNA to be repaired post replicatively. Much like the model at the replication fork, the lagging strand can be fully replicated, providing a template for the leading strand to replicate off and over the lesion, coming back down during a second end capture event to form a Rec-X structure (Figure 1.1K). These pathways are not mutually exclusive, and the current literature does not rule out the possibility for the first model; however, the evidence for a GR pathway is most

compelling, and so we will focus our review to this model, with the understanding that many of these observations could apply to both.

Evidence for post replicative gap repair goes as far back at 1968 when investigators noticed that single stranded gaps appeared in *E. coli* DNA following replication in the presence of UV. By measuring thymidine incorporation concomitantly with DNA density, they found that eventually these gaps were filled following bulk DNA replication [52, 53]. Four decades later, the explanation for these gaps was revealed when it was shown that the *E. coli* replisome can reprime downstream of a replication block on the leading strand template, in a manner that does not require fork regression, template switch, or a DSB [54]. Interestingly, this repriming was only necessary when the lesion was located on the leading strand, as a lesion on the lagging strand did not uncouple the replication machinery [54, 55].

That same year, single stranded gaps behind the fork in *S. cerevisiae* in response to UV were able to be visualized by EM [3]. Somewhat surprisingly, this phenomenon was not specific for UV, but rather, like the fork reversal events, a universal response to a variety of DNA damaging agents including MMS, HU, CPT, H_2O_2, and interstrand crosslinking agents [1]. Although these single stranded gaps are observed in a variety of organisms, from yeast to humans, the genetic requirements to prevent the accumulation of these gaps varies, indicating that different repair pathways may function in response to the same type of lesion [1-3]. Of note, Rad51 seems to be required to prevent ssDNA gap accumulation in yeast and *Xenopus*, but is not essential for alleviating these gaps in human cells [1, 2].

Whether this difference indicates a role for yeast Rad51 in lesion bypass at the replication fork, or whether it suggests a post replicative role to fill in the gap is not fully worked out, but most evidence favors the latter model. For one, post replicative repair machinery, spearheaded by the Rad6/Rad18 ubiquitin ligase complex and true to its name, can be uncoupled from replication and still provide damage tolerance to cells when activated in G2/M. Furthermore, ubiquitination of PCNA by this complex, which is required for Rad51-dependent template switch repair, persists after bulk replication, indicating that this process normally occurs following S-phase [7]. This gap repair is dependent on the activity of Pol δ and HR factors Rad51, Rad52, and Rad55, but independent of the strand annealing factor Rad59, implicated in Rad51-independent BIR, suggesting that this is a unique HR pathway [48].

Until recently, it was unknown whether GR occurred through a DSB intermediate or whether the strands remained intact. Using EM, Giannattasio, M. *et al.* was able to answer this question by visualizing Rad51/Rad52 –dependent X-structures in *sgs1Δ* yeast cells exposed to MMS [49]. While these structures initially appeared to be dHJs—an indicator of utilizing a GC pathway—they compared mung bean nuclease (MBN) sensitivity (see *Biochemical Distinction of Recombination Intermediates*) under uncrosslinked or psoralen crosslinked conditions, and found that while these structures were resistant to MBN when crosslinked, they were partially digested when uncrosslinked, leading the researchers to conclude that these structures were composed of both paranemically and plectonemically paired strands, consistent with a pseudo-dHJ (i.e. Rec-X) structure, and a break-independent repair pathway. In agreement with early studies measuring single stranded gap lengths, the hemi-catenated regions within the

crossover junctions were between 150 and 600 bp, demonstrating that the entire gap is repaired through an HR mediated event [49]. This pathway is consistent with certain types of DNA damage requiring HR machinery for repair in the absence of DNA breaks, and likely serves as a common repair pathway for many different types of DNA damage, including those known to trigger DSBs.

1.4 Recombination Intermediates

Each HR lesion bypass model uses a combination of just three structurally similar recombination intermediates: D-loops, HJs, and Rec-Xs (see highlighted boxes in Figure 1.1); but to complicate matters, these intermediates are fluid, with D-loops becoming HJs or Rec-Xs, and HJs coming in several varieties, including nicked-HJs, single HJs, and dHJs. Below we will describe the structural differences between these intermediates and the tools for distinguishing them.

1.4.1 D-loops

D-loops result from the first strand invasion step in all HR pathways and are prerequisite for both Rec-Xs and HJs. Following filament formation on a 3' extruding end, Rad51 undergoes a homology search and mediates strand invasion into a homologous section of duplex DNA. This invasion displaces one of the strands of the duplex, and Rad52 assists by annealing the invading strand to its complementary strand in the duplex. The resulting structure is thus composed of a DNA duplex between the invading strand (purple) and its complementary strand within the original duplex (red), and a displaced single strand from the original duplex (blue) (see Figure1.1B, C, & J). If a D-loop forms *via* strand invasion from a nicked end, it can become a Rec-X, as in the case of GR-TSR, but if formed *via* strand invasion from a fully broken end, which will

occur during GC, it can become a dHJ (Figure1.1J & C-D respectively). Consistent with this, overexpression of the helicase Srs2, known to displace D-loops, prevents the accumulation of MMS-induced X-structures in *sgs1Δ* mutants, where X-structures form independently of a break, and deletion of Srs2 leads to an increase in crossover levels following repair of a DSB [13, 14, 56]. Importantly, D-loops themselves can be the final recombination intermediate involving base pairing between damaged and template strands, as in the case of BIR, or SDSA (Figure1.1B & E). As a result, D-loops can also act as detrimental linkages if left unresolved, and so having enzymes that recognize and process these structures is vital for cell survival (see *Part 5. Resolvases*).

1.4.2 Holliday Junctions

The existence of HJs has been well established in the meiotic field, and they are known to be the recombination intermediate in response to a DSB [57, 58]. HJs take on a number of varieties: a nicked-HJ (nHJ), in which a discontinuity exists on one of the 4 branch points at a junction, is an intermediate substrate just prior to the second end capture step in GC, while completion of this second end capture will result in a dHJ (Figure 1.1D). Single HJs (sHJs) occur as a consequence of fork regression, when newly synthesized strands are peeled back off their parental templates and annealed to each other, creating a four-way junction (Figure1.1I). All HJs can occur in multiple isoforms *in vitro* including parallel and antiparallel stacked-X configurations, as well as the open planar, branch migratable form [59]. Whereas divalent cations (e.g. Mg^{2+}) stabilize a HJ into the antiparallel stacked-X isoform, many HJ resolvases bind and distort HJs into open planar configurations, suggesting both might be relevant structures *in vivo* [59, 60].

1.4.3 Rec-Xs

The existence of Rec-Xs has only recently come into acceptance within the last decade. Earlier observations that MMS-induced X-structures occurred in the absence of DSBs, and had ssDNA properties, strongly indicated that a recombination intermediate distinct from a HJ was being utilized to bypass MMS-induced lesions [13, 14, 61]. More recently, biochemical characterization and EM studies of MMS-induced X-structures in yeast, has confirmed that these structures do exist and are structurally distinct from HJs (see *Gap Repair-Template Switch Recombination* and *Chapter 2*) [49, 50]. These studies also strongly support Rec-Xs as being the recombination intermediates of GR-TSR, where the nascent lagging strand acts as a template for the lesion-blocked nascent leading strand. Although similar to a HJ in that it is a fully replicated joint molecule, a Rec-X is distinct in that its outer strands (made up of the parental template strands) are not plectonemically coiled (Figure 1.1H & J-K) [50, 51, 62].

1.4.4 Biochemical Differentiation of Recombination Intermediates

As most HR pathways initiate using a similar subset of enzymes, teasing out which pathway is utilized in response to a particular type of damage can be challenging; however, the recombination intermediates in each of these pathways are structurally distinct, and so being able to identify which recombination intermediate is present can provide insight into which pathway is triggered under certain conditions. D-loops are not fully replicated and have regions of both double and ssDNA; HJs are fully replicated and are fully double stranded; and Rec-Xs, while also being fully replicated, have single stranded outer strands capable of paranemic, but not plectonemic coiling. These distinctions become important for predicting how these structures will respond to

different biochemical tests. Currently, four biochemical tests, in combination with 2DGE and Southern blotting (2DGE-SB), are commonly employed to distinguish between these species. These tests include measuring branch migration in the presence or absence of Mg^{2+}, sensitivity to the single strand DNA nuclease, MBN, sensitivity to HJ resolvases (see *Part 5. Resolvases*), and strand denaturation to determine the size of strands that make up a four-way junction.

In the context of replication, all three of these recombination intermediates are composed of two linked sister chromatids with homology on either side of a junction, allowing them to freely branch migrate. However, due to the single stranded regions in D-loops and Rec-Xs, these structures are perpetually in an open configuration unlike a HJ which can easily convert back and forth between this open state and the stacked-X state. This open state is ideal for branch migration and thus D-loops and Rec-Xs are able to branch migrate even in the presence of Mg^{2+}, which restricts branch migration of a HJ by holding it in a stacked-X conformation [14, 59, 60].

Rec-Xs and D-loops have identical chemical properties in this test, and thus most D-loops that are transient precursors to Rec-Xs and HJs cannot be distinguished from Rec-Xs *via* 2DGE-SB; however, a subset of D-loops, namely those utilized at a fork, can be distinguished from Rec-Xs because their proximity to a replication fork restricts their size and shape. Therefore, while Rec-Xs are both fully replicated and bulky, D-loops employed during fork restart (e.g. BIR) are only partially replicated, and no bulkier than a replication fork; consequently, Rec-Xs will run within the X-spike on a 2DGE-SB while D-loops will run along the replication arc [49, 63]. The distinction between D-loops and replication forks can be made by determining whether branch migration occurs, as

replication forks are only 3-way junctions and consequently are not able to branch migrate into linear products.

The single stranded regions in D-loops and Rec-Xs also make these structures sensitive to digestion by MBN, whereas the fully double stranded nature of a HJ makes it resistant to this type of digestion. Digestion of Rec-Xs with MBN converts them to "double-Y" structures that migrate as an arc from the 1N spot up to the top of the X-spike on 2DGE-SB (see *Chapter 2*) [50, 64]. Digestion of D-loops will convert these structures to fork structures, reducing signal of the Y-arc, or, if a gap is present between the end of leading and the start of lagging strand synthesis, as in the case of BIR, they can be converted to linear products (see *Chapter 3)* [24].

A substrate's sensitivity to HJ resolvases has also been used to distinguish between these different recombination intermediates. As discussed below, HJ resolvases are structural endonucleases classified as such because of their ability to cleave *in vitro* HJ substrates; however, our group has proposed a model describing how a Rec-X can be converted to a transient HJ, thus making it sensitive to a HJ resolvase (see *Chapter 2*) [50]. Furthermore, Rec-Xs and D-loops have junctions similar to HJs, but the possibility that some HJ resolvases can recognize and cleave a Rec-X without this conversion step has never been tested. Given that almost all classical HJ resolvases bind and cleave HJs in their open conformation, it is likely that they could recognize and cleave a Rec-X and a D-loop as well. Indeed, RusA and Gen1, HJ resolvases that cleave HJs in their open conformation, have been shown to reduce MMS-induced X-structure levels in *sgs1Δ* mutants which are biochemically consistent with being Rec-Xs [14, 50, 65]. Interestingly, T4 endonuclease VII is distinct from all other HJ resolvases in that it binds specifically to

antiparallel stacked-X structures [66-68]. As a Rec-X and a D-loop cannot isomerize into this conformation, it is predicted that these two structures would be completely resistant to the activities of T4 endonuclease VII. Indeed, this has been shown for Rec-Xs [14].

Lastly, information regarding the size of each contributing strand to a recombination intermediate can shed light on the type of recombination intermediate being utilized. Both Rec-Xs and dHJs are fully replicated joint molecules and thus will have four strands of equal length. sHJs formed *via* fork reversal will have two sets of two strands of equal length, while D-loops or nHJs behind a fork will have three strands of equal length and two small strands whose sum is the length of one of the other strands. D-loops at the fork will have two strands of equal length and two smaller strands of differing length. These differences can be observed after running the products of a 2DGE in a third dimension under alkaline conditions. This will denature the strands, allowing the smaller strands to migrate faster, while the larger ones stay primarily in the X-spike[69]. Smaller strands will form an arc, indicative of different stages of repair occurring, however a ratio comparing this arc to the unmigrated full length fragments can indicate the type of replication intermediate present. Rec-Xs and dHJs will only be resolved into full length fragments and thus, will not have an arc corresponding to smaller fragments, single HJs formed *via* fork reversal, as well as D-loops at the fork will have a 1:1 ratio of full length to small fragments, and D-loops and nHJs will have a 3:1 ratio of full length to small. Caution should be used when quantifying *via* this technique as heterogeneity within the X-spike—i.e. the likelihood that both incomplete recombination intermediates (D-loops and nHJs) and complete recombination intermediates (Rec-Xs and dHJs) are present—can interfere with these ratios.

1.5 Resolution

Although HR allows for lesions to be bypassed during replication, this process introduces a new obstacle to genome integrity. Recombination intermediates formed during this process physically link sister chromatids together, and consequently, if left unresolved, can cause genomic instability when cells enter mitosis by facilitating aberrant chromosome breaks and aneuploidy. To ensure successful separation of sister chromatids prior to mitosis, a number of different mechanisms for resolving these linkages have evolved.

1.5.1 STR and SMC5/6 complexes

Dissolution by the Sgs1-Top3-Rmi1 (STR) complex is considered the primary mechanism for recombination intermediate resolution. The STR complex is made up of three proteins, the RecQ helicase, Sgs1, the topoisomerase, Top3, and the OB-fold containing protein, Rmi1, and is critical for maintaining genome integrity. It was first implicated in HR repair because of observations of increased genomic instability in cells from patients with Werner and Bloom Syndromes, and evidence in yeast showing *sgs1* and *top3* mutants had increased rates of recombination [56, 70-72]. Early studies demonstrated that WRN, BLM, and Sgs1 helicases could unwind 4-way junctions *in vitro*, and genetic studies in yeast showed that the synthetic sickness of *sgs1 srs2* mutants could be rescued by eliminating HR, hinting that the STR complex might be involved in recombination intermediate resolution; however, the seminal work that truly established the STR complex as a recombination intermediate resolvasome, came from Liberi *et al.*, who showed, *via* 2DGE-SB, that *sgs1* mutants accumulated Rad51-dependent X-structures that could be resolved upon induced expression of *SGS1* [14, 73-75].

While RecQ helicases are capable of resolving *in vitro* sHJs, dHJs have been touted as the primary recombination intermediate resolved by the STR complex as a whole. Multiple studies have shown that the STR complex as well as the human and *Drosophila* homologous BTR complexes are capable of resolving both short (14 bp) immobile synthetic dHJ substrates as well as long (165bp) mobile synthetic dHJs [50, 76-79]. This resolution activity is dependent on both the catalytic domains of Sgs1 and Top3, and occurs *via* convergent branch migration of the HJs into a single hemicatenane (Figure 1.1D left column) [79]. This reaction on a 165 bp mobile dHJ was further shown to be stimulated by RPA, suggesting that the helical unwinding activity of BLM/Sgs1 creates long stretches of ssDNA [79]. This is in line with models in which Sgs1 mediates the convergence of two HJs by unwinding the DNA behind the junctions until they merge to form a single hemicatenane which Top3, with the help of Rmi1, can then resolve through a transient nick in one strand of the hemicatenane followed by mediated strand passage and religation [78].

Our group also reported that the STR complex is capable of resolving a short (14 bp) immobile Rec-X structure more efficiently than an equivalent dHJ substrate, and this activity, although stimulated by the presence of Sgs1 and Rmi1, is not completely dependent on these complex members, as Top3 alone is capable of resolving the Rec-X substrate [50]. In contrast to dHJ dissolution, resolution of a Rec-X is thought to occur in a step-wise fashion with Sgs1 pushing the branch points together, and Top3 nicking and mediating strand passage for each linkage, requiring multiple decatenation steps (see *Chapter 2*) (Figure1.1J) [50]. This step-wise decatenation mechanism coupled with the

fact that a Rec-X contains regions of ssDNA already, is consistent with Top3's ability to act independently on this substrate while requiring assistance from Sgs1 to resolve a dHJ.

While the STR complex is the enzymatic contributor to recombination intermediate resolution, its success is dependent on signaling and structural support from another important DNA repair complex: the structural maintenance of chromosomes (SMC) 5/6 complex. Similar to mutations in the STR complex, mutations in any one of the SMC5/6 complex members results in increased MMS-induced X-structure accumulation. Evidence for the SMC5/6 complex in recombination intermediate resolution comes from studies showing that X-structures can be resolved by reexpressing WT Smc6 after their formation in *smc6-9* mutants [80]. Similarly to X-structures characterized in *sgs1Δ* mutants, X-structures in *smc5/6* mutants are consistent with being Rec-Xs [81]. Smc5/6 plays not only a structural role, but a signaling role in resolving X-structures, as made evident by the observation that a catalytically dead Mms21 mutant—the SUMO ligase component of the Smc5/6 complex—also accumulates MMS-induced X-structures [44, 81]. Recently, it was shown that Sgs1 and Top3 are both sumoylated in an Mms21-dependent manner, and this sumoylation, as well as physical association of Sgs1 with the Smc5/6 complex, is required for X-structure resolution [82, 83]. Thus, the X-structure accumulation observed for *smc5/6* mutants is likely due to a defect in STR complex recruitment to these structures.

The STR complex has also been implicated in other HR repair processes including fork stabilization and end resection. The STR complex potentially has two roles regulating fork stabilization, 1) altering DNA structure, and 2) recruiting other repair and replication factors. Indeed, the WRN and BLM helicases are capable of progressively

reversing fork structures up to 300 bp in length *in vitro*, suggesting a role for the BTR/STR complex in fork regression, however, examples of this occurring *in vivo* are not clear, and more data indicate that RecQ helicases could be involved in the unwinding of a regressed fork, rather than in its formation [43, 84-86]. This mechanism might be species specific as Sgs1 has not been implicated in this process in yeast, where fork reversal is not a common response to DNA damage. The STR complex as a whole however, has been shown to prevent fork collapse by stabilize polymerases E and α at stalled forks, and recruiting Rad53 specifically through the phosphorylated R1 domain of Sgs1 [87-89]. Whether this stabilization leads to alternative modes of repair has yet to be worked out.

Lastly, The STR complex is known to assist the exonuclease, Dna2, in 5'-to-3' end resection following a DSB. Sgs1 acts as the helicase to unwind the DNA, exposing ssDNA for RPA to bind, and Dna2 to resect, while Top3 and Rmi1 function as stimulatory components of this process, independent of Top3 catalytic activity [16, 78]. As previously stated, the increase in BIR observed in *sgs1* and *exo1* mutants is thought to be a result of decreased end resection, implying that the STR complex, not only has roles downstream of HR in resolving recombination intermediates, but also functions upstream by regulating pathway choice [37, 90].

1.5.2 HJ Resolvases

Following the discovery of HJs, a search for the enzymes that contributed to their resolution was underway. Canonical HJ resolvases were first discovered in bacteriophage, where both T7 Endonuclease I, and T4 endonuclease VII were shown to

cleave *in vitro* HJ structures [91, 92]. T7 endonuclease I resolves HJs by introducing symmetrical nicks to the continuous strands, in a sequence independent manner, while, T4 endonuclease VII appears to have opposite binding and cleaving specificity, as it cleaves the discontinuous strands of an anti-parallel stacked-X HJ [66-68, 93].

The first hint that HJs were utilized during DNA repair, came from studies in UV treated *E. coli*. UV-induced fork stalling was shown to lead to RecA-mediated fork reversal, resulting in a HJ. Further investigation into this fork restart mechanism led to the identification of the HJ resolvase, RuvC [94, 95]. Similar to T7 endonuclease I, RuvC acts as a homodimer, cleaving symmetrically to produce religatable products, but unlike T7, does so in a sequence specific manner [96]. It was then later discovered that *E. coli* harbor a second HJ resolvase, RusA, of prophage origin, which can become activated in the absence of a RuvABC pathway, in a RecG dependent manner, to aid in fork restart [97, 98]. RusA has a similar cleavage mechanism to RuvC, and also has a preferred, though different, cleavage sequence [96].

While the ability to bind to and cleave an *in vitro* 4-way junction is the main criteria for whether an enzyme can be classified as a HJ resolvase, the mechanism of cleavage is also telling. Despite the differences detailed above, an important similarity among bacterial and prophage HJ resolvases is that they all cleave junctions symmetrically, producing readily ligateable products without the need for further strand processing. This requirement brings into question whether some eukaryotic enzymes, originally classified as bona fide HJ resolvases actually act as such *in vivo*.

1.5.3 Eukaryotic HJ Resolvases

Unlike in prokaryotes, where HJ formation and resolution is well established as the primary mechanism for fork restart, evidence for this process occurring in eukaryotes is lacking. To date, there are four endonucleases with proposed roles in recombination intermediate resolution: Yen1/GEN1, Mus81-Mms4, Slx1-Slx4, and Rad1-Rad10. While all four enzymes have known roles in maintaining genome integrity, evidence suggests that they all have non-redundant roles and act preferentially on different substrates.

Yen1/GEN1

To date, Yen1 (GEN1 in mammals) has been the only nuclear endonuclease, whose structure specificity and mechanism of cleavage resembles that of canonical HJ resolvases in bacteria [22]. This enzyme is part of the Rad2/XPG nuclease family, and similarly to RuvC, is able to cleave the continuous strand of a synthetic HJ substrates symmetrically through dimerization [22, 99]. Despite HJ resolvases having important roles in DNA repair in bacteria, full gene deletions of *Yen1* in yeast only results in a minor sensitivity to DNA damaging agents, and does not reduce crossover rates, suggesting that Yen1/GEN1 functions primarily as a backup mechanism for recombination intermediate resolution during DNA repair [100, 101]. In support of this, Yen1 and GEN1 activities are restricted to mitosis, *via* phosphorylation and nuclear exclusion respectively, allowing noncrossover mechanisms (e.g. dissolution of joint molecules by STR/BTR complexes) to resolve the bulk of recombination intermediates in S and G2 phases [100, 102].

Mus81-Mms4

Mus81-Mms4 (MUS81-EME1 in mammals), a member of the Rad1/XPF nuclease family, has long been classified as the primary HJ resolvase in eukaryotes. Support for Mus81-Mms4 being a HJ resolvase comes predominantly from a number of studies detailing its relationship to Yen1 and the dHJ dissolvasome STR complex.

Mus81-Mms4 mutants are synthetic lethal when combined with deletion of any of the STR complex members. Interestingly, this lethality is rescued by deletion of HR, strongly suggesting that both of these complexes work in parallel to resolve recombination intermediates [103, 104]. Using temperature sensitive mutants, it was also shown that Mus81-Mms4 was required to remove MMS-induced X-structures in the absence of Sgs1, again supporting a role for this nuclease in resolving recombination intermediates [105]. It was postulated that these recombination intermediates were HJs because overexpression of HJ resolvases GEN1 and RusA were also able to resolve these structures [65]. Furthermore, *mus81* and *mms4* mutants were shown to be sensitive to DNA damaging agents, and have decreased rates of sister chromatid exchange [101, 106, 107]. As SCE is known to be caused by resolution of an HJ intermediate, these observations lent credence to the idea that Mus81-Mms4 resolved HJs.

In support of this, although *yen1Δ* single mutants have little sensitivity to DNA damaging agents, *yen1Δ mus81Δ* double mutants are more sensitive than *mus81Δ* single mutants, indicating they could be working in parallel pathways [101]. Given their activity on *in vitro* branched structures, it was hypothesized that these nucleases were resolving a common recombination intermediate. Insight into this mechanism led to observations that *yen1Δ mus81Δ* double mutants fail to both segregate their DNA and resolve replication

intermediates, and have an even larger reduction in crossovers than single *yen1Δ* or *mus81Δ* mutants, with a subsequent increase in BIR, again supporting a role for these nucleases in resolving HJs; however, recent investigation into the biochemical nature of these common recombination intermediates found that while they were sensitive to digestion by RuvC, they could be denatured into ssDNA fragments of differing size, consistent with these structures being nicked HJs and not intact HJs [69, 100, 101]. It is worth mentioning that a D-loop just prior to a second end capture event would also have these identical biochemical characteristics, so the possibility that Mus81-Mms4 and Yen1 are acting on precursors to Rec-Xs instead of or in addition to HJs is not out of the question.

Consistent with this later point, *in vivo* observations suggesting a role for Mus81-Mms4 in resolving HJs do not support *in vitro* structural characterizations that repeatedly have shown that a HJ is not an ideal substrate for Mus81-Mms4. Instead, Mus81-Mms4 favors 3' flaps, D-loops, and nicked HJs, structures expected to form in response to a stalled replication fork [40, 107-110]. These seemingly contradictory results however can be explained if the X-structures resolved by Sgs1 and Mus81-Mms4 are not HJs but instead are Rec-Xs. Our group and others have provided considerable evidence to lend support of this alternative, and intriguingly, the junctions of a Rec-X are very similar to a D-loop or a nicked HJ, making the Rec-X a potentially ideal substrate for the Mus81-Mms4 nuclease [14, 44, 49, 50]. That the Rec-X, and not the HJ, is the toxic intermediate upon DNA damage is further supported by the observation that *mus81Δ sgs1Δ* mutants are lethal while *mus81Δ yen1Δ* and *yen1Δ sgs1Δ* mutants are viable [100, 103].

Aside from likely roles in resolving Rec-Xs formed during GR-TSR, structure specificity of Mus81-Mms4 suggests that it might play a role in replication fork restart. Indeed, in mammals, DSBs associated with HU or aphidicolin treatment were found to be dependent on Mus81, and knockdown of Mus81 led to a reduction in recovery of stalled forks following HU or aphidicolin treatment, supporting a model in which stalled forks are purposefully cleaved to aid in restart [11]. Interestingly, unlike most structure specific endonucleases, Mus81-Mms4 cleaves a few base pairs away from a junction, a mechanism that would not favor HJ resolution, but that could aid in fork restart in a way that might actually prevent more deleterious HR pathways like BIR [40]. As previously stated (see *Break-dependent Pathway choice during Replication*), there is also evidence that Mus81 can cleave a "migrating bubble" replication fork—which resembles a D-loop—allowing for a transition of BIR repair into more favorable GC repair [34]. Interestingly, repair by BIR includes many template switches, which could be interpreted as SCEs, so Mus81's role in reducing recombination might be by preventing HJs from occurring in the first place [37]. That Mus81-Mms4 might function predominantly during GR-TSR or fork restart is also supported by observations that *mus81 yen1* double mutants, despite being synergistically sensitive to a variety of DNA damaging agents, have no sensitivity to IR which is known to cause DSBs [99]. As HJs are the known recombination intermediate of GC, this strongly supports Mus81-Mms4 playing an important role outside or upstream of GC recombination intermediate formation.

Slx1-Slx4

Slx1-Slx4 has also been shown to process *in vitro* HJ structures, however, unlike canonical HJ resolvases, Slx1-Slx4 does not resolve HJs into symmetrical religatable

products [107, 111]. This, combined with the observation that the synthetic lethality observed between mutations in Slx1 or Slx4 and the STR complex cannot be rescued by eliminating HR, led many to the conclusion that Slx1-Slx4 is not involved in recombination intermediate resolution [108]. Instead, Slx1-Slx4, shown to efficiently cleave 5' flaps and fork structures at the branchpoint into ligateable products, was thought to aid primarily in the resolution of stalled replication forks [111]. However, *in vivo* observations in human cells do point to an additional role for Slx1-Slx4 in HJ resolution, as SLX1 and SLX4 deficient cells were found to have a decrease in SCE events in the absence of BLM [106, 112]. Interestingly, while MUS81 deficient cells also displayed this phenotype, combined depletion of both SLX1 and MUS81 in BLM depleted cells did not further decrease SCE levels compared to depletion of just SLX1 or MUS81, prompting the investigation into whether these two protein complexes cooperated with each other during joint molecule resolution [112].

Indeed, SLX4 was found to act as a scaffold for both MUS81 and SLX1, and binding of these endonucleases to SLX4 was required for proper joint molecule resolution [112]. Intriguingly, while HJs are not ideal substrates for Mus81-Mms4, and are not cleaved to viable products by Slx1-Slx4, they can be cleaved *via* a coordinated nick and counternick mechanism through the combined activities of Slx1 and Mus81, respectively [107]. While this combined cleavage results in gaps and flaps within the linear products, and consequently does not produce readily religateable products, it does allow for potentially viable products that could be religated following additional end processing.

Rad1-Rad10

Rad1-Rad10 is another structure specific endonuclease important for genomic stability, and is particularly important during NER and HR repair (see [113]for a review on Rad1-Rad10s roles in NER). Although initial reports showed Rad1 had the ability to process an HJ in the presence of Mg^{2+} *in vitro*, these results were not reproducible, and an alternative role for Rad1-Rad10 as a 3' flap endonuclease became favored [114, 115]. Indeed, Rad1-Rad10 efficiently cleaves bubble structures, and 3' flaps at the junction of single stranded and double stranded DNA, thereby removing the 3' single stranded region, a process that is important for removing nonhomologous 3' flaps that occur following the annealing step in SSA (Figure 1.1G) [30, 110, 115, 116]. Rad1-Rad10 can also serve the same function for removing 3' flaps following D-loop dissolution during SDSA, and recruitment to these sites is dependent on Rad51 filament formation [117]. Given its close association with HR machinery, Rad1-Rad10 could play a role in processing Slx-Mus81 resolved HJs, although this mechanism has yet to be explored.

1.6 Conclusion

It is now clear that fork stalling and the accumulation of ssDNA gaps are the two universal responses to DNA damage, and depending on the type of DNA damage and the repair machinery available, repair of each of these structures can occur by a variety of HR mechanisms. Importantly, evidence strongly suggests that single stranded gaps and stalled forks are not repaired by the same HR pathway, with repair of single stranded gaps behind the replication fork likely being repaired primarily through a Rec-X mediated GR-TSR, while stalled forks are either regressed (in mammals) or cleaved and restarted by Rad51-dependent, error-free mechanisms (in yeast).The STR complex and

Mus81-Mms4 have multifaceted roles in both GS-TSR and restart of stalled forks, and thus it makes sense that STR and Mus81 mutants are consistently more sensitive to DNA damaging agents than canonical HJ resolvase mutants. This increased sensitivity to DNA damaging agents also strongly supports D-loops and Rec-Xs, and not HJs as the primary recombination intermediates utilized for lesion bypass during replication.

Our efforts to understand how the STR complex contributes to genome stability has led to novel observations and clearer insight into the specific HR repair pathways utilized in response to two different types of DNA damage. We find that in *sgs1Δ* mutants, MMS-induced damage is primarily bypassed through a Rec-X mediated GR-TSR mechanism while HU-induced fork stalling is counteracted through a DSB repair mediated fork restart mechanism. Furthermore, we highlight key functions of Top3 and the STR complex within these pathways, including Rec-X resolution and fork stabilization; and uncover a role for the Swi2/Snf2-related sumo-targeted ubiquitin ligase, Uls1, in HR repair pathway choice. While much progress has been made to understand how the STR complex and Mus81-Mms4 contribute to error-free repair downstream of HR, it will be interesting in the future to further uncover the mechanisms by which these complexes contribute to DNA repair and pathway choice upstream of recombination intermediate formation.

1.7 Figure Legends

Figure 1.1: Schematic of HR repair pathways. (**A-E**) Repair of a nick or break at a replication fork. A break at a replication fork (**A**) can be repaired by either BIR (**B**) or GC (**C-E**). During BIR, the nicked sister chromatid is ligated to the parental strand (**B**: *top*) to form an intact template for the broken sister chromatid to invade and replicate off of *via* a

"migrating bubble" D-loop (**B**: *bottom left: highlighted*), until it encounters another replication fork (not shown) or the end of a chromosome. Preceding GC (**C**), the fork is cleaved as to prevent ligation of the nicked sister chromatid with the parental strand. This allows for invasion of the 3' tail of the broken sister chromatid into the nicked sister chromatid and replication over the broken region (**C**: *middle*, *hig*hlighted). Following second end capture, and ligation of the broken ends, a dHJ is formed (**D**: *top row*), which can either be resolved into noncrossovers by the STR complex (*left column*) or through coordinated cleavage by HJ resolvases to produce noncrossover and crossover products (**D**: *right column*). Alternatively, a GC formed D-loop can be displaced (**E**) and annealed to its other broken end, allowing for religation and subsequent fork restart. If a break occurs behind a fork (**F-G**), it can either be repaired *via* GC as described above (**C-E**) or *via* SSA, in which extensive end resection (denoted by hash marks in **G**) occurs until at least 29 bp of homology exists to allow for Rad52-dependent annealing, and Rad1-Rad10 cleavage of the nonhomologous 3' flaps. This process leads to a loss of genetic information as denoted by the shorter sister chromatid (**G**: *bottom*). In the presence of a STL (**H**), lesion bypass an either occur *via* fork reversal (**I**) or through Rec-X mediated template switch (**J-K**). During fork reversal, the lagging strand gets replicated past the lesion (**H**) then pulled back, providing a template for the leading strand to replicate off of, creating a sHJ reversed fork. The sHJ can be branch migrated back to a replication fork, now bypassing the lesion (**I**: *left*), or the nascent strands can reinvade the parental strands, forming a dHJ and bypassing the lesion (**I**: *right*). Similarly to fork reversal initiation, TSR at the fork is initiated by the lagging strand replicating past the blocked leading strand (**H**). The leading strand then invades the lagging strand and replicates over the

lesion, forming a D-loop (**J**: *highlighted*). The leading strand then reanneals back to its original template *via* a second end capture event, creating a Rec-X (**J**: *highlighted*). This Rec-X is then resolved in a stepwise fashion by the coordinated actions of the Sgs1 helicase and Top3 topoisomerase, into noncrossover products. The same TSR bypass mechanism in (**J**) can also take place behind a fork to fill in a gap left following replisome repriming downstream of a lesion (**K**). Highlighted structures represent distinct recombination intermediates. Red labels represent lesion types encountered during replication.

Figure 1.1A-K

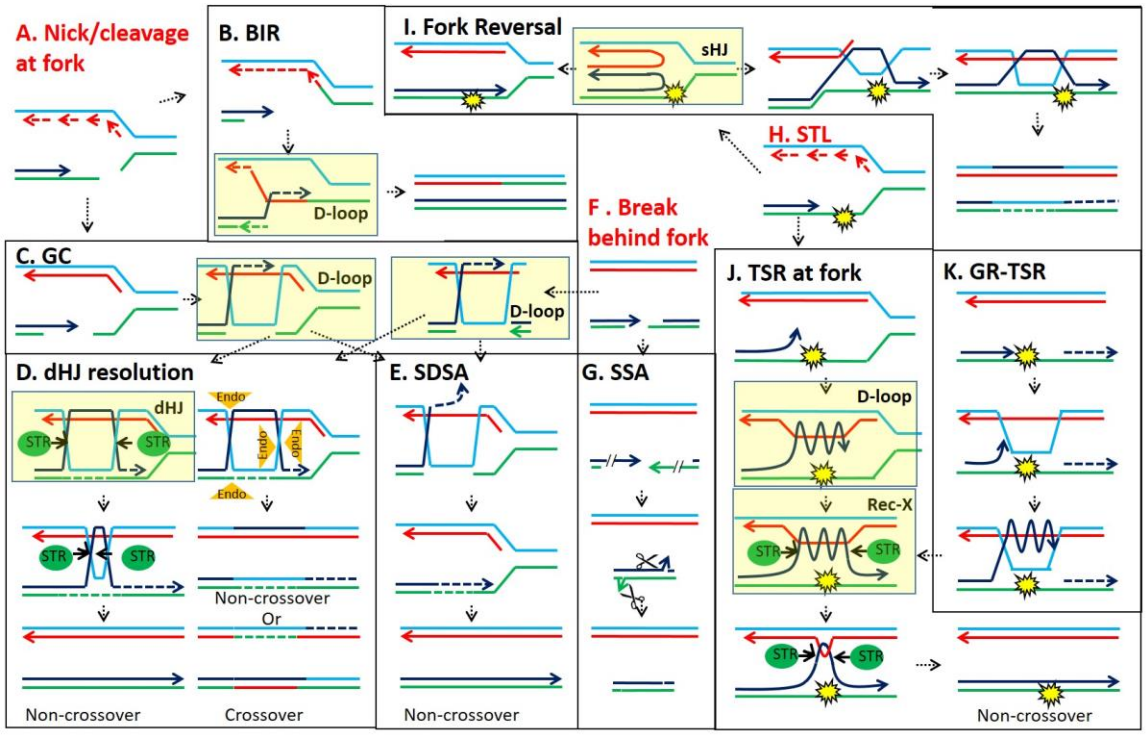
A. Nick/cleavage at fork
B. BIR
D-loop
I. Fork Reversal
sHJ
H. STL
F . Break behind fork
C. GC
D-loop
D-loop
J. TSR at fork
K. GR-TSR
D. dHJ resolution
dHJ
STR
STR
Endo
Endo
Endo
Endo
STR
STR
Non-crossover
Or
Non-crossover
Crossover
E. SDSA
Non-crossover
G. SSA
D-loop
Rec-X
STR
STR
STR
STR
Non-crossover

2. Resolution by unassisted Top3 points to template switch recombination intermediates during DNA replication

M. Rebecca Glineburg[1,2,*], Alejandro Chavez[1,2,3,5,*], Vishesh Agrawal[1], Steven J. Brill[4], and F. Brad Johnson[1,2,3]

Department of Pathology and Laboratory Medicine[1], Cell and Molecular Biology Group, Biomedical Graduate Studies[2], and Institute on Aging[3], University of Pennsylvania School of Medicine, Philadelphia, PA 19104, USA; [4]Department of Molecular Biology and Biochemistry, Rutgers University, Piscataway, New Jersey 08854, USA.

[5]Current address: Department of Pathology, Massachusetts General Hospital, Boston, MA 02215, USA

*These authors contributed equally to this work

Keywords: Top3, Sgs1, Rmi1, template switch recombination, STR complex, Holliday junction, Rec-X

Work in this chapter was published in *The Journal of Biological Chemistry* in 2013:

Glineburg, M.R., Chavez, A., Agrawal, V., Brill, S.J., and Johnson, F.B. *Resolution by unassisted Top3 points to template switch recombination intermediates during DNA replication.* J Biol Chem, 2013. **288**(46): p. 33193-20

2.1 Abstract

The evolutionarily conserved Sgs1/Top3/Rmi1 (STR) complex plays vital roles in DNA replication and repair. One crucial activity of the complex is dissolution of toxic X-shaped recombination intermediates that accumulate during replication of damaged DNA. However, despite several years of study the nature of these X-shaped molecules remains debated. Here we use genetic approaches and 2D gel electrophoresis of genomic DNA to show that Top3, unassisted by Sgs1 and Rmi1, has modest capacities to provide resistance to MMS and to resolve recombination-dependent X-shaped molecules. The X-shaped molecules have structural properties consistent with hemicatenane-related template switch recombination intermediates (Rec-Xs) but not Holliday junction (HJ) intermediates. Consistent with these findings, we demonstrate that purified Top3 can resolve a synthetic Rec-X but not a synthetic double HJ *in vitro*. We also find that unassisted Top3 does not affect crossing over during double strand break repair, which is known to involve double HJ intermediates, confirming that unassisted Top3 activities are restricted to substrates that are distinct from HJs. These data help illuminate the nature of the X-shaped molecules that accumulate during replication of damaged DNA templates, and also clarify the roles played by Top3 and the STR complex as a whole during the resolution of replication-associated recombination intermediates.

2.2 Background

The *S. cerevisiae* STR complex - consisting of the DNA helicase Sgs1, the type 1A topoisomerase Top3, and the OB-fold containing protein Rmi1 - functions in multiple facets of genome maintenance [118]. Loss of function mutations in STR complex

members cause sensitivity to a variety of DNA damaging agents, increased rates of chromosome loss, and chromosomal rearrangements [119-123]. Similarly, mice and humans lacking homologs of STR complex members, such as the Werner and Bloom syndrome DNA helicases, have phenotypes ranging from strong cancer predisposition to early embryonic lethality, highlighting the evolutionarily conserved importance of the complex in maintaining genomic integrity [124, 125].

How the STR complex functions to maintain genomic stability is an active subject of investigation with evidence pointing to roles in DNA damage checkpoint responses, replication fork stability, exonucleolytic processing of DNA ends and the resolution of homologous recombination (HR) intermediates [126]. Of note, emerging *in vitro* and *in vivo* evidence supports roles for the STR complex in the resolution of at least two different types of HR-dependent linkages: Holliday junctions (HJ) formed, for example, during double strand break repair (DSBR), and so-called Rec-X structures (also sometimes called sister chromatid junctions) formed during template switch recombination arising from the perturbation of DNA replication [14, 56, 57, 78, 127, 128]. In one type of HR-based DSBR, both broken ends invade the target, and following repair synthesis, each extended end is ligated to yield a double-Holliday junction (dHJ). The dHJ can be processed by a classical HJ resolvase, which can generate either crossover or non-crossover products. Alternatively, the STR complex can branch migrate the two HJs into one another to achieve dissolution without crossing over [129]. In the case of template switch recombination, when a replicating polymerase encounters a block to DNA synthesis, it is thought to switch to using the newly replicated strand of the sister chromatid as a template, and then eventually return to the original template once the stall-

inducing lesion has been bypassed. Alternatively, the switch could occur at a gap left behind the advancing replication fork. A Rec-X DNA intermediate is thus formed which links the sister chromatids and is characterized by entwined newly replicated strands and apparently unpaired original template strands. The Rec-X intermediate can then be dissolved by STR-catalyzed branch migration and dissolution (Figure 1) [130].

The supposition that the STR complex resolves HJs is supported by robust *in vitro* and *in vivo* evidence [57, 127, 128]. In contrast, evidence that the STR complex resolves Rec-X intermediates is based mostly on visualization and characterization of DNA intermediates using two-dimensional gel electrophoresis (2DGE) [14]. The initial studies examining MMS-induced recombination intermediates from *sgs1*Δ cells demonstrated a prominent near-vertical "spike" at the end of the replication arc, representing joint X-shaped linkages between sister chromatids. Further analysis revealed that these sister chromatid linkages are recombination-dependent, but unlike HJs can branch migrate in a fashion unimpeded by magnesium, are refractory to cleavage by the RuvC HJ resolvase, and can be cleaved by mung bean nuclease (MBN), an endonuclease specific for regions of ssDNA. These unique properties indicate that the intermediates that accumulate within MMS-treated *sgs1*Δ mutants are not HJs, but rather are Rec-Xs [5, 14, 61, 81]. Furthermore, restoration of Sgs1 expression caused a rapid loss of Rec-X intermediates in *sgs1*Δ mutants, indicating Sgs1 is highly suited to resolve these structures. Similar to the results with *sgs1*Δ cells, other loss-of-function mutations within the STR complex have been shown to accumulate recombination dependent X-shaped molecules, consistent with involvement of the whole complex for optimal resolution of Rec-X or dHJ intermediates [131, 132].

S. cerevisiae contains three topoisomerases, Top1, Top2 and Top3, which provide relief of topological stresses generated during DNA replication, repair and transcription. Unlike Top1 or Top2, which can relax both positive and negative DNA twist and supercoils in several contexts, Top3 is most active on negatively twisted (i.e. unwound) DNA [133]. To relieve negative twist, Top3 induces a single strand nick into the phosphodiester backbone by forming a covalent linkage between its catalytically essential tyrosine residue 356 and a phosphorus present in the DNA backbone. This reaction generates a transient gate through which the intact complementary strand of DNA can pass, thus relieving superhelical tension, and is followed by restoration of the phosphodiester backbone and release of Top3 [134-136]. Unlike Top1 and Top2, which provide the majority of *in vivo* topological relaxation, Top3 appears to function mainly in disentangling intermediates associated with DNA replication and repair [134-137]. Indeed, in support of such roles, *top3*Δ mutants display slowed chromosome replication, chromosome missegregation, inability to undergo meiosis and a strong sensitivity to genotoxic stressors [122, 138, 139]. Because Top3 interacts physically with Sgs1 and Rmi1, and mutations that disrupt these interactions compromise DNA repair activities, Top3 is generally thought to work only within the context of the STR complex [76, 140-144]. However, *sgs1*Δ *top3*Δ mutants are more sensitive to MMS than *sgs1*Δ mutants [144-146], suggesting that Top3 might have residual Sgs1-independent activities, but this possibility remains largely unexplored.

An essential requirement for resolution of both dHJs and Rec-Xs is that DNA strands pass through transient DNA breaks, and we reasoned that Top3 may thus be the most critical component of the STR complex for resolution of these X-shaped

intermediates. Although Sgs1 and Rmi1 stimulate Top3 catalysis, in principle, Top3 should have some intrinsic capacity to dissolve entangled DNA strands. Here we present evidence that Top3 indeed plays a more critical role than Sgs1 or Rmi1 in the resistance to MMS-induced DNA damage, and that in the absence of Sgs1 and Rmi1, Top3 has some capacity to resolve recombination intermediates. We utilize this Top3 dependent rescue to characterize the properties of the recombination intermediates that accumulate during replication of damaged DNA templates. Using genetic and biochemical assays, we show that the intermediates resolved by Top3 during bypass of stall-inducing lesions caused by MMS have characteristics of Rec-X structures rather than HJs. These findings clarify how the conserved STR complex promotes genome stability, and provide support for the role of Rec-X structures in DNA replication.

2.3 Experimental Procedures

Yeast strains:

All yeast strains are derived from the BY4741/2 background. Experiments using α-factor were carried out in *bar1Δ* strains. The following strains were constructed. **YAC174**: *sgs1Δ::HIS3;* YAC173: *sgs1Δ::HIS3, top3Δ::KanMX;* **YAC833**: *sgs1Δ::HIS3, rad52Δ::HYGMX;* **YAC1177**: *sgs1Δ::HIS3, top3Δ::KanMX, rad18Δ::HYGMX;* **YAC1637**: *sgs1Δ::HIS3, top3Δ::CaURA3;* **YAC1640**: *sgs1Δ::HIS3, top3Δ::CaURA3, mph1Δ::KanMX, shu1Δ::NatMX;* **YAC1644**: *sgs1Δ::HIS3, mph1Δ::KanMX, shu1Δ::NatMX;* **YAC1646**: *rmi1Δ::KanMX;* **YAC1887**: *sgs1Δ::HIS3, rad18Δ::HYGMX;* **YAC2005**: *sgs1Δ::HIS3, top3Δ::NatMX, Δrad52::HYGMX;* **YAC2341**: *rmi1Δ::KanMX, top3Δ::NatMX;* **YBB26** *sgs1Δ::KanMX, top3Δ::NatMX, bar1Δ::HYGMX.*

Plasmids:

All plasmids were based on Gateway-compatible pAG CEN/ARS vectors [147]. The constitutive *GPD* or *NOP1* promoters, which drive high or moderate levels of transcription, respectively, were each tested but gave indistinguishable results for *TOP3*-mediated rescue (data not shown). Plasmids used and constructed were as follows. pAG413GPD-ccdb; pAG415GPD-ccdb; pAG416GPD-ccdb; **AC207**: pDONR221-*TOP2*; **AC246**: pDONR221-*TOP1;* **AC273**: pAG416*NOP1*-ccdb; **AC739**: pDONR221-*TOP3;* **AC1314**: pAG416*TOP3*-MYC-ccdb (i.e. a *TOP3* promoter-driven vector); **AC1332**: pDONR221-hTOP3α; **AC1337**: pDONR221-*top3-Y356.*

Analysis of X-shaped Recombination Intermediates by 2DGE: Preparation of cell cultures, DNA, 2DGE, and Southern blots for analyzing the *ARS305* region has been previously described [64], and we employed the following modifications. Briefly, α-factor was added at a final concentration of 50 nM to logarithmically growing cultures for 4 hrs. The synchronized cells were collected by centrifugation and inoculated at 1.2 x 10^7 cells/ml into fresh YPAD containing a final concentration of 0.033% MMS. Samples were either harvested 1.5 hours later or the cells were washed at this point and inoculated into fresh YPAD (without MMS) at 4 x 10^6 cells/ml and were harvested 2 and 3 hours later. All comparisons were made between samples grown, prepared and run in parallel to remove inter-experimental variation. For 2DGE of the ribosomal DNA (rDNA) and the region adjacent to the *ARS305* region, DNA was digested with *Bgl II*, and run under identical conditions as for the *ARS305* region. The rDNA probe was made using PCR amplification of genomic DNA with primers rDNA-1053 and rDNA-447 as previously

described [148]. The *ARS305*-adjacent region probe was made using PCR amplification of genomic DNA with primers 5'-GTAGGAACAAAGGTTTGGCAGG-3' and 5'-CTTCGAGATAAGGCATGGGG-3'. Gels were quantified using Imagequant analyses of Phosphorimager scans. p-values for spike:arc ratios were calculated using one-tailed t-tests. Mung bean nuclease (MBN) sensitivity of X-shaped molecules was performed by digesting 1 μg of samples with *Bgl II* in NEB Buffer 2 followed by addition of 45 units of MBN (*NEB*) at 30º C for 1 hour. To confirm the specificity of MBN under these conditions, 0.5 fmol of a ^{32}P-5'-end labeled oligonucleotide (oligo 1*) by itself, or annealed into a synthetic HJ, was mixed with 1 μg of *Bgl II*-digested genomic DNA and treated with MBN as above. The synthetic HJ was based on J-11, built from oligos 1, 2, 3 and 4 [149], with two modifications: an error in the reported sequence of oligo 1 [149] was corrected to generate oligo 1* (GGCGACGTGATCACCAGATGATTGCTAGGCATGCTTTCCGCAAGAGAAGC), and a C was added to the 3' end of oligo 4 to generate oligo 4* (ACCGTTAGCAGTTCGCCTTGAGCCTAGCAATCATCTGGTGATCACGTCGCC) so that the HJ arm formed by oligos 1* and 4* was blunt ended and thus not subject to cleavage by MBN. Branch migration assays were performed as previously described (39), with the exception that the 65ºC incubation of samples was for 9 hrs.

Spot assays: Yeast were grown overnight at 23ºC in YPAD or, when required for plasmid maintenance, in selective media. 10^5 cells, and serial 10-fold dilutions, were then spotted to YPAD plates with or without MMS. Plates were incubated at either 30°C or 23°C

degrees and were imaged 2-3 days after spotting. For higher concentrations of MMS (0.02% and 0.03%) cells were spotted at 10^6 cells, with serial 10-fold dilutions.

Construction and characterization of dHJ and Rec-X substrates: Substrates were made using a two-step protocol modified from earlier constructions of dHJ from the dHJ1 and dHJ2 oligonucleotides [21, 150]. Oligonucleotide Rec-X1 (5'-CCACGTTTTCGTGGCGCTGGACTAACGCTCGACACCGACCAATGCTTTTGCATTGGTCGGACCTTCAGAACCGACCAGCG-3') was derived from dHJ1. The first step generated a covalently closed intramolecular circle from the Rec-X1 oligo (which self-anneals to form a structure containing a ligatable nick in one of its hairpinned duplex arms), and the second step generated the full Rec-X and dHJ products; this approach allowed for higher yield and purity of the Rec-X substrate. To ensure consistency between substrates, their components were processed identically and in parallel. For the first step, the dHJ1 and Rec-X1 oligonucleotides (12.5 pmol each) were phosphorylated using T4 polynucleotide kinase and a molar excess of [γ-^{32}P] ATP, followed by purification using Centri-Spin 20 columns (*Princeton Separations*) containing 10 mM Tris-HCl pH 7.5, 0.1 mM EDTA. The oligos were then subjected separately to annealing and ligation conditions (to which only Rec-X1 responded, by forming a closed circle) as follows: 6.25 pmol oligonucleotide was suspended in 35 µl containing 50 mM Tris-HCl pH 7.5, 10 mM $MgCl_2$, denatured at 95ºC for 3 minutes, shifted to 80ºC and cooled to 5ºC at a rate of 0.125º C/min. Samples were then ligated by addition of 1 mM ATP, 5 mM DTT, and 280 units of T4 DNA ligase (*NEB*) and incubated at 8ºC for 1 hr, 10ºC for 1 hr, 12ºC for 4 hrs, 16ºC for 12 hrs, and 20ºC for 12 hrs. The products were mixed 2:1

with formamide containing 0.1% bromophenol blue and xylene cyanol, and were resolved *via* electrophoresis through an 8% polyacrylamide gel (19:1 acrylamide:bisacrylamide) under denaturing conditions (7.8 M urea in 0.5X TBE). The gel was exposed to a Phosphorimager screen for ~15 minutes, and the image was printed out on a clear plastic sheet and placed over the gel to guide excision of the bands corresponding to the circularized Rec-X1 oligo and the linear dHJ1 oligo. The oligos were electroeluted from the gel slices using D-Tube Dialyzer Midi tubes (Novagen) with a 6-8 kDa cutoff at 6 V/cm for 1 hour in 0.5X TBE, followed by dialysis overnight at 4ºC *vs.* 1 L 10 mM Tris-Cl, pH 7.5, 0.1mM EDTA. In the morning the dialysis buffer was exchanged with fresh buffer and allowed to equilibrate for an additional two hours (this step was repeated twice). Samples were precipitated by adding 0.1 volume NaOAc pH 5.2, and 2.5 volumes 100% ethanol, and were washed with 70% ethanol.

For the second step, the pellets were resuspended in 20 µl 10 mM Tris-Cl pH 7.5, 0.1 mM EDTA containing 5'-phosphorylated dHJ2 (due to differences in substrate synthesis efficiency, dHJ2 was added at 100-fold molar excess to the Rec-X1; and at 15-fold molar excess to the dHJ1). Annealing, ligation, electrophoresis, gel extraction, electroelution, dialysis, and precipitation were performed as above. The final products were resuspended in 10 mM Tris pH 7.5, 0.1 mM EDTA at 0.5 fmol/µl. Substrate concentrations were estimated based on radioactive counts, measured using Imagequant analyses of Phosphorimager scans, compared to originally end-labeled oligos.

Confirmation of the Rec-X structure involved incubation of 0.5-1 fmol substrate with restriction enzymes (*NEB*) and exonucleases in 50 mM KAc, 20 mM Tris-acetate, 10 mM MgAc, 1 mM DTT, pH 7.9. RsaI (5 units) and HhaI (20 units) digests were

carried out at 37ºC for 3 hrs. Taq^{a}I (20 units) digests were carried out at 47ºC for 3 hours. *E. coli* Exo I (2.5 units; *USB*) and ExoIII (50 units; *Promega*) digests were carried out at 37ºC for 30 minutes. After digests, enzymes were heat inactivated at 80ºC for 20 minutes. Electrophoresis and image analysis were performed as above.

Top3 decatenation reactions: Top3 protein was prepared as described previously [151]. Reactions shown in Figure 8A-B were carried out using indicated amounts of protein, and 50 pM DNA substrate in 40 mM Hepes pH 7.0, 42% glycerol, 5 mM Na acetate, 65 mM NaCl, 60 mM KCl, 10 µg/mL BSA, 2 mM $MgCl_2$, 0.2 mM EDTA, 0.2 mM DTT, 0.002% NP-40, 0.02 mM PMSF, and 1 mM spermidine, at the indicated temperatures, for 2 hours. Reactions shown in Figure 8C-D and E-F were carried out as above but in 7% glycerol buffer, 5 mM ATP, no or 20 mM KCl, and 4 mM or 6 mM $MgCl_2$ respectively, at 37ºC. All reactions were stopped by the addition of 0.5% SDS and 0.05 mg/ml proteinase K, incubated at 37ºC for 20 minutes, and electrophoresis and image analysis were performed as above. p-values were calculated using two-tailed t-tests.

Western blot: Strains were grown to log phase and 10^8 cells were harvested by centrifugation and frozen for subsequent processing by mechanical disruption with glass beads in a 20% TCA solution. Samples were electrophoresed in 4-15% gradient acrylamide gels (*Bio-Rad*) and transferred to nitrocellulose membranes for probing with mouse anti-MYC antibody (Abcam #AB32) at a 1:2000 dilution, followed by HRP/chemiluminescence detection.

ADE2 crossover assay: Similar to a previously described crossover assay [152], a *URA3* marked ARS209-containing plasmid with a ~600 bp internal fragment of the *ADE2* locus was linearized at the Hpa1 site within the *ADE2* fragment. The resulting linear DNA was transformed into the desired yeast strains, cells were selected on SC-URA media and the percentage of red colonies was determined. Red colonies represent crossover (CO) repair events involving the formation of a dHJ that is resolved to disrupt the endogenous *ADE2* locus. White colonies represent non-crossover (NCO) events, e.g. repair events where the dHJs were convergently migrated and dissolved. p-values were calculated using two-tailed t-tests.

2.4 Results

2.4.1 Top3 promotes DNA damage tolerance in *sgs1*Δ mutants

As *sgs1*Δ *top3*Δ mutants are more MMS-sensitive than *sgs1*Δ cells [144-146], we hypothesized that Top3 might promote DNA damage tolerance, in an Sgs1-independent fashion, through the resolution of toxic recombination intermediates. The alternative explanation, that Top3 impacts checkpoint responses or cell cycle kinetics in *sgs1Δ* mutant cells, has been ruled out previously [138]. To first confirm that Top3 confers DNA damage tolerance in our genetic background, we compared the growth of MMS-treated *sgs1*Δ and *sgs1*Δ *top3*Δ mutants and found a ten-fold increase in DNA damage sensitivity when *TOP3* was deleted from *sgs1*Δ cells (Figure 2A). To provide further evidence for autonomous Top3 activity, we tested if overexpression of Top3 might further promote DNA damage tolerance in cells lacking Sgs1. A small (five-to-ten-fold) but repeatable increase in MMS resistance was observed upon Top3 overexpression in

*sgs1*Δ but not in wild-type cells, suggesting that the beneficial activity of Top3 is limiting, at least when Sgs1 is absent (Figure 2B and data not shown). These data prompted us to further investigate the mechanism of Top3-dependent DNA damage resistance.

2.4.2 Rescue of *sgs1Δ* mutants by topoisomerase activity is specific to Top3, and can be conferred by its human ortholog Top3α

To test if the identified role for Top3 in promoting DNA damage resistance within *sgs1*Δ cells is specific to Top3 or might be a general property of topoisomerases, we compared the capacity of Top1, Top2 or Top3 overexpression to rescue the MMS sensitivity of *sgs1*Δ and *sgs1*Δ *top3*Δ mutants. Unlike Top3, overexpression of Top1 or Top2 provided no increased DNA damage resistance in either context (Figure 2D). The catalytic activity of Top3 was required for rescue, because overexpression of the *top3-Y356F* mutant, which is defective in the formation of the 5' phospho-tyrosine covalent bond between DNA and Top3, was unable to rescue DNA damage sensitivity in *sgs1*Δ or *sgs1*Δ *top3*Δ mutants, despite equal accumulation of wild-type and Y356F proteins (Figure 2E-G) [134, 145].

The selective role for Top3 in the rescue of MMS sensitivity prompted us to ask if this role might be conserved and thus shared by the human Top3 ortholog *TOP3α* [153]. Remarkably, expression of *TOP3α,* which might be expected to interact poorly with endogenous yeast proteins, provided robust rescue of *sgs1*Δ *top3*Δ DNA damage sensitivity (Figure 3A). This finding supports the idea that Top3 can function

independently to confer resistance to MMS, and raises the possibility that this function is conserved between yeast and human cells.

2.4.3 Top3 promotes DNA damage tolerance independent of other STR complex members

In addition to its association with Sgs1, Top3 binds the OB-fold containing protein Rmi1 [119, 120]. Because Rmi1 binds DNA and is reported to stimulate Top3 reaction kinetics *in vitro*, we asked if DNA damage tolerance provided by Top3 depends upon Rmi1 [76, 78, 151]. No role for Rmi1 in Top3-mediated rescue was found as *rmi1*Δ *top3*Δ mutants were more sensitive to MMS than *rmi1*Δ controls, and Top3 overexpression in *rmi1*Δ mutants provided MMS resistance (Figure 3B & C). Furthermore, Rmi1 overexpression did not augment MMS resistance provided by Top3 overexpression in *sgs1*Δ cells (Figure 3C). Altogether, our findings indicate that even without assistance by other STR-complex members Top3 can provide some resistance to MMS-induced DNA damage.

2.4.4 Recombination intermediate resolution by unassisted Top3 provides DNA damage tolerance

We sought to determine whether the same DNA repair factors that enable the accumulation of HR intermediates during replication of MMS-treated *sgs1*Δ mutants are also required for the MMS resistance provided by unassisted Top3. Previous biochemical and biophysical analyses employing 2DGE indicated that these intermediates are Rec-Xs [14, 61, 81]. On 2D gels, Rec-Xs run as a prominent near-vertical spike originating at the end of the replication arc (e.g. see Figure 5A, below), as would be expected for joint

linkages arising from template switch recombination between sister chromatids. Importantly, not all molecules running within the X-spike are HR-dependent, as low levels of X-shaped species are still observed in homologous recombination-deficient *rad51*Δ or *rad52*Δ strains, particularly near origins of replication [154]. However, the elevated levels of Rec-Xs that accumulate when *sgs1*Δ mutants replicate through damaged DNA templates are entirely HR-dependent [14].

Several factors are necessary for Rec-X formation in *sgs1*Δ mutants, including the HR factor Rad52 and the post-replicative repair protein Rad18 [5, 14, 81]. Furthermore, it was shown recently that cells defective in another protein complex critical for Rec-X resolution, the Smc5/6 complex, accumulate Rec-X intermediates in a fashion dependent on the DNA helicase Mph1 and the pro-recombination Shu protein complex (consisting of Shu1, Shu2, Psy3 and Csm2) [44, 132, 155, 156]. Combined deletion of *MPH1* and *SHU1* completely suppresses Rec-X formation in *smc5/6* mutants, and given the biochemical similarity between the Rec-X molecules in *smc5/6* and *sgs1* mutants, we predicted and confirmed similar suppression of X-shaped molecule formation in *sgs1*Δ *top3*Δ by combined deletion of *MPH1* and *SHU1* (data not shown). Therefore, *MPH1* or *SHU1*, like *RAD52* and *RAD18*, are required for accumulation of X-shaped structures in *sgs1*Δ *top3*Δ mutant cells.

If the Sgs1-independent functions of Top3 involve resolution of Rec-X intermediates, Top3 should not impact MMS resistance in backgrounds lacking Sgs1 and factors required for Rec-X formation. As predicted, *sgs1*Δ *rad52*Δ, *sgs1*Δ *shu1*Δ *mph1*Δ and *sgs1*Δ *rad18*Δ mutants showed little to no effect of *top3* deletion (Figure 4A).

Similarly, Top3 overexpression did not improve the MMS sensitivity of these mutants (Figure 4B).

To test directly for effects of Top3 on replication intermediates, we employed 2DGE followed by Southern blotting to visualize events at different genomic regions. As is standard [14, 48, 65, 105], higher levels of MMS (0.016% - 0.033%) were used in 2DGE assays to enable visualization of enhanced X-structure levels under conditions where cells are exposed to MMS for only a single S-phase and where replication must be perturbed in any given genomic fragment that is visualized; importantly, we confirmed that Top3 overexpression improves growth even when cells are exposed to these higher levels of MMS (Figure 2C).

Logarithmically growing cells were synchronized with α-factor, and released into media containing MMS. Samples were taken at 1.5 hours after treatment, and also at two and three hours after release from MMS into fresh YPAD. In agreement with our MMS-resistance analyses, Top3 overexpression within *sgs1*Δ *top3*Δ mutants decreased X-shaped intermediates during recovery from MMS treatment (Figure 5). Whereas there was a trend toward suppression by Top3 overexpression of X-shaped molecule accumulation in a genomic fragment containing *ARS305*, this suppression did not achieve statistical significance in our assays (Figure 5 and data not shown). We reasoned that the background of origin-dependent X-structures may have obscured a difference in the MMS-dependent X-structures. To address this, we examined genomic fragments replicated by forks emanating from origins outside the fragments, including an rDNA region containing the replication fork block (RFB) and a region adjacent and telomeric to the fragment containing *ARS305*. Significant and reproducible suppression of X-shaped

molecules by Top3 overexpression was observed within both of these fragments (Figure 5). Overall, our findings indicate that Top3 is capable of providing MMS resistance and promoting the resolution of recombination intermediates independently of other STR members.

2.4.5 Unassisted Top3 does not resolve HJ intermediates efficiently

Recently, HJ-cleaving enzymes (RusA, Gen1, Mus81/Mms4) were shown to diminish levels of MMS-induced X-shaped molecules within STR complex mutants, leading to the suggestion that the X-structures may be HJs rather than Rec-Xs (see *Discussion*) [65, 105]. Because Top3 confers resistance to DNA damage and decreases the level of X-shaped molecules that accumulate in STR mutant cells, we used Top3 manipulation to further dissect the nature of the X-shaped molecules. The X-shaped molecules that accumulate during DSBR are known to be HJs [57], and we therefore tested whether Top3, independent of Sgs1, could affect the outcomes of DSBR. We employed a previously characterized *ADE2* recombination repair assay [152] in which the rate of crossover (CO) and non-crossover (NCO) events are reflected by the frequencies of red and white colonies, respectively. As demonstrated previously, *sgs1*Δ mutants show a statistically significant increase in the ratio of CO events as compared to wild-type strains (Figure 6A) [56]. However, in contrast to its effects on MMS resistance and replication-associated X-shaped molecules, and consistent with earlier findings, the deletion of *TOP3* from *sgs1*Δ mutants causes no additional change in CO events [56, 157]. Similarly, overexpression of Top3 in the *sgs1*Δ *top3*Δ background did not alter the frequency of CO events (Figure 6B). These findings are consistent with the idea that

Top3 cannot by itself resolve HJ intermediates, and support the idea that the X-shaped intermediates that are resolved by such unassisted Top3 during replication are likely not HJ intermediates.

2.4.6 The X-shaped molecules that accumulate without Top3 are Rec-X structures

Previous analyses of the MMS-induced recombination intermediates that accumulate within *sgs1*Δ mutants revealed that they are Rec-X structures which, unlike HJs, can branch migrate unhindered by magnesium and are susceptible to cleavage by mung bean nuclease (MBN) [14]. Although we expected a similar identity for the X-structures in *sgs1*Δ *top3*Δ, it was conceivable that they were instead HJs or regressed forks (i.e. "chicken foot" structures). We examined samples from cells grown for 1.5 hours in 0.033% MMS, prior to Top3-induced differences in X-structure resolution. As predicted, the MMS-induced X-shaped molecules in *sgs1*Δ *top3*Δ mutants showed an equivalent capacity to be branch migrated to resolution in the presence or absence of Mg^{2+} (Figure 6C & D). Furthermore, they demonstrated sensitivity to cleavage by MBN as well as a migration pattern consistent with the digested products of Rec-X structures (Figure 6E). MBN specificity under these conditions was confirmed by demonstrating efficient cleavage of trace quantities of ^{32}P-5'-end labeled ssDNA but not HJ substrates added into genomic DNA digestion reactions that were otherwise identical to those above (Figure 6F).

2.4.7 Unassisted Top3 decatenates Rec-X but not dHJ substrates in vitro

To confirm that unassisted Top3 can directly and selectively resolve Rec-Xs, we generated synthetic Rec-X and dHJ substrates, and tested their resolution by purified

Top3 *in vitro*. The dHJ substrate has been described previously [21, 128, 150] and was assembled from two 80mers, each forming intrastrand hairpinned duplex arms and two interstrand plectonemically coiled duplexes, each ~ 1.4 helical turns in length (Figure 7A). The Rec-X was derived from the dHJ 80mers, with one strand modified such that the two strands formed only one of the duplexes, and had unpaired "outside" strands (Figure 7A & B; see Materials and Methods). The Rec-X structure was confirmed using site-specific endonucleases together with exonucleases (Figure 7C). Each substrate contained a single ^{32}P-labeled strand and a total of two interlinks between strands.

Top3 was incubated with each substrate and strand decatenation was assessed using denaturing PAGE to separate the substrates from products (Figure 8). A range of temperatures was examined, because Top3 topoisomerase activity is enhanced at elevated temperatures [135, 151, 158]. Consistent with previous studies demonstrating that the dHJ substrate is resistant to Top3 alone but can be completely dissolved by Top3 combined with Sgs1 [78], Top3 was unable to decatenate the dHJ substrate even at high temperatures. However, Top3 displayed robust decatenation activity on the Rec-X substrate (up to 76%), in a temperature-dependent fashion (Figure 8A-B). Increased temperature alone did not result in decatenation of the Rec-X substrate, as evidenced by the no protein control, which was also treated at the highest temperature (47º C). We suspect that increased temperature could allow the Rec-X to adopt partial ssDNA character, making it a better substrate for Top3. However, we note that this does not appear to explain the specificity of Top3 for the Rec-X substrate because elevated temperature should affect the dHJ substrate similarly. It is also clear that the Rec-X retains significant duplex character at elevated temperatures because it is cleaved

efficiently by the *Taq*^{a}I endonuclease at 47ºC (Figure 7). Decatenation of the Rec-X was dependent on the catalytic activity of Top3, as the catalytically inactive Top3-Y356F was incapable of resolving the structure (Figure 8C & D). As expected, incubation with the entire STR complex showed robust decatenation of both the dHJ and the Rec-X (Figure 8C & D). The fact that the STR complex is more active than Top3 in the resolution of the Rec-X is consistent with our *in vivo* data showing that although unassisted Top3 has some capacity to resolve X-shaped replication intermediates and provide some resistance to MMS, it does not do so as robustly as the full STR complex. These findings are also consistent with the capacity of purified human TOP3α to decatenate entwined single-stranded circles, in a fashion stimulated by BLM and RMI1 [76]. Interestingly, the STR complex as a whole was almost twice as active on the Rec-X than on the dHJ at lower temperatures, and showed considerably more activity on the Rec-X than the dHJ at low protein concentrations, consistent with the idea that the STR complex processes Rec-X as well as dHJ substrates *in vivo* (Figure. 8, *C–F*). We note that Rmi1 does enable weak resolution by Top3 of the dHJ, as well as slightly stimulate the ability of Top3 to resolve the Rec-X (Figure. 8, *E* and *F*, and see Figure. 8, *A* and *B*; and data not shown). This contrasts with the activity of *TOP3* unassisted by *SGS1 in vivo*, for which *RMI1* does not enable crossover inhibition or stimulate resistance to MMS. A possible explanation for these apparent discrepancies is that the two interlinks between the entwined strands of the synthetic Rec-X and dHJ substrates are fewer in number than the interlinks between X-structures *in vivo*. Rmi1 has been shown to stimulate Top3 activity particularly at the final decatenation step [78], and thus might provide greater assistance to Top3 on the synthetic substrates than on highly interlinked substrates *in vivo*.

2.5 Discussion

Here we show that the type 1A topoisomerase Top3 can confer significant resistance to MMS-induced DNA damage in the absence of its STR complex partners, Sgs1 and Rmi1. This function of Top3 requires its catalytic activity and also involves HR pathways, as strains defective in the accumulation of X-shaped recombination intermediates (*sgs1*Δ *rad52*Δ*, sgs1*Δ *shu1*Δ *mph1*Δ or *sgs1*Δ *rad18*Δ mutants) failed to show altered DNA damage sensitivity upon *TOP3* deletion or overexpression. Consistent with these findings, Top3 overexpression diminished X-structures visualized by 2DGE and Southern blotting, indicating that Top3 promotes resolution of X-structures.

Although we have no reason to believe that Top3 functions apart from the STR complex under natural conditions, we took advantage of its unassisted activity to investigate the MMS-induced X-shaped replication intermediates, whose structure has been a matter of debate [159]. In particular, recent investigations of factors (e.g. HJ resolvases) capable of resolving recombination intermediates that accumulate within STR mutants have concluded that the X-shaped intermediates previously characterized as Rec-Xs instead represent unresolved HJs [65, 105]. However, to our knowledge, in all cases where X-structures induced by replication in the presence of MMS have been examined at a biochemical level, they have been found to have features most consistent with Rec-X species rather than HJs [5, 14, 81]. These features include branch migration unimpeded by Mg^{2+}, susceptibility of the "outside" single-stranded regions to cleavage by MBN, and relative resistance to cleavage by nucleases that cleave HJs, including T4 endonuclease VII and RuvC. On the other hand, it is clear that X-shaped intermediates formed during

DSBR such as during meiotic crossover events are HJs [58]. During DSBR, the STR complex promotes the branch migration of double HJs and ultimately their mutual removal by a dissolution mechanism. Consistent with a role for unassisted Top3 in the resolution of Rec-X intermediates but not HJs, we found that Top3 overexpression did not impact CO frequencies in a DSBR assay, and that *sgs1*Δ *top3*Δ mutants had CO levels no greater than *sgs1*Δ mutants. These observations are in agreement with previous studies [56, 157]. We also note that although conversion of a stalled replication fork to a DSB is presumably followed by formation of a HJ during HR-dependent resumption of replication, MMS does not actually cause significant levels of DSBs, consistent with MMS-induced X-structures not being HJs [13].

How then, can one reconcile the apparently conflicting viewpoints concerning the nature of replication-related X-structures? We suggest two non-mutually exclusive possibilities. First, the HJ resolvases identified as assisting in the resolution of X-shaped molecules within STR complex mutants (Mus81/Mms4, RusA, and Gen1 (1-527)) may process Rec-X substrates, although perhaps inefficiently. These nucleases clearly process HJs, but when carefully tested *in vitro,* each of these nucleases also binds and cleaves additional substrates [22, 96, 99, 160-162]. Because the discovery of Rec-X intermediates is still rather new, none of these identified HJ resolvases have been tested to see if they possess *in vitro* activity against Rec-X molecules. Indeed, to our knowledge, our *in vitro* studies with Top3 represent the first construction of a synthetic Rec-X substrate. We speculate that because Rec-X molecules have properties in common with HJs and replication forks, both of which Mus81/Mms4, RusA and Gen1 all bind and act upon, it would not be surprising if each of these enzymes can process Rec-X molecules.

Mus81/Mms4 in particular is a good candidate Rec-X resolvase as it cleaves HJs very inefficiently *in vitro* [163], but nonetheless has been demonstrated to be the enzyme responsible for resolution of MMS-induced X-spikes in the absence of the STR complex [105, 164]. The second possibility is that Rec-Xs might transiently assume a more HJ-like character, potentially allowing processing by HJ resolvases. This conversion of a Rec-X into a HJ might take place by base-pairing the "outside" strands at a Rec-X junction (*via* paranemic coiling) to generate a HJ (Figure 9). The very slow rate at which X-spikes are removed by overexpressed HJ resolvases is consistent with both of these models [65, 105]. Ultimately, to settle this issue it will be important to test the activity of HJ resolvases on model Rec-X structures and also to perform more detailed structural studies on the X-shaped molecules that accumulate during replication of damaged templates.

2.6 Figure Legends

Figure 2.1: Bypass of a replication-stalling lesion through the use of Rec-X-based template switch recombination (after Liberi *et al.* *[14]*). (**A**) A replication fork is shown with the nascent leading strand (dark blue) encountering a stall-inducing lesion. (**B**) The leading strand switches to use of the nascent strand of the sister chromatid as a template, bypassing the lesion. (**C**) The leading strand returns to its original template. (**D**) A Rec-X intermediate, which is resolved by the STR complex (**E, F**). A Rec-X could also form during the repair of gapped DNA left behind an advancing replication fork (not shown).

Figure 2.2: Top3 provides DNA damage resistance in *sgs1*Δ mutants. Spot assays comparing the effects of MMS on the growth of (**A**) *sgs1*Δ and *sgs1*Δ *top3*Δ mutants, (**B**) *sgs1*Δ mutants without or with a *TOP3* overexpression plasmid, (**C**) *sgs1*Δ *top3*Δ mutants without or with a *TOP3* overexpression plasmid showing resistance at higher levels of MMS, (**D**) *sgs1*Δ and *sgs1*Δ *top3*Δ mutants with control vector or plasmids overexpressing *TOP1, TOP2,* or *TOP3,* and (**E**) *sgs1*Δ or *sgs1*Δ *top3*Δ cells with control vector or plasmid expressing the catalytically inactive *top3-Y356F* allele. Ten-fold dilutions of strains were spotted onto YPAD alone or containing the indicated concentrations of MMS and grown as indicated for 48 (and for C up to 72) hours. (**F**) Western blot from log-phase *sgs1*Δ *top3*Δ cells containing plasmids expressing *TOP3* promoter-driven *MYC-TOP3* or *MYC-top3-Y356F* and probed with an anti-Myc tag antibody. (**G**) Ponceau S staining of the same membrane as in (**F**) to confirm equal loading of protein. Molecular weight markers are indicated (kDa).

Figure 2.3: MMS resistance provided by unassisted Top3 is evolutionarily conserved and can occur without *RMI1*. Spot assays comparing effects of MMS on the growth of (**A**) *sgs1*Δ *top3*Δ cells containing either control vector or human *TOP3α* expression plasmid, (**B**) *rmi1*Δ or *rmi1*Δ *top3*Δ mutants, and (**C**) *rmi1*Δ cells with vector or *TOP3* overexpression plasmid and *sgs1*Δ strains containing a *TOP3* overexpression plasmid together with an additional control vector or plasmid overexpressing *RMI1*.

Figure 2.4. Rescue by unassisted Top3 requires factors that enable the accumulation of unresolved recombination intermediates within *sgs1*Δ mutants. (**A**) *sgs1*Δ cells lacking additional factors which render them unable to accumulate recombination

intermediates, with or without endogenous *TOP3*, were spotted onto YPAD containing the indicated concentrations of MMS. (**B**) Identical to (**A**) except comparing the effects of *TOP3* overexpression.

Figure 2.5: Top3 overexpression reduces the level of X-shaped molecules within *sgs1*Δ *top3*Δ cells. (**A**) Representative two-dimensional gel electrophoresis Southern blots examining replication intermediates that accumulate in *sgs1*Δ *top3*Δ cells containing either vector or *TOP3* overexpression plasmid during exposure to MMS and following release into MMS-free medium. An rDNA fragment containing the RFB, a fragment adjacent to an *ARS305*-containing fragment, as well as the *ARS305*-containing fragment, are shown on the *left* and *middle*, and *right* sets of panels, respectively. *MMS* indicates cells grown for 1.5 hours in 0.033% MMS, and *2 hrs*, *3 hrs* and *4 hrs* indicate cells 2, 3, and 4 hours after release from MMS. *Right:* Schematic showing the location of DNA structures visualized by 2DGE, including the 1N spot containing non-replicating duplex, Y-shaped fragments containing single replication forks, and the X-spike containing two duplexes interlinked at different positions along their lengths. (**B**) Quantification of the ratio of X-shaped molecules to those running within the replication arc (n = 3 biological replicates for the rDNA fragment and *ARS305* adjacent fragment, and error bars represent the s.e.m; * p = 0.034, ** p = 0.009).

Figure 2.6: Unassisted Top3 promotes Rec-X resolution but not HJ resolution. (**A**) Wild-type, *sgs1*Δ and *sgs1*Δ *top3*Δ cells were transformed with the *ADE2* cassette, and the ratios of crossover-containing (CO) to total (CO + non-crossover (NCO)) colonies are plotted on the y-axis. Data are from three independent experiments and error bars

represent the s.e.m; * $p<0.05$, *NS* = not significant. (**B**) Identical to (**A**) except testing the effects of Top3 overexpression. (**C-D**) *Schematic:* resolved products are indicated by the new spot in the right panel. Southern blot of genomic DNA extracted from *sgs1*Δ *top3*Δ cells containing either vector or *TOP3* overexpression plasmid, showing resolution of X-shaped molecules into branch migrated products (*arrows*) at the *ARS305* adjacent fragment (**C**) and rDNA fragment (**D**). Samples were incubated at 65^{o} C in branch migration buffer (*BMB*) +/- Mg^{2+} between the first and second dimensions of electrophoresis. Percentages of branch migrated products are indicated in top right corner of panels. (**E**) Mung bean nuclease (*MBN*) treatment of genomic DNA extracted from *sgs1*Δ *top3*Δ cells containing either vector or *TOP3* overexpression plasmid, showing alteration in rDNA migration, consistent with Rec-X structures as indicated in the schematic. (**F**) 8% native polyacrylamide gel showing MBN digestion products of a ^{32}P-5'-end labeled 50 base long oligonucleotide alone (*ssDNA*) or annealed into a synthetic HJ substrate that were added into genomic DNA MBN digests under the same conditions as in E. The percentages of substrates digested are shown on the *right*. Note that the samples for **C** and **E** are from cells grown for 1.5 hours in 0.033% MMS, prior to Top3-induced differences in X-structure resolution, whereas samples for **D** are from cells 2 hours after release from MMS.

Figure 2.7: Characterization of synthetic Rec-X structure. (**A**) Schematic representations of the Rec-X and dHJ substrates, showing where the two oligonucleotides are topologically interlinked. For simplicity, the helical turns are not drawn in subsequent figures. (**B**) Rec-X map showing the sequences of the RecX1 and dHJ2 oligos that

compose it, regions of double stranded DNA, and RsaI, HhaI, and Taq^{a}I cut sites. The ^{32}P-labeled phosphate is indicated by an asterisk. (**C**) 8% polyacrylamide denaturing gel confirming the structure of Rec-X. Lane 1 (*M*), ^{32}P-5'-end labeled 10 bp DNA Step ladder (Promega); *second lane 2* (*S*) standard comprising Rec-X, and ligated and unligated forms of the 80-nt long RecX1 oligo; *third* and *fourth lanes*, Rec-X without restriction enzyme treatment; *fifth* and *sixth lanes*, digested with RsaI; *seventh* and *eighth lanes*, digested with HhaI; *ninth* and *tenth lanes*, digested with Taq^{a}I. *Fourth, sixth, eighth*, and *tenth lanes*, samples were further treated with *E. coli* ExoI and ExoIII, which degrade single-stranded and double-stranded DNA, respectively, in a $3' \rightarrow 5'$ direction. Note that the Taq^{a}I digest was performed at 47 °C, indicating that the inter-strand duplex region remained at least partially double stranded during the Top3 decatenation experiments, even at an elevated temperature. In addition we independently confirmed the structure of dHJ in a fashion similar to the characterization of the Rec-X (data not shown), as described previously [150].

Figure 2.8: Top3 decatenates a Rec-X but not dHJ substrate. (**A, C, E**) Samples were run on denaturing polyacrylamide gels. (**A**) Decatenation of Rec-X but not dHJ by Top3. DNA substrates were incubated alone or with 40 nM Top3 at the indicated temperatures. The products of Top3-mediated decatenation migrate with the closed circular form. (**C**) Decatenation of a Rec-X by Top3 alone, but not by catalytically inactive Top3, and decatenation of a Rec-X and a dHJ by the STR complex. DNA substrates were incubated alone (*NP*), with 40 nM Top3-Y356F (*T-Y*) or Top3 (*T*), or 40 nM Top3-Rmi1 together with 0.6 nM Sgs1 (*STR*) at 37º C. (**E**) Decatenation of a Rec-X

and a dHJ by the STR complex. DNA substrates were incubated alone (*NP)*, or with 1.2 nM Sgs1 and 0, 5, 10, or 25 nM of Top3-Rmi1. (**B, D, F**) Quantification of the data in (**A**), (**B**), and (**C**) respectively. The mobility standard (*S*) for all gels was made by mixing equal amounts of duplex substrate (Rec-X or dHJ), and circular and linear forms of the labeled strand. Percentages were corrected for background by subtracting the value of the no protein control for each substrate (n = 3 for B, D), *p < 0.05, **p<0.01, ***p<0.0002.

Figure 2.9: Models for Rec-X – HJ isomerization, and for Rec-X resolution *via* Top3 *vs*. a HJ resolvase. *Top*: Model for how a Rec-X can isomerize into a HJ. The "outside" strands are capable of base pairing (**A**), which would be limited by stress induced by the positive twist in the region of base-pairing and paranemic coiling. This stress could be absorbed by compensatory negative twist in the adjacent stretch(es) of the outside strands (not shown), and so base-pairs should be able to form at least transiently. Here such base-pairing is shown adjacent to the right junction, thus forming a HJ (**B**). *Lower left*: Model for how a Rec-X can be resolved by Top3. Top3 binds the Rec-X and cleaves one of the plectonemically coiled strands (*red*; **C**), enables passage of the intact strand (*black*), then religates the strand (**D**). The resulting negative twist is relieved by duplex rotation (**E**), leading to a Rec-X with one less linkage (**F**). (**G-H**) The products expected after steps C-F are repeated one and two more times respectively. *Lower right:* Model for how a Rec-X can be resolved by a HJ resolvase. The transient HJ described above is cleaved by the HJ resolvase (**I**), allowing the original "outside" strands to coil plectonemically around each other (**J**). This enables the linkage on the left to form a HJ that is subsequently cleaved by

the HJ resolvase (**K**). Note that crossing-over does not occur with resolution by Top3, but can occur with resolution *via* HJ resolvases.

Figure 2.1A-J

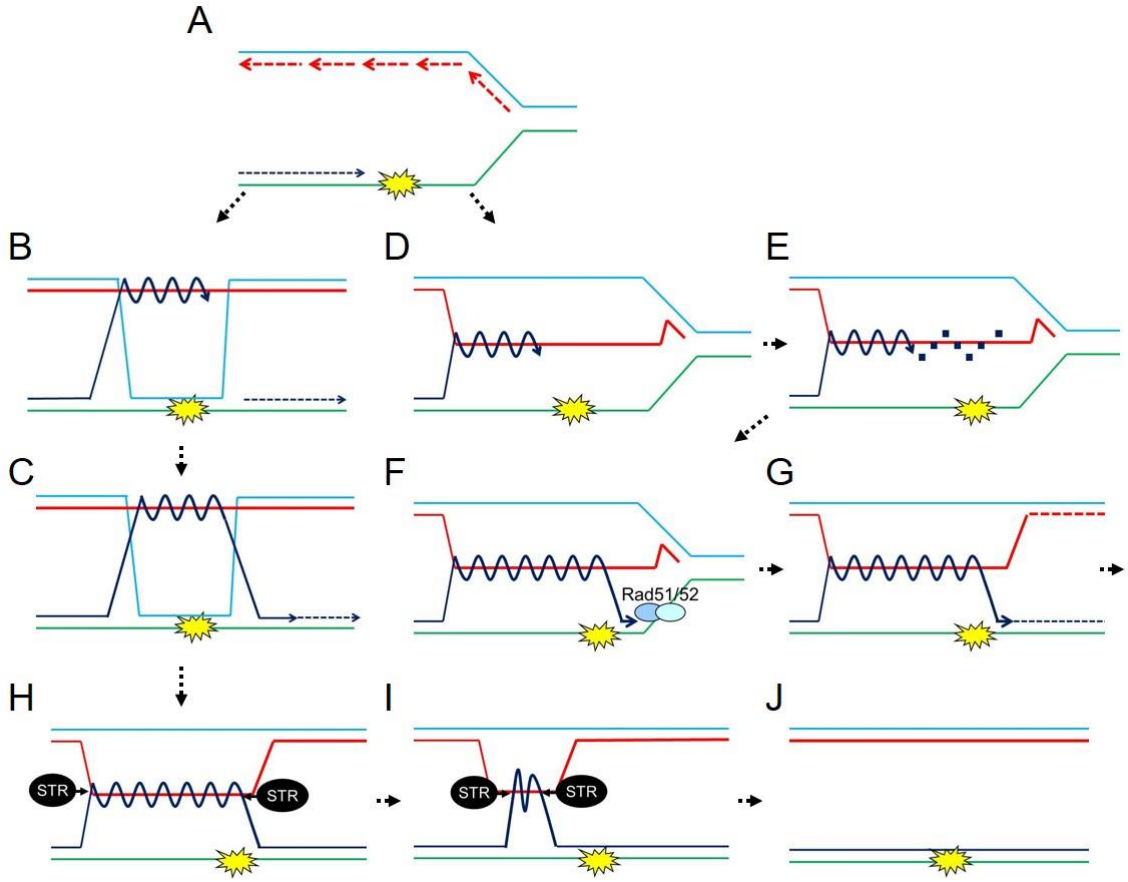

Figure 2.2A-G

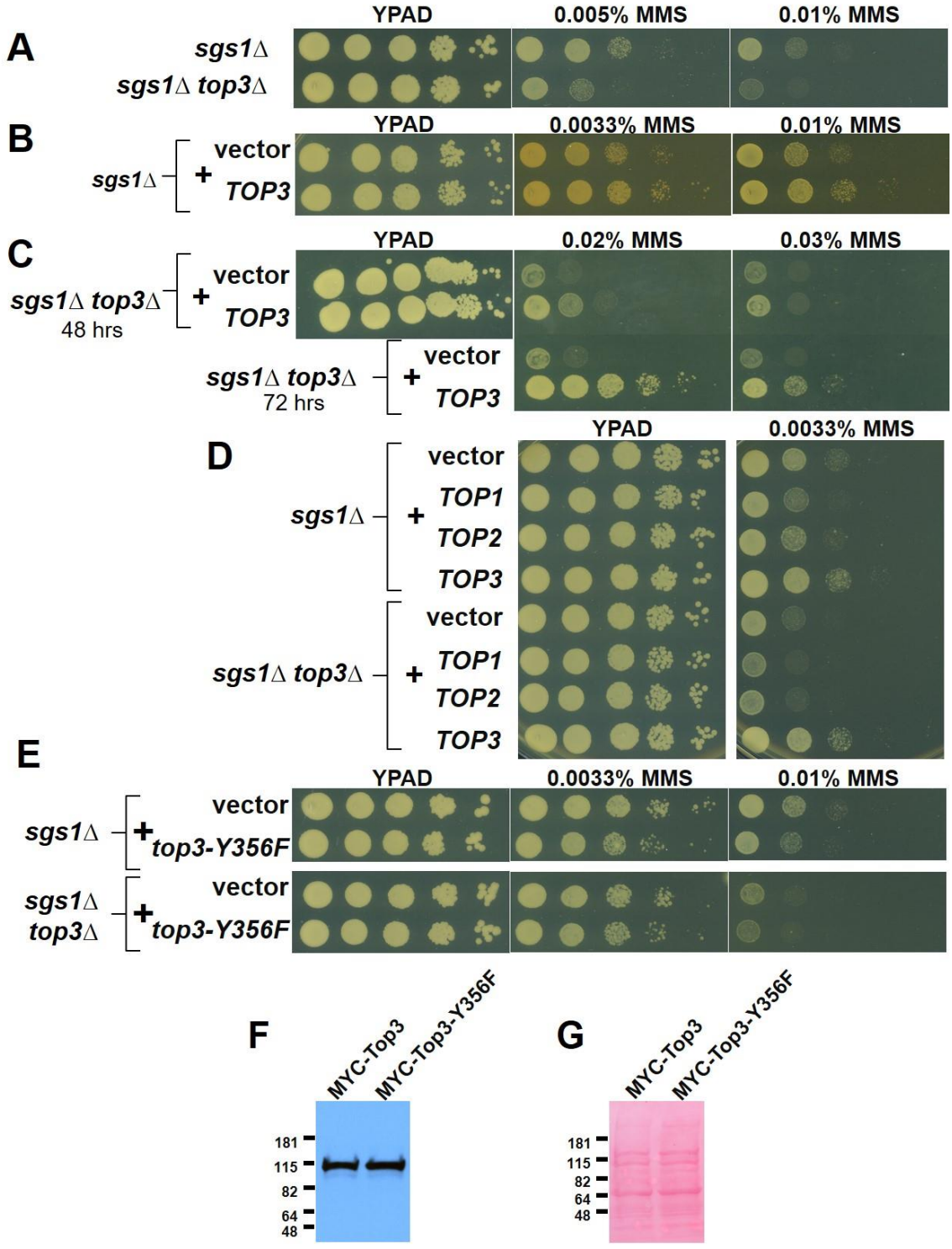
A
YPAD
0.005% MMS
0.01% MMS
sgs1Δ
sgs1Δ top3Δ
B
YPAD
0.0033% MMS
0.01% MMS
sgs1Δ
+
vector
TOP3
C
YPAD
0.02% MMS
0.03% MMS
sgs1Δ top3Δ
48 hrs
+
vector
TOP3
sgs1Δ top3Δ
72 hrs
+
vector
TOP3
D
YPAD
0.0033% MMS
sgs1Δ
+
vector
TOP1
TOP2
TOP3
sgs1Δ top3Δ
+
vector
TOP1
TOP2
TOP3
E
YPAD
0.0033% MMS
0.01% MMS
sgs1Δ
+
vector
top3-Y356F
sgs1Δ
top3Δ
+
vector
top3-Y356F
F
MYC-Top3
MYC-Top3-Y356F
181
115
82
64
48
G
MYC-Top3
MYC-Top3-Y356F
181
115
82
64
48

Figure 2.3A-C

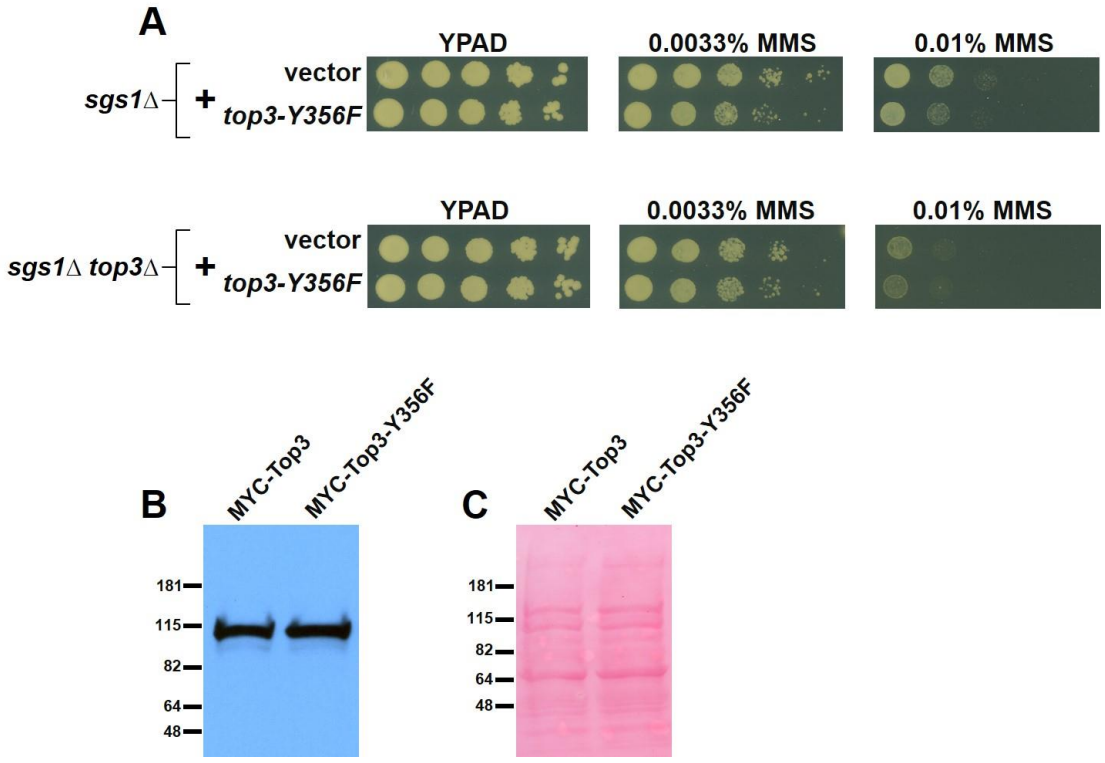
A
YPAD
0.0033% MMS
0.01% MMS
sgs1Δ
+
vector
top3-Y356F
sgs1Δ top3Δ
+
vector
top3-Y356F
YPAD
0.0033% MMS
0.01% MMS
B
MYC-Top3
MYC-Top3-Y356F
181
115
82
64
48
C
MYC-Top3
MYC-Top3-Y356F
181
115
82
64
48

Figure 2.4A-B

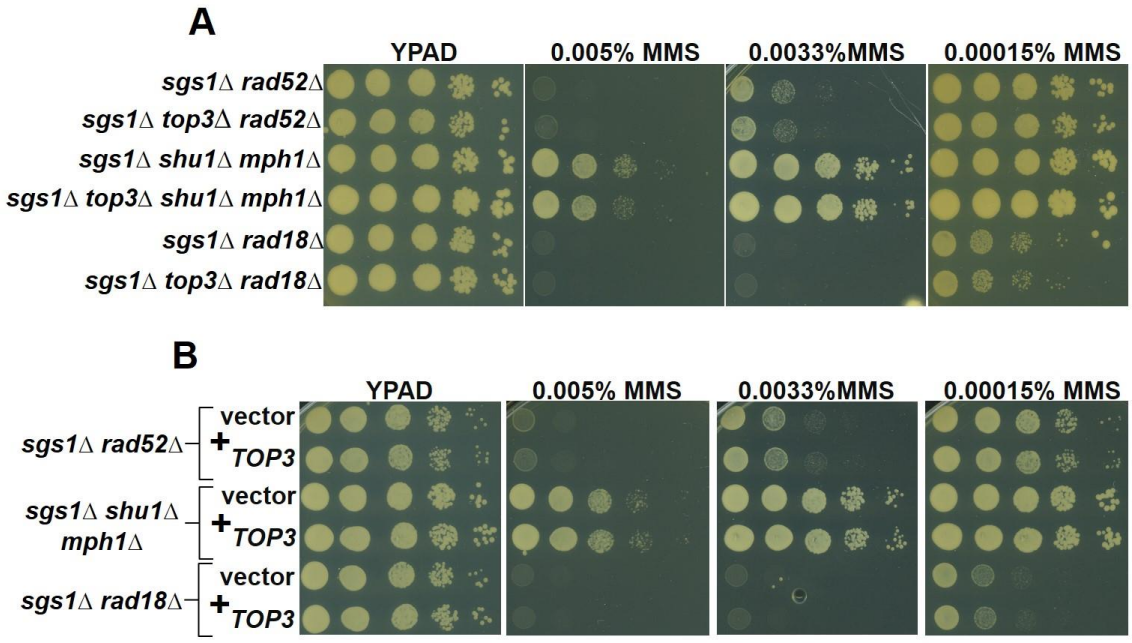
A
YPAD
0.005% MMS
0.0033%MMS
0.00015% MMS
sgs1Δ rad52Δ
sgs1Δ top3Δ rad52Δ
sgs1Δ shu1Δ mph1Δ
sgs1Δ top3Δ shu1Δ mph1Δ
sgs1Δ rad18Δ
sgs1Δ top3Δ rad18Δ
B
YPAD
0.005% MMS
0.0033%MMS
0.00015% MMS
sgs1Δ rad52Δ
vector
+TOP3
sgs1Δ shu1Δ mph1Δ
vector
+TOP3
sgs1Δ rad18Δ
vector
+TOP3

Figure 2.5A-B

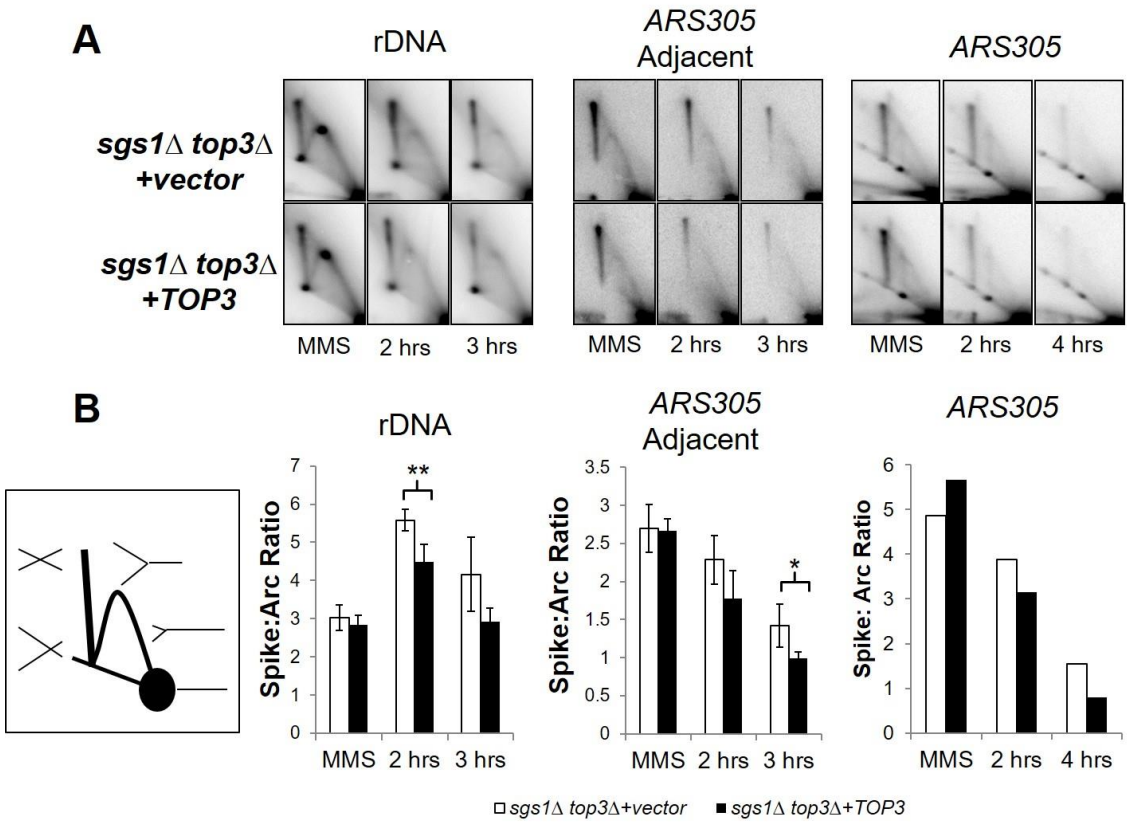
A
rDNA
ARS305 Adjacent
ARS305
sgs1Δ top3Δ +vector
sgs1Δ top3Δ +TOP3
MMS 2 hrs 3 hrs
MMS 2 hrs 3 hrs
MMS 2 hrs 4 hrs
B
rDNA
ARS305 Adjacent
ARS305
Spike:Arc Ratio
**
*
MMS 2 hrs 3 hrs
MMS 2 hrs 3 hrs
MMS 2 hrs 4 hrs
sgs1Δ top3Δ+vector
sgs1Δ top3Δ+TOP3

Figure 2.6A-F

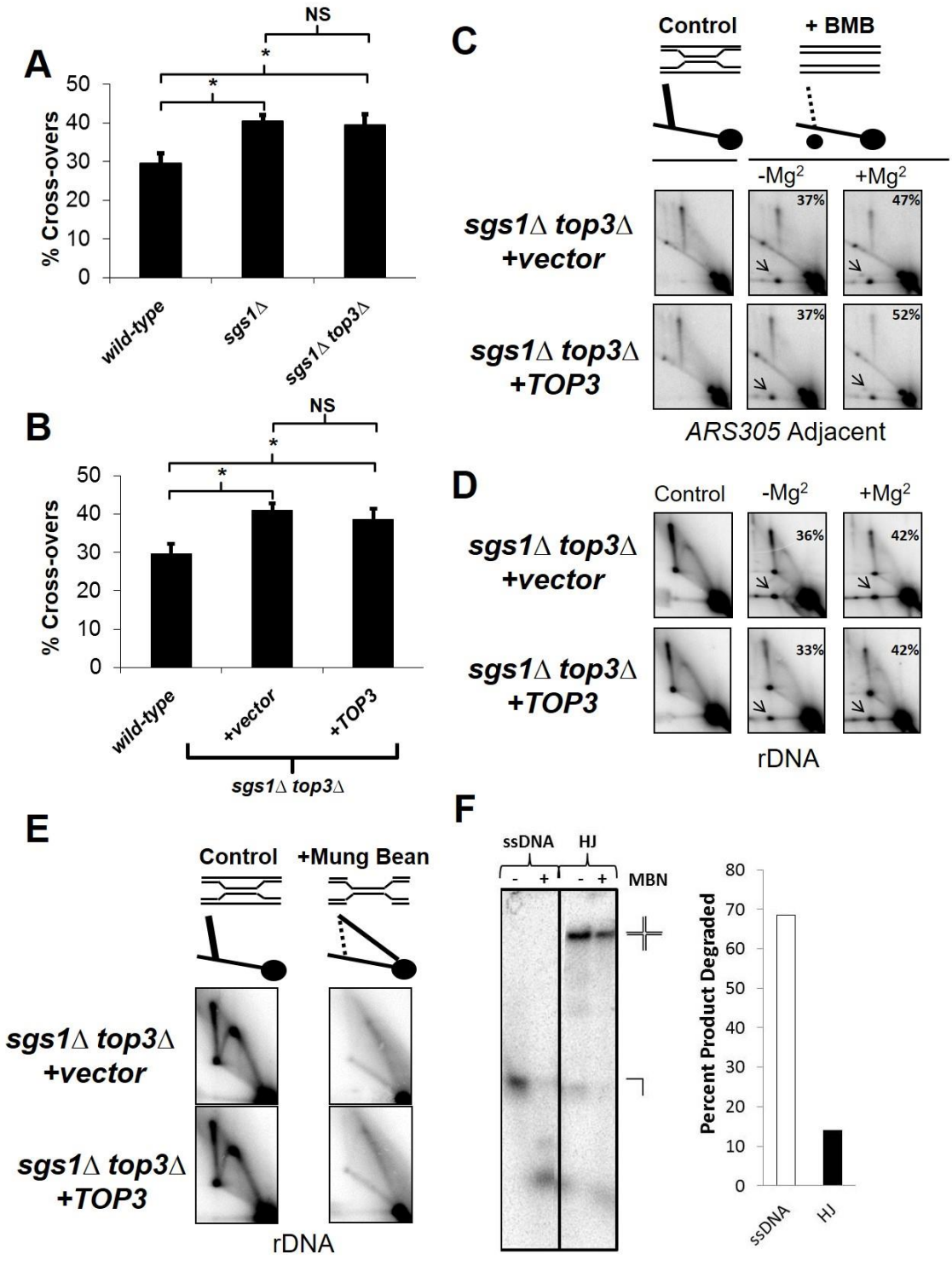
A
NS
*
*
% Cross-overs
50
40
30
20
10
0
wild-type
sgs1Δ
sgs1Δ top3Δ
B
NS
*
*
% Cross-overs
50
40
30
20
10
0
wild-type
+vector
+TOP3
sgs1Δ top3Δ
C
Control
+ BMB
-Mg2
+Mg2
sgs1Δ top3Δ +vector
37%
47%
sgs1Δ top3Δ +TOP3
37%
52%
ARS305 Adjacent
D
Control
-Mg2
+Mg2
sgs1Δ top3Δ +vector
36%
42%
sgs1Δ top3Δ +TOP3
33%
42%
rDNA
E
Control
+Mung Bean
sgs1Δ top3Δ +vector
sgs1Δ top3Δ +TOP3
rDNA
F
ssDNA
HJ
- + - +
MBN
Percent Product Degraded
80
70
60
50
40
30
20
10
0
ssDNA
HJ

Figure 2.7A-C

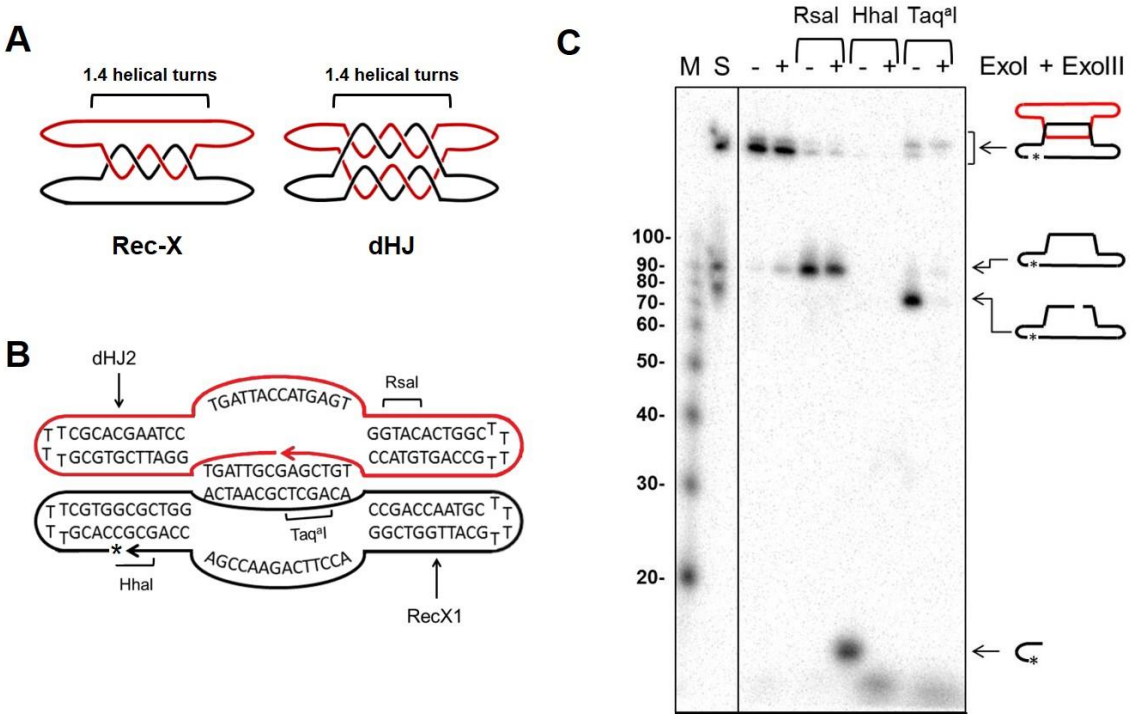
A
1.4 helical turns
1.4 helical turns
Rec-X
dHJ
B
dHJ2
RsaI
TGATTACCATGAGT
TTCGCACGAATCC
TTGCGTGCTTAGG
GGTACACTGGCTT
CCATGTGACCGTT
TGATTGCGAGCTGT
ACTAACGCTCGACA
TTCGTGGCGCTGG
TTGCACCGCGACC
CCGACCAATGCTT
GGCTGGTTACGTT
TaqαI
HhaI
AGCCAAGACTTCCA
RecX1
C
RsaI HhaI TaqαI
M S - + - + - + - +
ExoI + ExoIII
100-
90-
80-
70-
60-
50-
40-
30-
20-

Figure 2.8A-F

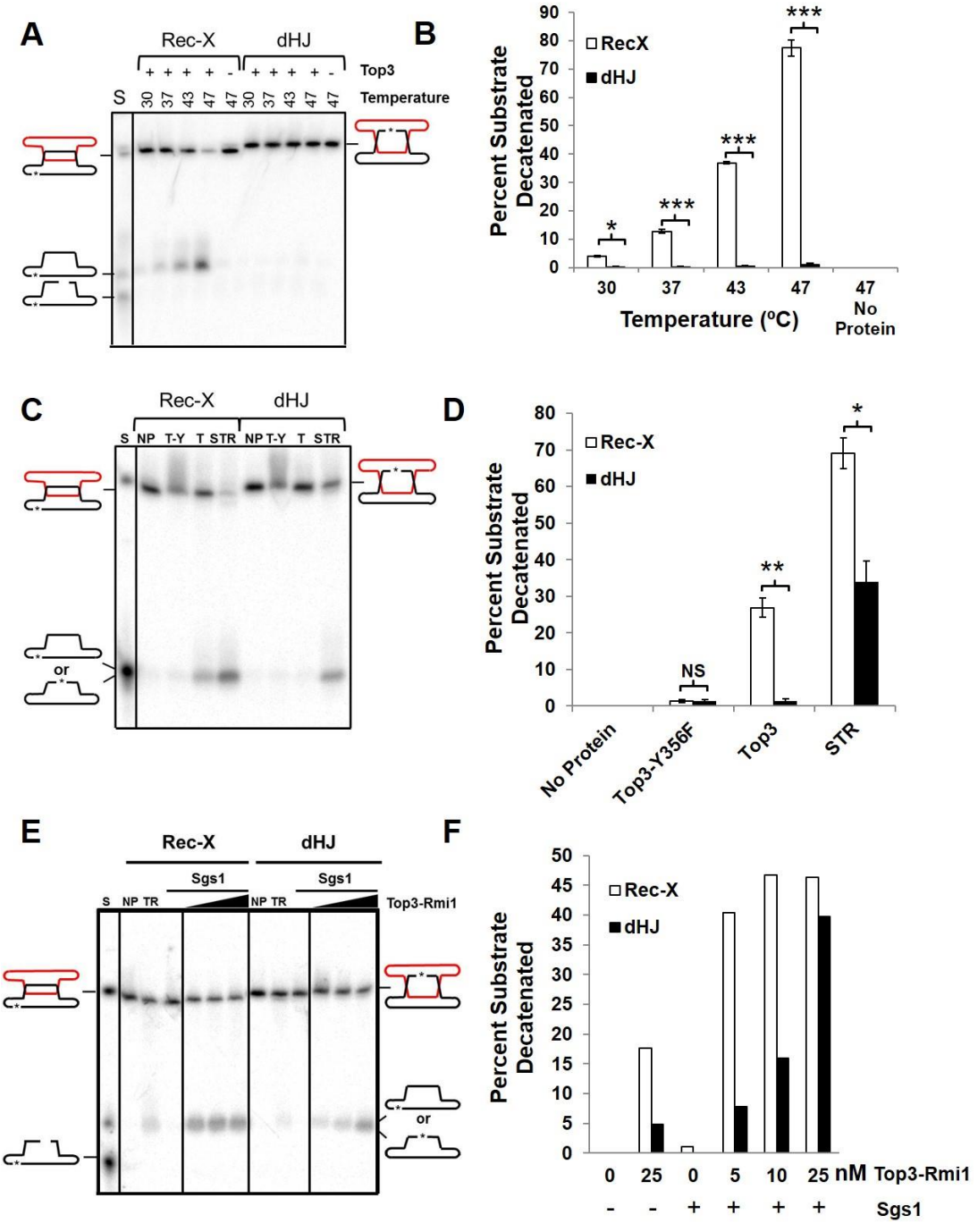
A
Rec-X
dHJ
Top3
Temperature
S
30 37 43 47 47 30 37 43 47 47
B
RecX
dHJ
Percent Substrate Decatenated
Temperature (°C)
No Protein
C
Rec-X
dHJ
S NP T-Y T STR NP T-Y T STR
or
D
Rec-X
dHJ
Percent Substrate Decatenated
NS
No Protein
Top3-Y356F
Top3
STR
E
Rec-X
dHJ
Sgs1
Sgs1
S NP TR NP TR
Top3-Rmi1
or
F
Rec-X
dHJ
Percent Substrate Decatenated
0 25 0 5 10 25 nM Top3-Rmi1
- - + + + + Sgs1

Figure 2.9A-K

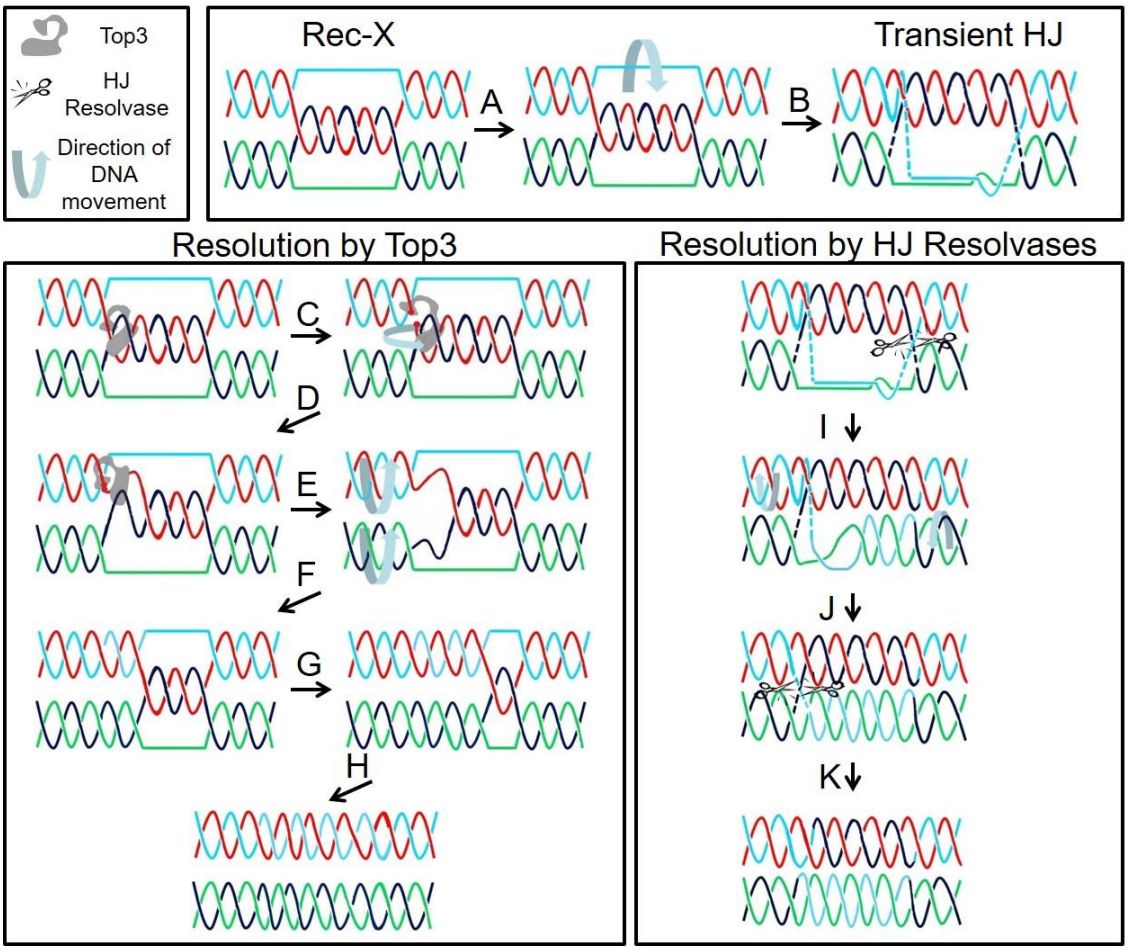
Top3
HJ Resolvase
Direction of DNA movement
Rec-X
Transient HJ
A
B
Resolution by Top3
Resolution by HJ Resolvases
C
D
E
F
G
H
I
J
K

3. Deletion of *ULS1* confers damage tolerance in *sgs1* mutants through a Top3-dependent D-loop mediated fork restart pathway

3.1 Abstract

Homologous recombination (HR)-based repair during DNA replication can apparently utilize several partially overlapping repair pathways in response to any given lesion. A key player in HR repair is the Sgs1-Top3-Rmi1 (STR) complex, which is critical for removing X-shaped recombination intermediates formed following bypass of methyl methanesulfonate (MMS)-induced damage. However, STR mutants are equally sensitive to the ribonucleotide reductase inhibitor, hydroxyurea (HU), but unlike MMS-sensitivity, this sensitivity is not accompanied by X-structure accumulation, and it is thus unclear how STR functions in this context. Here we provide evidence that HU-induced fork stalling enlists Top3 upstream of recombination intermediate formation. We demonstrate that Top3 can provide rescue to *sgs1Δ* mutants on HU, specifically in the absence of the sumo-targeted ubiquitin ligase, Uls1, and that Top3 is required for coordinated breaks and subsequent D-loop formation at forks stalled at the ribosomal DNA (rDNA) replication fork block (RFB). We also find that this rescue depends on the catalytic activity of the E3 SUMO ligase, Mms21, and includes a rapid Rad51-dependent restart mechanism that is different from the slow Rad51-independent HR fork restart mechanism operative in *sgs1Δ ULS1+* mutants. These data support a model in which repair of HU-induced damage in *sgs1Δ* mutants involves an error-prone break-induced

replication pathway but, in the absence of Uls1, switches to one with more fidelity, and provides evidence for D-loops in the repair and restart of stalled replication forks, particularly within the rDNA.

3.2 Background

Maintaining genome integrity is vital for cell survival and cancer prevention, and this maintenance is particularly challenging in the context of replication, where DNA repair machinery must coordinate activities with the replisome. It is well established that cells have a number of partially overlapping pathways that can repair DNA damage during replication, but how pathway choice is decided is still unclear. Recently, it has become evident that an intimate crosstalk occurring between the replication machinery, chromatin structure, and DNA repair complexes can strongly influence repair pathway choice. Understanding how DNA damage is repaired in the context of replication can provide insight into how these different pathways assist and compensate for one another to repair a given lesion and could provide insight into alternative chemotherapeutic strategies.

The ribonucleotide reductase inhibitor, hydroxyurea (HU) predominantly induces replication fork stalling, and in some DNA repair mutant backgrounds this stalling can be converted to reversed forks [46, 165, 166]. Interestingly, while fork reversal is one of the primary reactions of a stalled replication fork in mammalian cells, likely due to the action of PARP, it is a rare event in yeast; fork stalling and restart in yeast thus must arise by some other mechanism [1, 3, 47, 167].

The STR complex, comprising the RecQ helicase, Sgs1—often described as the "caretaker of the genome,"—the topoisomerase, Top3, and the OB-fold containing protein, Rmi1, maintains genome integrity, particularly in the context of HR repair, and serves as an ideal candidate for aiding in replication fork restart. Mutations in any of the STR complex members lead to increased rates of aberrant recombination, and increased steady state as well as MMS-induced X-shaped recombination intermediates [14, 50, 56, 61, 65, 131]. Both *in vitro* and *in vivo* studies strongly indicate a direct role for this complex in resolving recombination intermediates, through the combined catalytic activities of the Sgs1 helicase unwinding DNA and the Top3 topoisomerase transiently nicking and mediating strand passage to decatenate joint molecules [50, 65, 78, 79, 131, 137]. Previous work from our own lab has also shown that Top3 is also capable of working independently from its complex members to resolve a specific type of template switch recombination intermediate termed a Rec-X [50].

However, *STR* mutants are similarly sensitive to HU, which unlike MMS, does not result in X-structure accumulation, indicating that the STR complex could have important functions outside of recombination intermediate resolution [14, 65]. Indeed Sgs1 has also been implicated in earlier steps of HR repair of damaged forks including polymerase stabilization, Rad53 recruitment and 5' end resection, with Top3 and Rmi1 having only stimulatory but not catalytic roles in these contexts [16, 78, 87-89]. These functions likely aid in fork stabilization, but whether other functions of the STR complex are important at the fork and whether Top3 is capable of additional independent roles outside of Rec-X resolution are not fully worked out. Interestingly, deletion of *SGS1* results in increased rates in break-induced replication (BIR) and a compensatory loss of

gene conversion (GC) events following a double strand break (DSB), suggesting Sgs1, and possibly the entire STR complex can mediate repair pathway choice in this setting; how these activities might influence DNA repair during replication has not been explored [37, 38].

Recently it has been shown that genetic inactivation of a Swi2/Snf2-related sumo-targeted ubiquitin ligase (STUbL), *Uls1,* provides damage tolerance to *sgs1Δ* mutants in a post replicative, HR-dependent manner [168, 169]. Given our previous observations that overexpression of Top3 can also provide rescue to *sgs1Δ* mutants on DNA damaging agents, we investigated whether the rescue conferred by deletion of *ULS1* required these same Top3 functions. We find that rescue of *sgs1Δ* mutants in the absence of Uls1, while dependent on Top3, is not through Top3-mediated Rec-X resolution but instead through a novel Top3-mediated break-induced fork restart mechanism. Furthermore, we provide evidence that repair of HU-induced stalled forks occurs predominantly through D-loop intermediates to restart replication, and that deletion of *ULS1* confers resistance in *sgs1Δ* mutants by switching this D-loop mediated repair from a Rad51-independent to a Rad51-dependent pathway.

3.3 Experimental Procedures

Yeast Strains and plasmids

All yeast strains used were derived from the BY4741/2 background, with the exception of the HO-inducible crossover assay strains (derived from JMK background strains gifted by Jim Haber). *bar1Δ* strains were used for all synchronization assays. Table 1 provides a list of all strains constructed.

Spot Assays: Yeast were grown overnight at 23°C and spotted in 10-fold serial dilutions on YPAD or YPAD + drug plates as previously described [50]. Experiments were performed at 30°C, and images were taken at 48 hrs unless otherwise indicated. At least 3 independent experiments were conducted for each spot assay.

Analysis of Recombination Intermediates via 2D-gel electrophoresis & Southern Blotting: Preparation of cell cultures, DNA purification, and 2DGE-SB for analyzing the rDNA, region adjacent to ARS305 and telomeres were performed as previously described [50, 64]. G1 synchronized cells were released into fresh YPAD containing 200mM HU and allowed to grow for 1 hr. At this time, cells were either harvested, or spun down and resuspended in fresh YPAD containing no drug and grown for the times indicated prior to harvest. For experiments utilizing *in vivo* crosslinking, cells were grown and harvested as above. At the time of harvest, cells were resuspended in 5mL cold dH_2O at 4 $x10^8$ cells/mL and crosslinked 5 times with 300uL of 200ug/ml psoralen in EtOH for 5min with 5 min incubations on ice in between as described [64]. Branch migration assays were performed after the first dimension at 65°C for 6 hrs as described [64]. MBN assays were performed using 45units/1 ug of DNA as described [50, 64]. All 2DGE-SB experiments were performed in duplicate, and samples run in parallel to account for variation in gel preparation. Gels were quantified using Imagequant analyses of Phosphorimager scans. *p*-values for spike:arc and RFB:arc ratios were calculated using one-tailed t-tests.

Morphology Assays: Cells were grown as described above for 2DGE-SB, and samples were collected and immediately photographed and quantified at the specified time points.

We note that extended exposure to α-factor can influence cell morphology, and so an additional wash of the cells with fresh YPAD prior to exposure to HU was performed to eliminate all traces of α-factor. Cells were counted as aberrant if they presented as a cluster of three or more intact cells. Each cluster was counted as one cell. Cells were photographed on the bright field setting at 40X magnification using MagnaFire2.1C software. *p*-values are calculated from a Fisher's exact test.

rDNA break Assay: Cells were grown as described above for 2DGE-SB experiments, in 5 ml volumes. Plug preparation, digest, running conditions, and southern blotting for the rDNA break assay has been described previously (Weitao, T., 2003). In brief, cells were imbedded into agarose plugs with zymolyase and digested in a 6 well plate sequentially: 2X zymolyase at 37C for 24 hrs, 2X 1mg/ml proteinase K and 2.5% Sarkosyl at 50C for 24 hrs, 1X 40ug/ml PMSF for 1 hr, washed with TE 1hr at 50C, 1X 100ug/ml RNase A, at 50C for 3 hrs, and digested with Bgl II overnight at 37C. Plugs were washed with TE prior to loading on a 1% agarose gel in 1X TBE. ER5A-up, 5′-GCC ATT TAC AAA AAC ATA ACG-3′ and ER5A-lower, 5′-GGG CCT AGT TTA GAG AGA AGT-3′ were used to make Probe A *via* PCR amplification of genomic DNA (Weitao, T., 2003). Breaks were quantified using Imagequant analyses of Phosphorimager scans. The proportion of breaks was determined by dividing the 2.3Kb band over the 4.6Kb band. Each sample was harvested in triplicate and quantification for two individual colonies for each genotype are shown. *p*-values for 2.3Kb:4.6Kb ratios were calculated using two-tailed t-tests.

Crossover Assays: The ADE2 crossover assay (Glineburg et al., 2013, Tay Y. D., 2010), and the HO-inducible crossover assay (Ira, G., 2003), have been previously described. *p*-values for comparing *sgs1Δ* to *sgs1Δ uls1Δ* were quantified using two-tailed t-tests for the ADE2 crossover assay and for the 6 hr time point for the HO-inducible crossover assay. Fisher's exact test was used to calculate *p*-values for comparing *sgs1Δ* and *sgs1Δ uls1Δ* differences in the single colony analysis.

3.4 Results

3.4.1 Rescue of *sgs1Δ* by deletion of *ULS1* is dependent on Top3

Inactivation of Uls1, has previously been shown to provide rescue to *sgs1Δ* mutants on MMS and HU, in a HR-dependent manner [168, 169]. Furthermore, this rescue *via* deletion of *ULS1* appeared to be specific for *sgs1Δ* mutants, as deletion of *ULS1* was unable to provide rescue of *top3Δ* and *rmi1Δ* mutants [168, 169]. Although it normally functions within the full STR complex, Top3 is capable of working independently from its complex members to provide rescue on DNA damaging agents in a HR-dependent manner, and so we investigated the possibility that the rescue of *sgs1Δ* mutants observed with *ULS1* deletion requires Top3 [50]. To address this, we first confirmed that deletion of *ULS1* does indeed confer damage tolerance to *sgs1Δ* mutants exposed to DNA damaging agents in our strain background (Figure 1A). We next examined whether deletion of *ULS1* was still able to confer damage tolerance to *sgs1Δ* mutants in the absence of Top3. There was no difference in growth observed in *sgs1Δ top3Δ vs sgs1Δ top3Δ uls1Δ* mutants on MMS or HU indicating that Top3 is required for the damage tolerance observed when *ULS1* is deleted in *sgs1Δ* mutants (Figure 1A).

Consistent with our previous findings [50], the ability of *sgs1Δ* mutants to be rescued by deletion of *ULS1* is independent of Rmi1, supporting an independent role for Top3 outside of its canonical functions within the STR complex. Furthermore, in HU treated cells, when Top3 was overexpressed (OE) in *sgs1Δ uls1Δ* mutants, there was a small, but reproducible, increase in damage tolerance compared to *sgs1Δ uls1Δ* or *sgs1Δ* with Top3 OE, indicating that in the absence of Uls1, Top3 activity becomes even more important for rescue (Figure 1B). We noted that the rescue observed by deletion of *ULS1* in *sgs1Δ* mutants was consistently more prominent in the presence of HU than MMS, and furthermore, that Top3 OE rescued *sgs1Δ* and *sgs1Δ uls1Δ* mutants to similar degrees on MMS but not on HU. This led us to hypothesize that in the absence of Uls1, Top3 functions independently of its known X-structure resolution activity to provide rescue to *sgs1Δ* mutants on HU. We thus chose to focus our investigation on the role of Top3 in conferring tolerance to HU-induced damage in *sgs1Δ* mutants lacking Uls1.

3.4.2 Rescue of *sgs1Δ* mutants by deletion of *ULS1* is through an accelerated Top3-dependent DNA repair mechanism

Fork stalling by HU causes filamentous growth in which cells continue to replicate their DNA without full cytokinesis and form elongated hyphal structures containing multiple nuclei. In normal *S. cerevisiae* cells, HU-induced filamentous growth occurs in a Mec1/Rad53 dependent manner that is reversible following release from HU [170]. We wondered whether the Top3-dependent damage tolerance conferred by deletion of *ULS1* in *sgs1Δ* mutants was through this pathway. Indeed, we observed a statistically significant decrease in the percentage of cells with aberrant morphology—

defined as clusters of three or more interlinked cells—in *sgs1Δ uls1Δ* compared to *sgs1Δ* mutants following 12 hours of recovery from HU, whereas no difference was observed between *sgs1Δ, sgs1Δ top3Δ* and *sgs1Δ top3Δ uls1Δ* mutants (Figure 2A). These observations support a role for Uls1 and Top3 in alleviating HU-induced filamentous growth

We next wondered whether Top3 and deletion of *ULS1* inhibited the induction of filamentous growth or whether they promoted faster resolution of this phenotype in *sgs1Δ* mutants. To this end, we followed the progression of cell morphology over time in *sgs1Δ*, *sgs1Δ uls1Δ, sgs1Δ top3Δ*, and *sgs1Δ top3Δ uls1Δ* cells exposed to and following recovery from HU. In steady state growth, all cell types had an elevated population of cells in apparent G2/M, typical of DNA repair mutants. The majority of these cells responded to α-factor as if in G1 as evidenced by the large number of "shmoo doublets" (Figure 2B arrows), indicating that most cells had actually completed mitosis at this time point. We found that all genotypes examined entered S-phase in the presence of HU at similar rates, as determined by bud morphology. During the three hours following recovery from HU, all strains accumulated equivalent levels of filamentous growth, with no change in cell number, suggesting that Top3 and deletion of *ULS1* do not prevent filamentous growth in *sgs1Δ* mutants (Figure 2B-2D). However, at 4.5 hours following release from HU, we observed a sudden decrease in the number of filamentous cells in all cell types, with the most dramatic decrease (~two-fold) occurring for *sgs1Δ uls1Δ* (Figure 2B and 1C). These decreases correlated with an equivalent increase in cell number, again with *sgs1Δ uls1Δ* mutants having the most dramatic (two-fold) increase in cell number

(Figure 2D). These increases in cell numbers within this 1.5 hr time frame could not be attributed to growth from the 20-28% of normal cells within the population, indicating that even in the absence of Sgs1, these cells can recover from HU. Importantly, these observations place the activity of Top3 downstream of HU-induced fork stalling, and support a model in which deletion of *ULS1* promotes faster recovery from damage rather than affecting an earlier stage by preventing damage.

3.4.3 Rescue of *sgs1Δ* mutants by deletion of *ULS1* is through Top3-mediated fork restart

Given the dependence of DNA replication stress-induced filamentous growth on Rad53, we speculated that this HU-induced phenotype could be due to cells entering mitosis without completing replication and/or without resolving DNA linkages formed during HR. Previous work has implicated Uls1 activity occurring upstream of recombination intermediate formation [168, 169]; however, it has been well established that Top3 has roles downstream of recombination intermediate formation [50, 65, 83, 131]. The observation that deletion of *ULS1* results in fewer of these filamentous cells over time (Figure 2) prompted us to investigate whether deletion of *ULS1* prevented formation of recombination intermediates or whether it led to their faster resolution. To test this, we performed two-dimensional gel electrophoresis and Southern blotting (2DGE-SB) to compare X-structure levels in *sgsΔ vs sgs1Δ uls1Δ* mutants recovering from HU. No differences in X-structure levels were observed at a fragment adjacent to ARS305, consistent with previous observations of *sgsΔ vs sgs1Δ uls1Δ* mutants exposed to MMS, or within the rDNA on a fragment containing the RFB (Figure 3A-B &

Supplemental Figure 1) [169]. However, there was a reproducible and statistically significant (1.3-fold) increase in large fork structures in the *sgs1Δ uls1Δ* mutants *vs sgs1Δ* mutants recovering from HU in the rDNA fragment (Figures 3A-3B & 4D-4E). To rule out the possibility that deletion of *ULS1* could be stabilizing easily branch migratable X-structures, which might resolve spontaneously during sample preparation and thus be difficult to detect in the assay, we also used psoralen crosslinking of cells to stabilize DNA structures prior to their isolation. Again, we noticed no difference in X-structure levels at a fragment adjacent to ARS305 or within the rDNA fragment, suggesting that they do not accumulate, but we did observe an even larger increase (1.9-fold) in large fork structures in *sgs1Δ uls1Δ* mutants compared to *sgs1Δ* mutants, again only within the rDNA fragment, suggesting that these structures are unstable (Supplemental Figure 2A-2B). Intriguingly, this increase in large fork structures, which we initially interpreted as fork stalling, was also dependent on Top3 activity, as *sgs1Δ uls1Δ top3Δ* mutants consistently had reduced large forks compared to *sgs1Δ uls1Δ* mutants and did not have a statistically significant increase in large forks compared to *sgs1Δ* mutants (Figure 3A-3B). This observation led us to hypothesize that Top3, instead of having its traditional roles downstream of X-structure formation (i.e. in their resolution), could actually be acting upstream, perhaps to stabilize stalled forks and prevent their collapse.

To determine if Top3 was helping to stabilize forks in the absence of Uls1, we measured the amount of breaks at the rDNA locus in cells exposed to HU using a previously published system [171]. In brief, DNA was digested to produce rDNA fragments of 4.6 Kb in length with ~2.3 Kb of sequence on either side of the RFB (Figure 3C). Distinct bands of 3, 2.3 and 2.2 Kb are visualized in this system, the latter two

indicative of broken forks stalled at the RFB, while the origin of the former is not clear [171]. To our surprise, we observed not a decrease, but an increase in RFB-specific breaks in *sgs1Δ uls1Δ* mutants compared to *sgs1Δ* mutants, and this increase in breaks was dependent on Top3 (Figure 3C-D). As breaks during S-phase are predominantly repaired *via* HR mechanisms, this new observation suggests a requirement for HR machinery for *uls1Δ*-mediated rescue of *sgs1Δ* mutants. Although this requirement has previously been shown, the HR mechanism utilized was not immediately apparent, as no difference in X-structure levels was observed upon 2DGE analysis [169, 172]. This led us to investigate whether the replication intermediates migrating as apparent large stalled forks were indeed stalled forks or another species that might be HR-dependent.

3.4.4 Rescue of *sgs1* mutants by deletion of *ULS1* is through HR-mediated fork restart

To determine the biochemical nature of these structures, we incubated our samples in branch migration buffer between the first and second dimensions of 2DGE. HJs and reversed forks are known to form antiparallel stacked-X structures in the presence of Mg^{2+}, which greatly impedes branch migration, while hemicatenanes and Rec-Xs are able to branch migrate to similar degrees with or without Mg^{2+} [60, 64]. The HU-induced replication intermediates migrating with mobilities that had led us to interpret them initially as “large stalled forks” under control conditions, were able to branch migrate in the absence of Mg^{2+}, which would not be expected for a stalled fork, and furthermore were able to branch migrate even more so in the presence of Mg^{2+}, indicating a different structure entirely. Interestingly, branch migration occurred in two

directions, either forming two linear products, or branch migrating up and off the arc into a cone (Figure 4A-B). Reversed forks have been shown to migrate within this cone shape, however, reversed forks are bona fide HJs and should not be able to be resolved into linear fragments in the presence of Mg^{2+} (Figure 4C) [46]. Instead, we propose that these structures are D-loops. Like Rec-Xs, D-loops exist in an open conformation, that cannot isomerize into a stacked X configuration, making them resistant to Mg^{2+} entrapment. Branch migration of a D-loop will either lead to linearized fragments, corresponding in size to the full length intact sister chromatid and the smaller broken sister, or to a bulky not fully replicated 5 or 4-way junction (Figure 4A-B). Indeed we see two distinct linear fragments derived from the RFB, one that runs as a full length fragment (spot b in Figure 4A), and one that runs smaller (spot c in Figure 4A) and likely represents a newly invaded D-loop at the RFB that has not undergone any synthesis. In addition to these fragments, we also observed another branch migration derived spot that runs as a full length fragment (spot a in Figure 4A), with a smear down to spot c. We interpret these signals as linear fragments derived from D-loops that have been extended *via* DNA synthesis to different extents, and under untreated conditions migrate as "large stalled forks". Lastly, we see the appearance of a cone that hyperextends off of the arc, past the upper mobility limit of the X-spike seen in the untreated cells, and thus likely represents these not fully replicated 4 and 5-way branch migration intermediates, the latter that we would predict to be bulkier than a classic HJ and thus have slower mobility in the second dimension. No larger species are seen branch migrated from the RFB, which is in line with our assessment that the D-loops at this stage have not been extended, and thus likely branch migrate to linear fragments quickly.

To further characterize these species, we treated our samples with the single strand specific nuclease, mung bean nuclease (MBN). D-loops have regions of single stranded DNA and should be sensitive to MBN while reversed forks should be resistant. Indeed, "large stalled forks" in *sgs1* mutants exposed to HU are sensitive to MBN (Supplemental Figure 3). Furthermore, despite their potentially bulky nature, D-loops have been shown previously to migrate along the replication arc in 2DGE performed in fission yeast [63]. That these structures are D-loops is also consistent with the observation that they were more prominent in *sgs1Δ uls1Δ* mutants following crosslinking. As D-loops contain only one invading end, they do not have the stability of a complete HJ or Rec-X, and could largely dissociate into linear products during the DNA extraction process. Furthermore, we point out that the rDNA RFB creates a natural concentration of stalled events leading to D-loops at defined points, which makes it possible to observe the roles for Sgs1 and Uls1 in HU-exacerbated fork stalls.

We next sought to determine whether these D-loops arose from the same or different HR repair pathways. While all HR repair pathways require Rad52, Rad51 is required only for GC and some forms of template switching, while being dispensable for BIR and single-strand annealing (SSA) [8, 23, 27, 173]. We compared HU-induced replication intermediates in *sgs1Δ* and *sgs1Δ uls1Δ* strains to HU-induced replication intermediates in *sgs1Δ rad51Δ* and *sgs1Δ uls1Δ rad51Δ* strains, and found that D-loops were Rad51-dependent specifically in the *sgs1Δ uls1Δ* strains but not in the *sgs1Δ* strains (Figure 4D-F). That *sgs1Δ* mutants have Rad51-independent D-loops is consistent with previous reports showing increased rates of BIR in *sgs1Δ* mutants [28, 37]. Intriguingly, and as detailed in the *Discussion*, deletion of *ULS1* seems to result in a

switch of repair pathway choice, channeling repair of rDNA away from a Rad51-independent pathway into a Rad51-dependent pathway.

3.4.5 Suppression of aberrant rDNA recombination by *ULS1* deletion occurs upstream of HR pathway choice

A reliance on Rad51-dependent D-loops in the absence of Uls1 might seem contradictory to the previous demonstration that deletion of *ULS1* reduces recombination rates in the rDNA in *sgs1Δ* mutants [169]. However, such rates were measured by loss of a marker inserted into one of the tandem rDNA repeats, which reflects recombination errors and not necessarily overall HR efficiency. At the rDNA, we can envision marker loss to be reduced through four different mechanisms: 1) reduction in breaks within the rDNA, allowing fewer opportunities for recombination, 2) promotion of non-homologous end joining (NHEJ) following a break, 3) promotion of non-crossover pathways following formation of a dHJ (e.g. *via* STR-mediated dissolution), or 4) promoting recombination through error-free HR pathways over error-prone ones (e.g. *via* restriction of the type of break, and thus prevention of broken ends that would feed into error-prone HR pathways such as SSA or BIR). Our observation that *sgs1Δ uls1Δ* mutants have more breaks within the rDNA than *sgs1Δ* eliminates the first possibility. Previously published data showed that rescue of *sgs1Δ* mutants by deletion of *ULS1* requires HR [169], and we also confirm here that this rescue is independent of NHEJ machinery (Figure 5A), eliminating option 2. To determine whether deletion of *ULS1* could affect recombination rates in *sgs1Δ* mutants following dHJ formation, we implemented a crossover assay utilizing an induced site-specific DSB, where homology exists on either side of the break

and thus repair by GC dominates with dHJs as intermediates. In this assay, deletion of *ULS1* did not alter crossover rates in *sgs1Δ* mutants (Figure 5B). Furthermore, in a system in which a DSB was induced and GC could be followed over time[56], *sgs1Δ* and *sgs1Δ uls1Δ* mutants again had no difference in crossover rates and also had similar rates of repair (Figure 5C & data not shown). That deletion of *ULS* has no effect on crossover rates following dHJ formation, and actually leads to more specific DSBs in the rDNA, strongly supports the fourth option: that reduced marker loss in the rDNA of *sgs1Δ* mutants results from the promotion of specific error-free HR pathways. Importantly, the type of break utilized in our assays does not fully recapitulate repair of a break during replication, as the homology on both sides precludes the use of BIR or SSA mechanisms (the former of which can occur following replication encounter of a nicked template), and indeed, we speculate that specific cleavage of the replication fork itself could be the mechanism by which deletion of *ULS1* confers resistance to *sgs1Δ* mutants on HU. We propose that in the absence of Uls1, stalled forks are stabilized potentially through a sumoylated target of Uls1, thus allowing for accurate enzymatic cleavage and strand invasion *via* an error-free HR pathway (e.g. GC), limiting the need for extensive end processing and a homology search required for error-prone pathways such as BIR and SSA. This activity would be particularly beneficial at the tandemly repeated rDNA locus, where if allowed to break at random, rDNA repeats could recombine with each other, leading to deleterious expansions or contractions of the repeat array.

3.4.6 Rescue of *sgs1Δ* by deletion of *ULS1* is dependent on Mms21 SUMO ligase activity

Uls1 has predicted STUbL activity [174], and so (as hinted above) we hypothesized that it might normally function by ubiquitinating sumoylated proteins and targeting them for proteasomal degradation following DNA repair. Thus, in the absence of Uls1, a subset of DNA repair proteins might remain that could provide benefit in the absence of Sgs1. We reasoned that if the damage tolerance in *sgs1Δ* mutants observed with deletion of Uls1 was due to the persistence of a sumoylated DNA repair protein, then removing the SUMO ligase responsible for that modification would eliminate the sumoylated form of that protein, and consequently abrogate any benefit from deletion of *ULS1*. *S. cerevisiae* only have three SUMO ligases, Mms21, Siz1, and Siz2, and so we determined whether any were required for rescue of *sgs1Δ* mutants in the absence of Uls1. Interestingly, we found that deletion of *ULS1* not only was unable to confer damage tolerance to *sgs1Δ mms21-sp* mutants, in which the SUMO ligase domain is defective, on HU and MMS, but the combined deletion of *ULS1* with *mms21-sp* resulted in a slow growth phenotype on rich media (Figure 6 and Supplemental Figure 4). This interaction was specific to Mms21 and not representative of all SUMO ligases, as deletion of the two other *S. cerevisiae* SUMO ligases, Siz1 and Siz2 did not abrogate rescue of *sgs1Δ* mutants by *ULS1* deletion (Figure 6). In addition to being a SUMO ligase, Mms21 is also part of the Smc5/6 complex, which has important roles in DNA replication and repair and has close interactions with the STR complex [44, 82, 83, 175]. Recently, Mms21 was shown to sumoylate Top3 [82, 83], and so these observations raise the possibility that

sumoylation of Top3 or another target of Mms21 sumoylation could be assisting Top3 in providing rescue to *sgs1Δ* mutants in the absence of Uls1.

3.5 Discussion

Although roles for Top3 downstream of recombination intermediate formation are well documented, the mechanisms by which Top3 can act prior to recombination intermediate formation are not fully understood. Hints that Top3 has roles outside of post replicative repair come from studies showing that Top3 levels go up in S-phase, and that *top3* mutants are defective in the intra S-phase checkpoint [138, 176]. Indeed, Top3 has known Sgs1-dependent functions prior to recombination intermediate formation including stabilizing polymerases at stalled replication forks, and 5'-3' end resection, but whether it functions independently at earlier steps of HR repair is not known [16, 78, 88]. Here, we provide novel evidence supporting a Sgs1-independent role for Top3 in fork processing and restart. We show that in the absence of Sgs1 and Uls1, Top3 enhances the induction of site specific breaks and subsequent increase in D-loop formation within the rDNA to restart stalled replication forks. We further show that restart of HU-induced fork stalling occurs primarily through a break-induced D-loop intermediate, and not *via* a fork reversal mechanism. Importantly, deletion of *ULS1* alters the genetic requirements for this D-loop formation, resulting in a switch from Rad51-independent D-loops in *sgs1Δ* mutants to Rad51-dependent D-loops in *sgs1Δ uls1Δ* mutants.

How then, might this repair pathway switch confer resistance to HU in *sgs1* mutants? We hypothesize that in the absence of Sgs1, forks become compromised (possibly as a consequence of replisome destabilization) and break, resulting in collapse

of one strand or, as depicted, both the leading and lagging strands (Figure 7A-B). Repair of the lagging strand template would need to occur through SSA (Figure 7C-D), while the leading strand could reinvade *via* BIR (Figure E-F). Both of these processes can lead to a loss of repeats within the rDNA, with BIR becoming particularly problematic in the context of HU, as more ssDNA is available, allowing for more opportunities for Rad51-independent strand annealing, leading to an even further loss of repeats. Deletion of *ULS1* leads (directly or indirectly) to stabilization of replication forks, specifically at the rDNA RFB. We propose that Top3 aids in this stabilization by rewinding exposed ssDNA (i.e. using its strand passage activity to reanneal strands), preventing aberrant fork collapse, and subsequent homology search (Figure 7G-K). Forks in this context are cleaved specifically at the rDNA RFB (Figure 7L). The structure specific endonuclease Mus81-Mms4 is a likely candidate for this role as *uls1Δ mus81Δ* double mutants have known synergistic sensitivity to DNA damaging agents and a delay in S-phase completion following MMS-induced damage [168]. Furthermore, Mus81-Mms4 has been shown *in vitro* to cleave fork structures in such a way as to leave a 5' flap on the leading strand template, and a single strand gap on the lagging strand template, a discontinuity that could potentially favor a GC fork restart event over BIR [40, 163]. Confirmation that *uls1Δ mus81Δ* double mutants do indeed have an increase in stalled, unbroken forks would further support this mechanism. Following cleavage by Mus81-Mms4 (or an alternative endonuclease), Rad51-mediated GC can initiate to restart the fork (Figure 7M-N). The distinction between GC and BIR is an important one, as BIR can not only lead to loss of repeats, but can also trigger extensive template switching leading to increased mutagenesis [32, 33]. Furthermore, the switch from a Rad51-independent repair pathway

to a Rad51-dependent pathway is also important as Rad51 has been shown to displace Rad52-RPA filaments from ssDNA, a function that would like inhibit SSA events [17]. Consequently, deletion of *ULS1* in *sgs1Δ* mutants results in a switch from an error-prone HR fork restart pathway to a relatively error-free one. Interestingly, initiation of DNA synthesis following BIR is significantly delayed compared to synthesis following GC (4 hrs vs 30 min) [28], and we speculate that this difference could account for the observed delay in recovery from HU-induced filamentous growth in *sgs1Δ vs sgs1Δ uls1Δ* mutants (Figure 2B). Thus, deletion of *ULS1* could be providing benefit to *sgs1Δ* mutants *via* two means: 1) by accelerating the onset of DNA synthesis following acute damage, and 2) by inhibiting mutagenic DNA synthesis during chronic exposure to HU. Finally, based on observations showing a lack of X-structure accumulation in *sgs1Δ* mutants exposed to HU, we hypothesize that most fork restart events get channeled through a synthesis dependent strand annealing pathway (Figure 6O-P) rather than through formation and resolution of a dHJ intermediate. In the future, it will be interesting to address how Top3 aids in this process, whether it can diminish levels of ssDNA at a replication fork or if it cooperates with Mus81-Mms4 or some other endonuclease in fork processing.

Recently it was shown that Top3 can also be sumoylated in an Mms21-specific manner [82, 83], and thus, the possibility that Top3 becomes hypersumoylated in the absence of Uls1 could be the defining characteristic that allows Top3 to function independently of Sgs1 during HR-mediated fork restart. Curiously, Top3 sumoylation is dependent on the presence of Sgs1, but whether this loss of sumoylated Top3 seen in *sgs1Δ* mutants is due to an inability to be sumoylated by Mms21 or whether it results from a rapid turnover of sumoylated Top3 *via* Uls1-dependent ubiquitination and

proteosomal degradation has not been explored [83]. That sumoylation of Top3 might be required specifically for its fork restart activity and not for recombination intermediate resolution is particularly intriguing as overexpression of Top3 in the presence of Uls1, while previously shown to provide rescue to *sgs1Δ* mutants on MMS *via* Rec-X resolution, is not able to confer any resistance to *sgs1Δ* mutants on HU, where stalled fork are the primary lesion ([50] and data presented here). In contrast, deleting *ULS1* does allow Top3 to provide rescue to *sgs1Δ* mutants on HU, but only has a modest effect in the context of MMS. HU and MMS are often used interchangeably in experiments, and although they both can lead to stalled forks and single strand gaps as detected by EM, different repair pathways clearly dominate in each. This is most evident *via* 2DGE-SB analyses in *sgs1Δ* mutants, which clearly show that MMS induces Rec-X mediated repair, while HU induces repair *via* fork restart ([14, 46, 50, 165] and data presented here). These observations strongly support two context-specific roles for Top3 in DNA repair: sumoylation-independent functions involving Rec-X resolution, and sumoylation-dependent functions involving replication fork restart. Interestingly, while the benefit of *ULS1* deletion to *sgs1Δ* mutants on MMS is modest, it becomes much more noticeable in a *smc5/6*-deficient background (Appendix Figure 2B). Why a *smc5/6*-deficient background allows deletion of *ULS1* to provide rescue to *sgs1Δ* mutants could be explained by differences in primary DNA repair responses to HU and MMS. Very few DNA breaks occur in yeast following MMS treatment [13], and we hypothesize that this might be due in large part to the Smc5/6 complex stabilizing stalled forks, thereby limiting their collapse and promoting Rec-X mediated repair. Indeed, the Smc5/6 complex is known to associate with replicating DNA particularly at regions with

unidirectional replication (e.g. the rDNA and telomeres), and studies in *S. pombe* support its role in Rad52-dependent fork stabilization [177, 178]. Therefore, in the absence of a fully functional Smc5/6 complex, we would predict more fork collapse during MMS treatment, which would create a setting in which deletion of *ULS1* becomes beneficial.

These findings provide new insight into a mechanism regulating repair pathway choice to restart stalled forks, and suggest a novel role for Top3, independent of its complex members, in mediating DNA repair at a stalled fork, though we cannot rule out the possibility that the presence of Sgs1 and Rmi1 could aid in this process. In the future, it will be interesting to investigate how Top3 functions at a stalled fork, whether it rewinds ssDNA, acts directly with an endonuclease, or both to restart a fork. Furthermore, determining whether sumoylation of Top3 is affected in the absence of Uls1, and whether constitutively sumoylated Top3 alone is enough to confer HU resistance in *sgs1Δ* mutants will help clarify this rescue mechanism. Numerous DNA repair proteins are sumoylated in an Mms21-dependent manner in response to DNA damage so it is likely that the mechanism of rescue *via ULS1* deletion is much more complex than presented here. Ultimately, identifying these factors and understanding how they contribute to fork restart will further enhance our understanding of the complexity of DNA repair, and may shed light on alternative factors contributing to repair pathway choice.

3.6 Figure Legends

Figure 3.1: Rescue of *sgs1Δ* mutants by deletion of *ULS1* is dependent on Top3. (**A**) Spot assay comparing the effects of MMS and HU on growth of *sgs1Δ, sgs1Δ uls1Δ,*

sgs1Δ top3Δ, sgs1Δ top3Δ uls1Δ, sgs1Δ rmi1Δ, and sgs1Δ rmi1Δ uls1Δ mutants. (**B**) Spot assay comparing the effects of MMS and HU on growth of *sgs1Δ,* and *sgs1Δ uls1Δ* with or without a *TOP3* overexpression plasmid.

Figure 3.2: Deletion of *ULS1* accelerates the repair process following HU-induced damage in *sgs1Δ* mutants. (**A**) Quantification of the proportion of cells with aberrant morphology in *sgs1Δ, sgs1Δ uls1Δ, sgs1Δ top3Δ,* and *sgs1Δ top3Δ uls1Δ* mutants following 12 hours of recovery from 200mM HU treatment. 407 (*sgs1Δ),* 922 (*sgs1Δ uls1Δ),* 360 (*sgs1Δ top3Δ*), and 625 (*sgs1Δ top3Δ uls1Δ*) cells were counted for each genotype. p-values calculated using Fisher's exact test; ***p*-value = 0.0019. (**B**) Light microscopy images showing HU-induced filamentous growth in *sgs1Δ, sgs1Δ uls1Δ, sgs1Δ top3Δ,* and *sgs1Δ top3Δ uls1* mutants over time. Arrows point to "G1-doublets". (**C**) Quantification of the percentage of aberrant cells in *sgs1Δ, sgs1Δ uls1Δ, sgs1Δ top3Δ,* and *sgs1Δ top3Δ uls1Δ* mutants. (**D**) Quantification of intact cells (*not nuclei)* for genotypes listed in (**C**) over time.

Figure 3.3: Deletion of ULS1 increases species that run as stalled forks in *sgs1Δ* mutants in a Top3-dependent manner. (**A**) Representative 2DGE-SB examining replication intermediates that accumulate in *sgs1Δ, sgs1Δ uls1Δ,* and *sgs1Δ top3Δ uls1Δ* mutants, 1 hour after HU treatment, and 2 hrs following release from HU. An rDNA fragment containing the RFB is shown. (**B**) Quantification of X-structures relative to small arc (*left*) and RFB relative to small arc (*right*). *n*=2, and error bars represent standard deviation;**p*-value= 0.04. (**C**) (*Left*) schematic depicting RFB in relation to sites of restriction enzyme digest and *in vivo* break site. (*Right*) one dimensional gel-SB

examining breaks at the rDNA replication fork block in WT and *sgs1Δ, sgs1Δ uls1Δ,* and *sgs1Δ top3Δ uls1Δ* mutants. (**D**) Quantification of (**C**): Broken fragments (2.3KB) were normalized by dividing over the intact locus fragment (4.6KB). *n*=2, and error bars represent standard deviation.

Figure 3.4: Structures running as large forks are Rad51-dependent D-loops. (**A**) (*Top*) Schematic of replication intermediates following 2DGE-SB under untreated (control) and branch migratable conditions (+BMB) following the first dimension. (*Bottom*) representative 2DGE-SB examining replication intermediates in *sgs1Δ* and *sgs1Δ uls1Δ* mutants untreated (*left column*), or branch migrated in the absence (*middle column*) or presence of Mg^{2+} (*right column*) following the first dimension. Arrows point to linearized branch migrated products. Brackets indicate limited mobility branch migrated products. (**B**) Schematic of D-loop branch migration intermediates and corresponding gel migration patterns on a 2DGE-SB. D-loops utilized to restart a stalled fork will migrate similarly to forks. In the presence of branch migration buffer, these D-loops can either branch migrate into two linearized products (*bottom right*), or into incompletely replicated 5 and 4 ended structures with limited mobility (*top middle* and *top right* diagrams respectively). (**C**) Schematic of reversed fork branch migration in the presence or absence of Mg^{2+}. In the absence of Mg^{2+}, reversed forks will first migrate up into a four-way junction and eventually into linearized products (*bottom* images); however, in the presence of Mg^{2+}, reversed forks will be converted to the immobile antiparallel stacked-X structure, and will not be able to branch migrate into linearized fragments. (**D**) Representative 2DGE-SB examining replication intermediates in *sgs1Δ,*

sgs1Δ rad51Δ, sgs1Δ uls1Δ and *sgs1Δ uls1Δ rad51Δ* mutants exposed to 200mM HU for 1 hour and following 45 minutes after release from HU. An rDNA fragment containing the replication fork block is shown. (**E**) Quantification of D. *n*=2, and error bars represent standard deviation; **p*-value ≤ 0.05.

Figure 3.5: Deletion of ULS1 does not affect crossover rates during DSBR in *sgs1Δ* mutants. (A) Spot assay comparing the effects of HU on growth of *sgs1Δ lig4Δ, sgs1Δ lig4Δ uls1Δ, sgs1Δ yku70Δ, sgs1Δ yku70Δ uls1Δ, sgs1Δ yku80Δ,* and *sgs1Δ yku80Δ uls1Δ*. B) *sgs1Δ* and *sgs1Δ uls1Δ* mutants were transformed with the *ADE2* cassette and ratios of crossovers to total are shown on the Y-axis. *n*=4, error bars represent standard deviation C) HO endonuclease was induced in *sgs1Δ* and *sgs1Δ uls1Δ* mutants with galactose and ratios of crossovers to total were determined 6 hours after induction (all repair events) and in single colonies following 3 days of growth (viable events). Three independent experiments were performed for calculating crossovers at 6 hours. A representative experiment is shown (*left*). 152 single colonies from *sgs1Δ* and 149 single colonies from *sgs1Δ uls1Δ* were compared to calculate viable crossover events following repair of the HO inducible DSB (*right*). *p*-values calculated using Fisher exact test.

Figure 3.6: Rescue of *sgs1Δ* mutants by deletion of ULS1 is dependent on SUMO ligase Mms21. Spot assay comparing the effects of MMS and HU on growth of *sgs1Δ, sgs1Δ uls1Δ, siz1Δ sgs1Δ, siz1Δ sgs1Δ uls1Δ, siz2Δ sgs1Δ, siz2Δ sgs1Δ uls1Δ, mms21-sp sgs1Δ*, and *mms21-sp sgs1Δ uls1Δ* mutants.

Figure 3.7: Schematic of Replication fork restart following HU-induced damage. (**A-F**) Model for replication fork restart in *sgs1Δ* mutants. (**A**) HU induces replisome uncoupling, leading to long stretches of ssDNA at the fork. (**B**) In the absence of Sgs1, forks become unstable, leading to breaks on both template strands, (**C**) followed by limited 5' end resection of the lagging strand, which allows for (**D-E**) recombination of the lagging strand *via* SSA. (**F**) The leading strand can then reinvade the newly repaired lagging strand, *via* BIR to reestablish the fork. (**G-P**) Model for replication fork restart in *sgs1Δ uls1Δ* mutants. (**G**) In the absence of Uls1, Top3 recognizes and binds the ssDNA at the fork, and (**H-K**) reduces negative supercoiling at the fork by making transient nicks in one strand and mediating strand passage to rewind the fork. (**L**) This provides an ideal substrate for an endonuclease to cleave the fork, (**M-N**) allowing for Rad51-mediated HR, and (**O-P**) subsequent synthesis dependent strand annealing to reestablish the fork.

3.7 Supplemental Figure Legends

Supplemental Figure 3.1: Deletion of *ULS1* does not alter abundance of HU-induced replication intermediates in *sgs1Δ* mutants at a region adjacent to ARS305. Representative 2DGE-SB examining replication intermediates at a region adjacent to ARS305 in *sgs1Δ*, *sgs1Δ uls1Δ*, and *sgs1Δ top3Δ uls1Δ* mutants exposed to 200mM HU for 1 hour and 2 hrs following recovery.

Supplemental Figure 3.2: Deletion of *ULS1* leads to increased structures migrating as stalled forks in *sgs1Δ* mutants. (**A**) Representative 2DGE-SB examining replication intermediates in *sgs1Δ* and *sgs1Δ uls1Δ* mutants exposed to 200mM HU for 1 hour. Cells

were psoralen crosslinked *in vivo* prior to DNA extraction. (**B**) Quantification of A. *n*=2; error bars represent standard deviation; *p*-value=0.02.

Supplemental Figure 3.3: HU-induced structures, migrating as stalled forks are sensitive to MBN. *sgs1Δ* mutants were either untreated or treated with MBN prior to 2DGE-SB analysis.

Supplemental Figure 3.4: *mms21-sp uls1Δ* double mutants are synthetically sick. Spot assay comparing the effects of MMS and HU on growth of *siz1Δ, siz1Δ uls1Δ, siz2Δ, siz2Δ uls1Δ, mms21-sp,* and *mms21-sp uls1Δ* mutants.

Table 3.1

YB352	sgs1Δ::HIS3, mat a
YB778	sgs1Δ::HIS3, uls1Δ::G418, mat a
YB314	sgs1Δ::HIS3, top3Δ::CaURA, mat a
YB318	sgs1Δ::HIS3, uls1Δ::G418, top3Δ::CaURA, mat a
YB852	sgs1Δ::HIS3, rmi1Δ::Ura3, mat a
YB853	sgs1Δ::HIS3, uls1Δ::G418, rmi1Δ::Ura3, mat a
YB310	sgs1Δ::HYG + 415-gpd-ccdB
YB311	sgs1Δ::HYG + 415-gpd-Top3
YB557	sgs1Δ::HYG, uls1Δ::G418 + 415-gpd-ccdB mat a
YB558	sgs1Δ::HYG, uls1Δ::G418 + 415-gpd-Top3 mat a
YB653	sgs1Δ::HIS3, bar1Δ::NAT, mat a
YB621	uls1Δ::G418, sgs1Δ::HIS3, bar1Δ::NAT, mat a
YB633	sgs1Δ::HIS3, top3Δ::CaURA, uls1Δ::G418, bar1Δ::NAT, mat a
YB89	sgs1::leu,bar1::kan,rad51::HYG, Mat a
YB818	sgs1::Leu, uls1::Ura, bar1::G418, rad51::HYG, mat a
YB533	mms21-sp::URA3 cir0, mat a
YB534	mms21-sp::URA3, uls1Δ::HYG cir0, mat a
YB535	mms21-sp::URA3,sgs1Δ::HIS3 cir0, mat a
YB536	mms21-sp::URA3,sgs1Δ::HIS3, uls1Δ::HYG cir0, mat a
YB143	siz1Δ::HYG, mat a
YB325	uls1Δ::G418, siz1Δ::HYG, mat a
YB142	siz1Δ::HYG, sgs1Δ::HIS3, mat a
YB323	sgs1Δ::HIS3, uls1Δ::G418, siz1Δ::HYG, mat a
YB665	siz2Δ::LEU2, mat α
YB667	siz2Δ::LEU2, uls1Δ::HYG, mat α
YB669	siz2Δ::LEU2, sgs1Δ::HIS3, mat α
YB671	siz2Δ::LEU2, sgs1Δ::HIS3, uls1Δ::HYG, mat α

Figure 3.1A-B

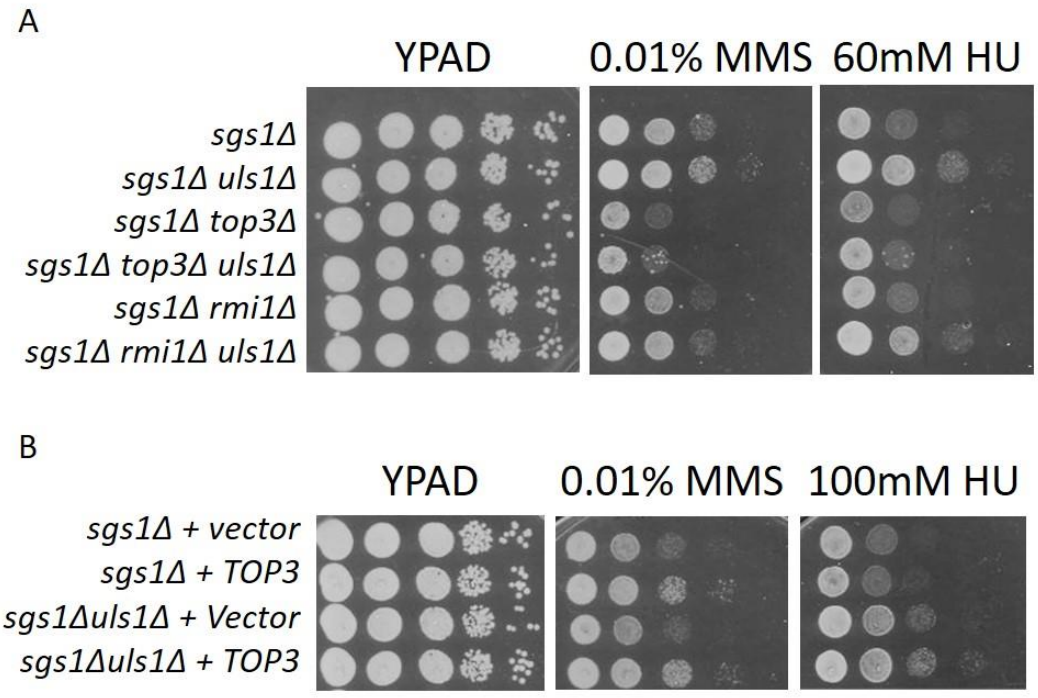
A
YPAD
0.01% MMS
60mM HU
sgs1Δ
sgs1Δ uls1Δ
sgs1Δ top3Δ
sgs1Δ top3Δ uls1Δ
sgs1Δ rmi1Δ
sgs1Δ rmi1Δ uls1Δ
B
YPAD
0.01% MMS
100mM HU
sgs1Δ + vector
sgs1Δ + TOP3
sgs1Δuls1Δ + Vector
sgs1Δuls1Δ + TOP3

Figure 3.2A-D

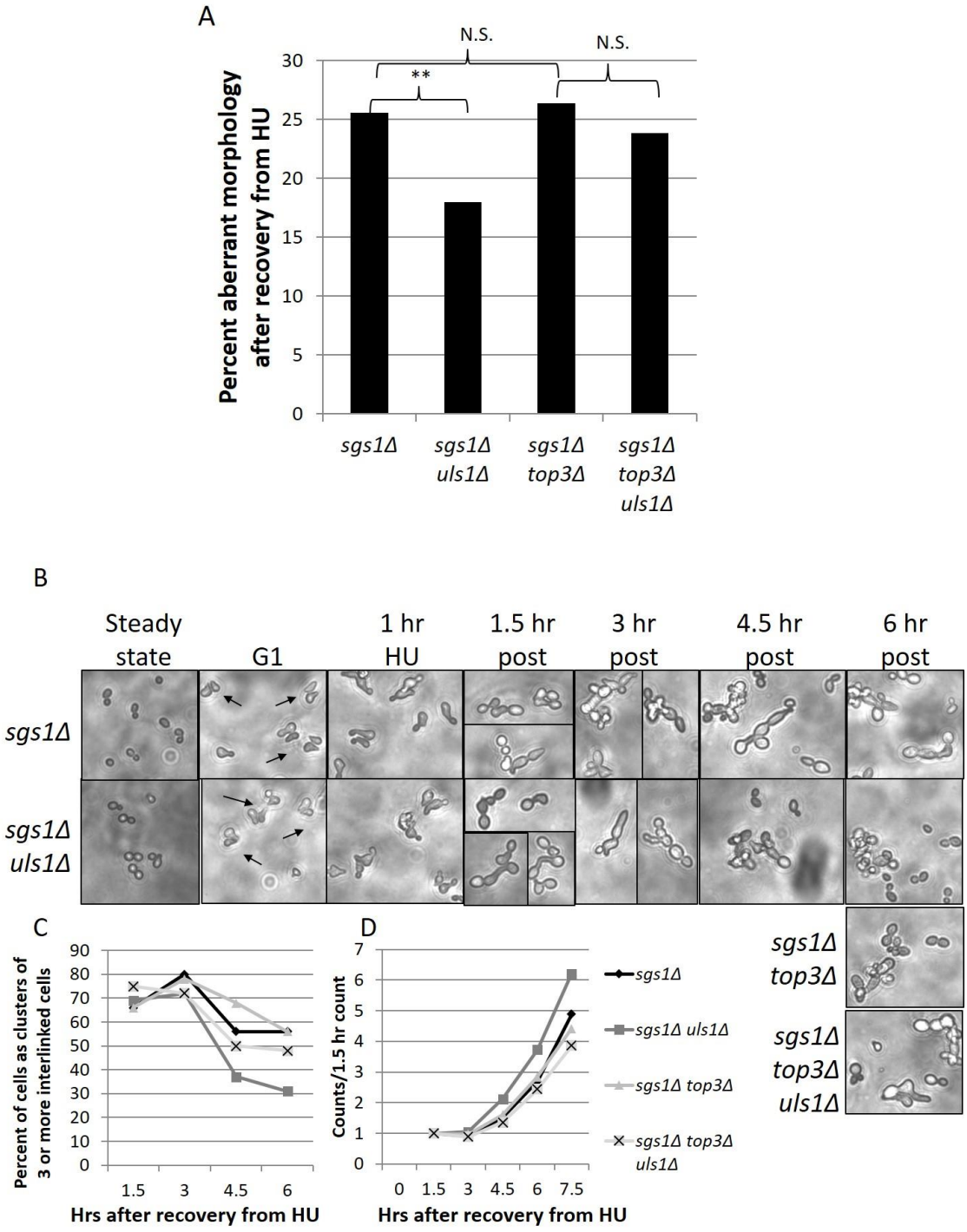
A
N.S.
N.S.
**
Percent aberrant morphology after recovery from HU
30
25
20
15
10
5
0
sgs1Δ
sgs1Δ uls1Δ
sgs1Δ top3Δ
sgs1Δ top3Δ uls1Δ
B
Steady state
G1
1 hr HU
1.5 hr post
3 hr post
4.5 hr post
6 hr post
sgs1Δ
sgs1Δ uls1Δ
sgs1Δ top3Δ
sgs1Δ top3Δ uls1Δ
C
Percent of cells as clusters of 3 or more interlinked cells
90
80
70
60
50
40
30
20
10
0
1.5
3
4.5
6
Hrs after recovery from HU
D
Counts/1.5 hr count
7
6
5
4
3
2
1
0
0
1.5
3
4.5
6
7.5
Hrs after recovery from HU
sgs1Δ
sgs1Δ uls1Δ
sgs1Δ top3Δ
sgs1Δ top3Δ uls1Δ

Figure 3.3A-D

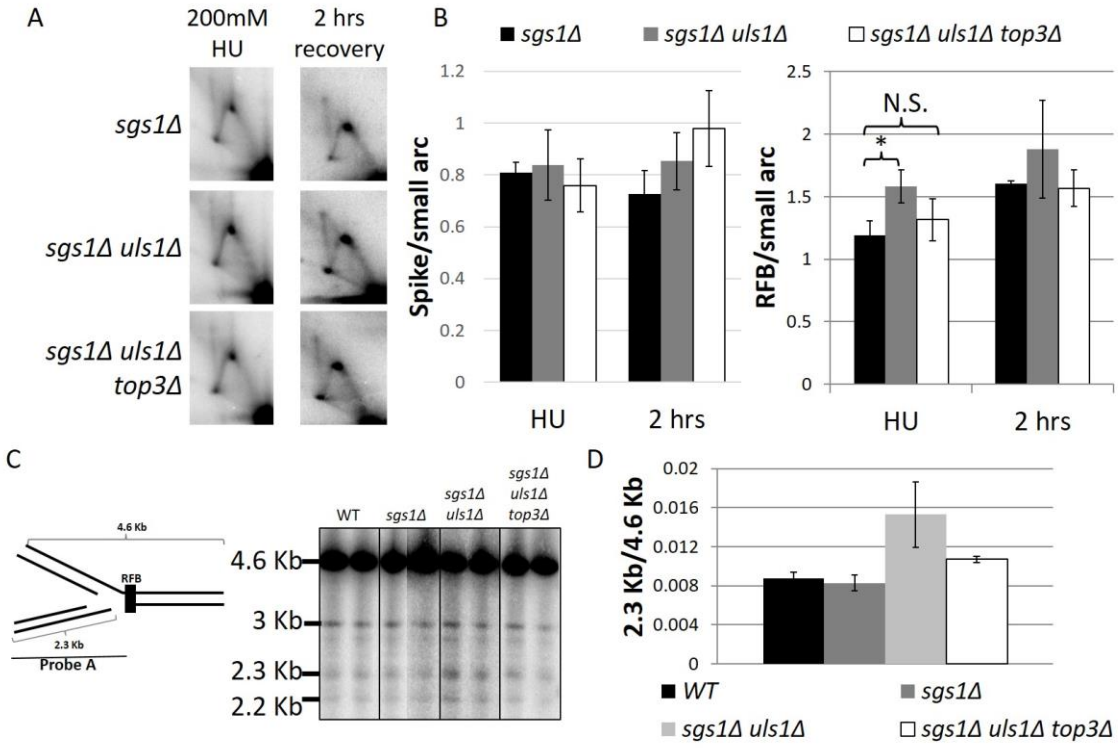
A
200mM HU
2 hrs recovery
sgs1Δ
sgs1Δ uls1Δ
sgs1Δ uls1Δ top3Δ
B
sgs1Δ
sgs1Δ uls1Δ
sgs1Δ uls1Δ top3Δ
Spike/small arc
RFB/small arc
N.S.
*
HU
2 hrs
C
4.6 Kb
RFB
2.3 Kb
Probe A
WT
sgs1Δ
sgs1Δ uls1Δ
sgs1Δ uls1Δ top3Δ
4.6 Kb
3 Kb
2.3 Kb
2.2 Kb
D
2.3 Kb/4.6 Kb
WT
sgs1Δ
sgs1Δ uls1Δ
sgs1Δ uls1Δ top3Δ

Figure 3.4A-C

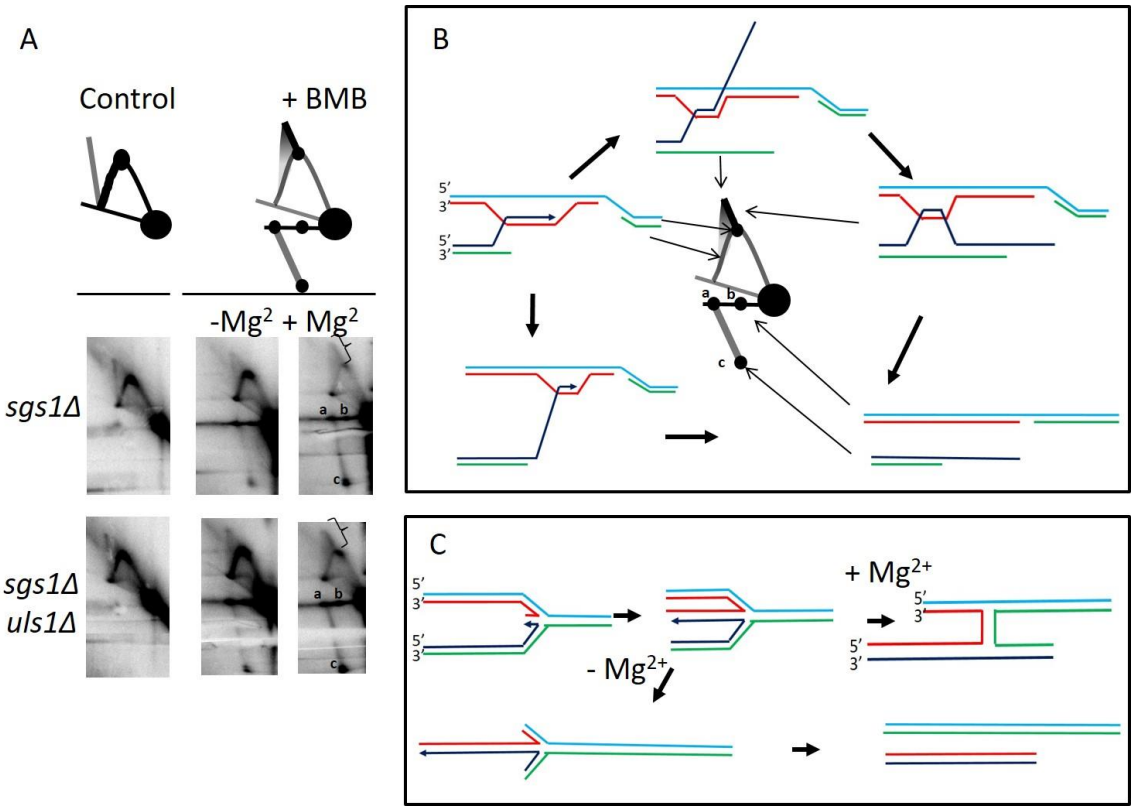
A
Control
+ BMB
-Mg2 + Mg2
sgs1Δ
sgs1Δ
uls1Δ
a b
c
B
5′
3′
5′
3′
a b
c
C
5′
3′
5′
3′
- Mg2+
+ Mg2+
5′
3′
5′
3′

Figure 3.4D-E

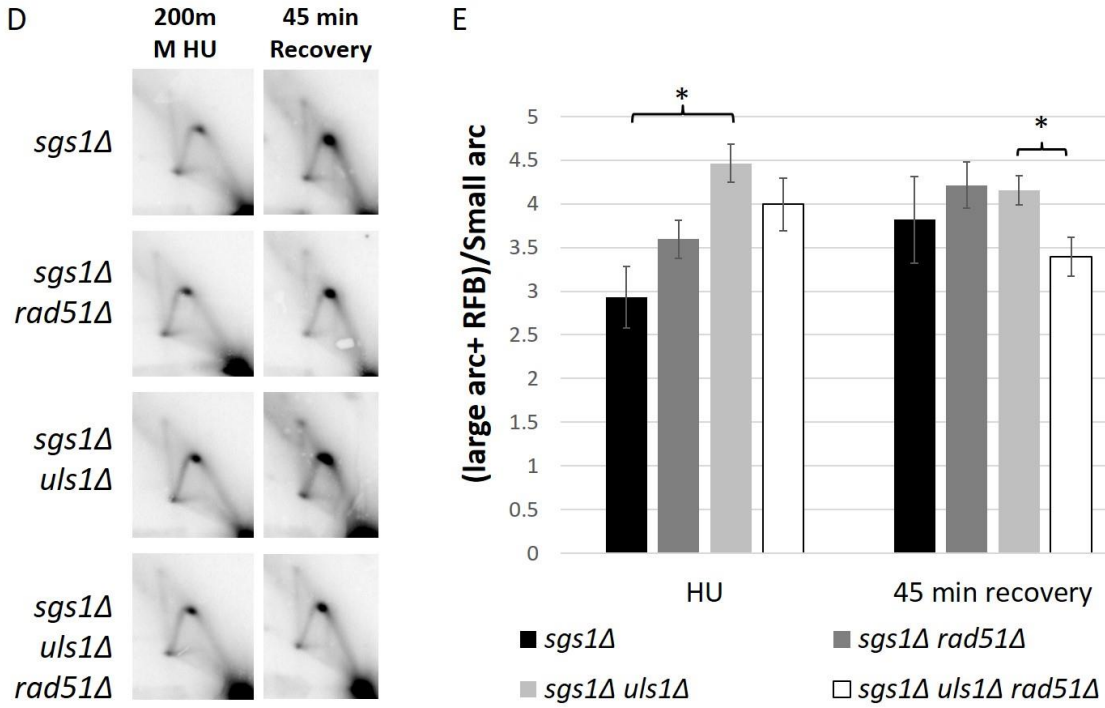
D
200m M HU
45 min Recovery
sgs1Δ
sgs1Δ rad51Δ
sgs1Δ uls1Δ
sgs1Δ uls1Δ rad51Δ
E
(large arc+ RFB)/Small arc
5
4.5
4
3.5
3
2.5
2
1.5
1
0.5
0
*
*
HU
45 min recovery
sgs1Δ
sgs1Δ rad51Δ
sgs1Δ uls1Δ
sgs1Δ uls1Δ rad51Δ

Figure 3.5A-C

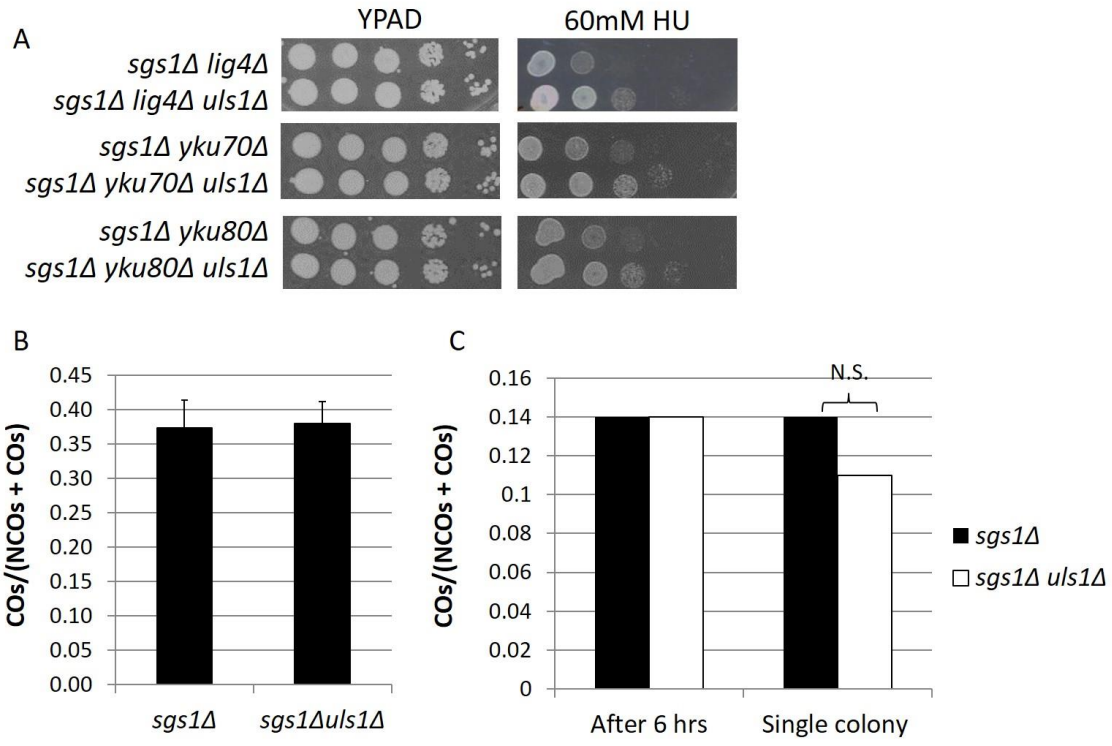
A
YPAD
60mM HU
sgs1Δ lig4Δ
sgs1Δ lig4Δ uls1Δ
sgs1Δ yku70Δ
sgs1Δ yku70Δ uls1Δ
sgs1Δ yku80Δ
sgs1Δ yku80Δ uls1Δ
B
COs/(NCOs + COs)
0.45
0.40
0.35
0.30
0.25
0.20
0.15
0.10
0.05
0.00
sgs1Δ
sgs1Δuls1Δ
C
COs/(NCOs + COs)
0.16
0.14
0.12
0.1
0.08
0.06
0.04
0.02
0
N.S.
After 6 hrs
Single colony
sgs1Δ
sgs1Δ uls1Δ

Figure 3.6

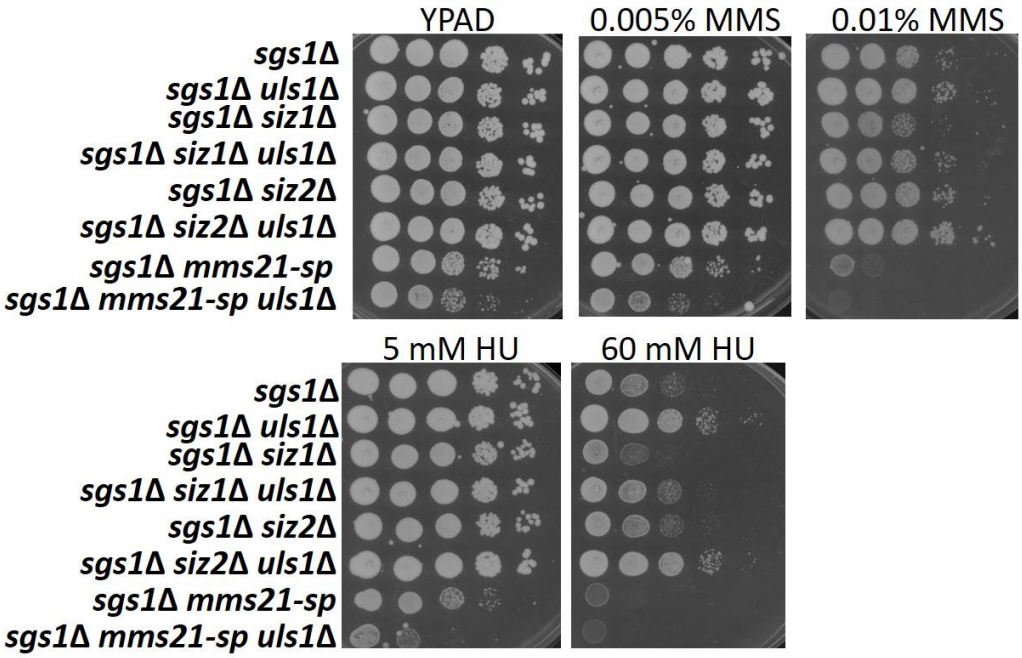
YPAD
0.005% MMS
0.01% MMS
sgs1Δ
sgs1Δ uls1Δ
sgs1Δ siz1Δ
sgs1Δ siz1Δ uls1Δ
sgs1Δ siz2Δ
sgs1Δ siz2Δ uls1Δ
sgs1Δ mms21-sp
sgs1Δ mms21-sp uls1Δ
5 mM HU
60 mM HU
sgs1Δ
sgs1Δ uls1Δ
sgs1Δ siz1Δ
sgs1Δ siz1Δ uls1Δ
sgs1Δ siz2Δ
sgs1Δ siz2Δ uls1Δ
sgs1Δ mms21-sp
sgs1Δ mms21-sp uls1Δ

Figure 3.7A-P

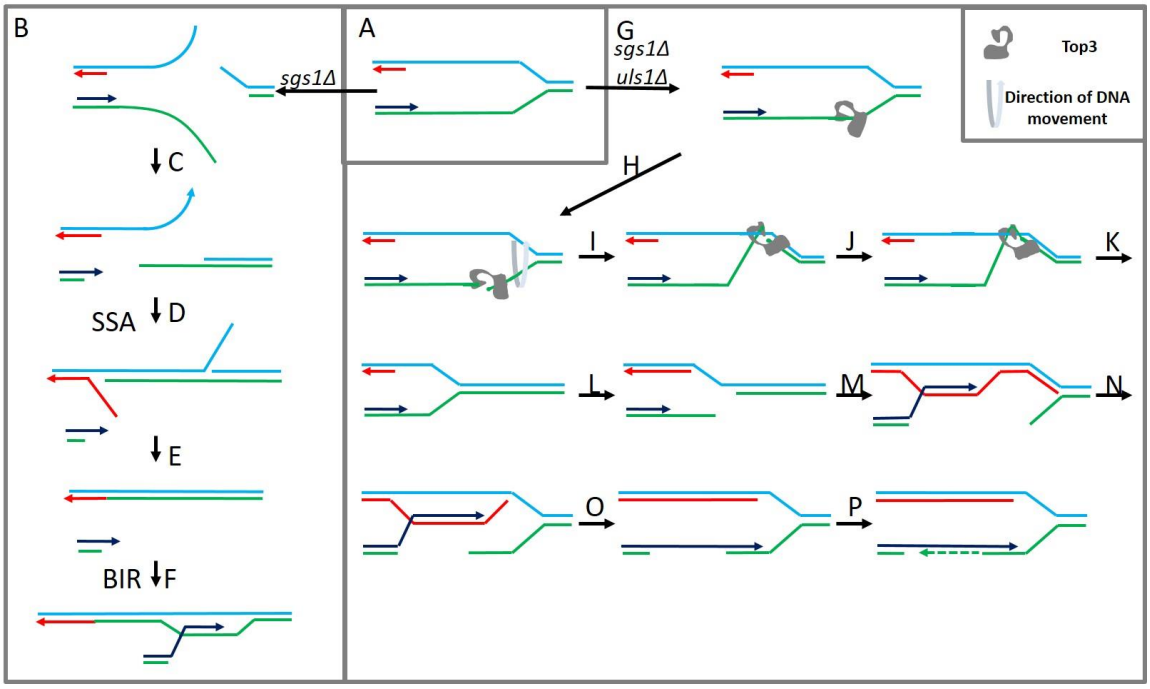
B
A
G
sgs1Δ
uls1Δ
sgs1Δ
Top3
Direction of DNA movement
C
H
SSA
D
I
J
K
E
L
M
N
BIR
F
O
P

Supplemental Figure 3.1

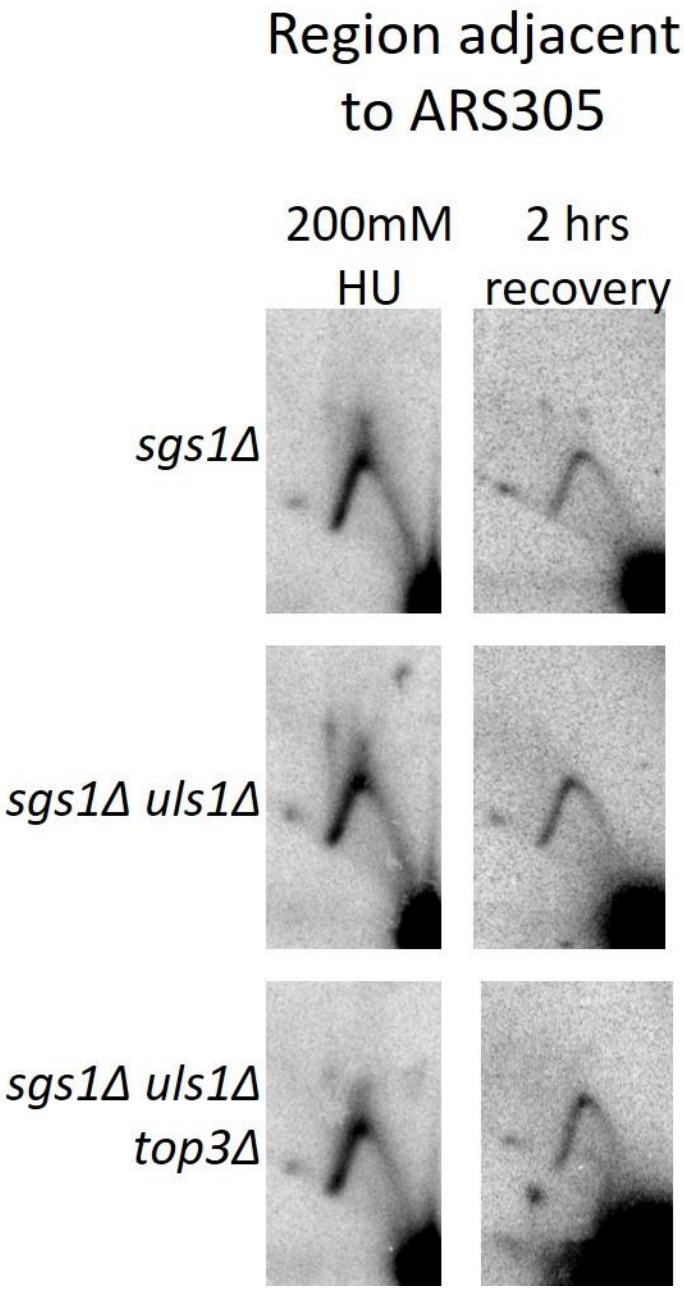

Supplemental Figure 3.2A-B

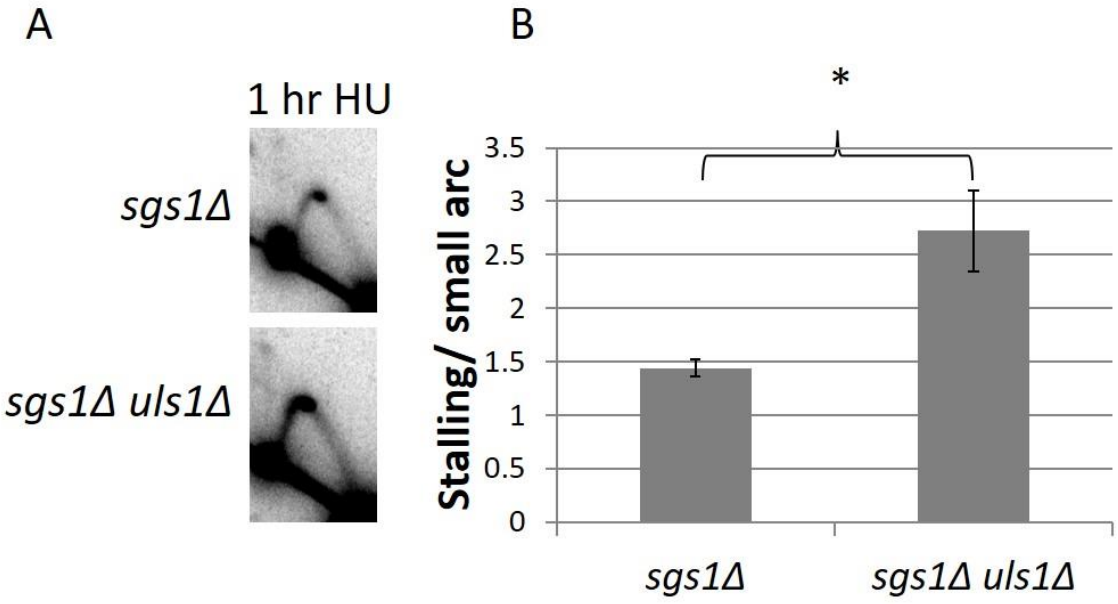

Supplemental Figure 3.3

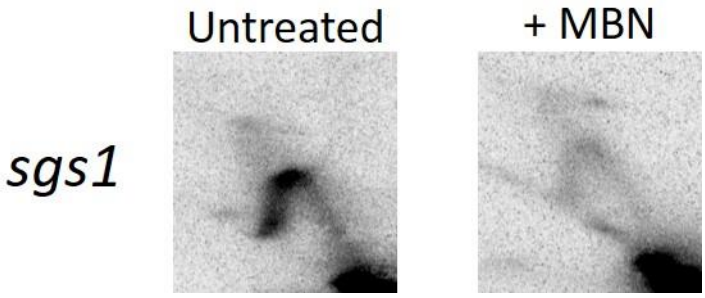

Supplemental Figure 3.4

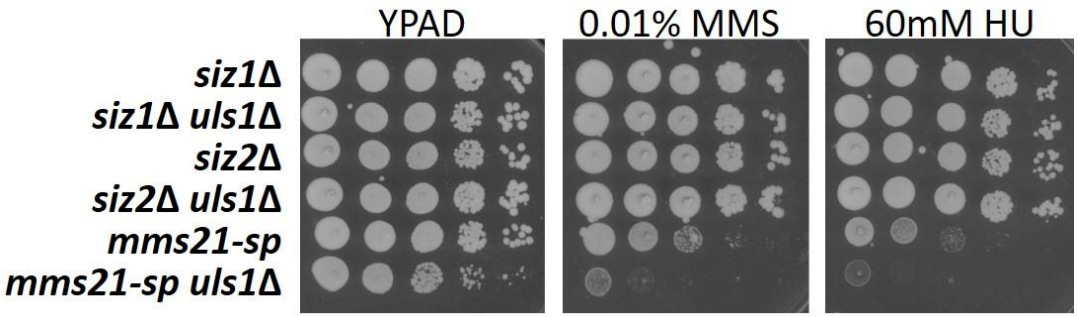

4. Discussion and Future Directions

4.1 Roles for Top3 in Rec-X Resolution and Fork Stabilization

Recent investigation into the nature of DNA lesions resulting from a variety of agents causing replicative stress and DNA damage, has revealed that all such insults lead primarily to the accumulation of two different replication-dependent structures: stalled forks and single stranded gaps behind the fork [1-3]. Stalled forks can occur during an encounter with a lesion, or during uncoupling of replication machinery; if caused by the latter, (e.g. due to treatment with the ribonucleotide reductase inhibitor, hydroxyurea (HU), this uncoupling can ultimately result in an excess of negatively supercoiled DNA behind the fork. Single stranded gaps can also result from replication uncoupling or lesion encounter if the replication machinery reprimes downstream of a lesion or gap. Both stalled forks and gaps contain stretches of single stranded DNA (ssDNA) that are more susceptible to DNA damage, and trigger the DNA damage response. While RPA can mask this ssDNA, eliminating it is a more favorable option. The data described here strongly support a role for Top3 in responding to and repairing both of these primary lesions. Why Top3 in particular becomes important for repairing these structures is likely due to its substrate specificity: Top3 is unique to other topoisomerases in that its activity is stimulated by ssDNA, allowing it to preferentially act on negatively supercoiled DNA [133]. Thus, it can untangle and rewind this exposed ssDNA, preventing downstream instability. We hypothesize that this rewinding activity not only stabilizes DNA but could also be required to provide a substrate for further processing by other repair enzymes (e.g. cleavage by Mus81-Mms4), for example, to initiate fork restart. This catalytic

activity allows Top3 to function in a number of contexts including double Holliday junction (dHJ) dissolution, and as we have demonstrated, Rec-X dissolution (*Chapter 2*) and stalled fork processing leading to D-loop based fork restart (*Chapter 3*) [21, 50, 65, 131].

Top3 naturally functions, at least in part, in concert with the Sgs1 DNA helicase, however the work presented here examines the Sgs1-independent functions of Top3 in providing resistance to DNA damaging agents. In Chapter 2, we have shown that Top3 is capable of providing rescue to *sgs1Δ* mutants on MMS, and this rescue is dependent on HR machinery. Overexpression of Top3 leads to a global reduction in X-structure levels in *sgs1Δ top3Δ* mutants, and biochemical characterization of these X-structures indicates that they are Rec-Xs and not HJs. Furthermore, we find that Top3 is capable of resolving a synthetic Rec-X but not an equivalent dHJ *in vitro*, and overexpression of Top3 has no effect on crossover rates in the context of a DSB where dHJs are known intermediates. Because the STR complex has substantial effects on crossovers, *via* resolution of DSB-induced dHJs, this confirms that resistance to MMS provided by Top3 is *via* a mechanism distinct from dHJ dissolution. Together, these data strongly support a model in which template switch recombination *via* a Rec-X intermediate (gap repair *via* template switch recombination (GR-TSR)) is the primary mechanism for repairing MMS-induced damage, and are consistent with other reports that show that MMS does not induce *in vivo* DSBs [13].

In Chapter 3, we investigated the role of Top3 in providing resistance to *sgs1Δ* mutants in the context of HU. We have found that while Top3 overexpression does not,

by itself, provide any rescue to *sgs1Δ* mutants on HU, deletion of the STUbL, Uls1, does provide rescue to *sgs1Δ* mutants, and does so in a Top3-dependent manner. Surprisingly, in a *sgs1Δ uls1Δ* double mutant, Top3 was required for both appropriate fork breakage and D-loop formation at the rDNA locus, suggesting a Sgs1-independent role for Top3 in fork processing and restart. Despite evidence for Top3 involvement in this process, many questions remain unanswered in regard to how Top3 aids in stabilization at a stalled replication fork. Namely, whether Top3 works through its catalytic domain, by altering DNA topology (e.g. rewinding the fork), and/or through recruitment of specific DNA repair factors is unknown. Furthermore, whether these activities are regulated by the sumoylation status of Top3, and whether this posttranslational modification is required for both restart of stalled forks and Rec-X resolution, or if this requirement is structure specific has not yet been tested.

4.2 Sumoylation and the STR complex

We and others have shown that the benefit of deletion of *ULS1* in *sgs1Δ* mutants primarily involves repair of the rDNA [169]. As rDNA resides within the nucleolus, and conjugated sumo is found predominantly in the nucleolus, it is plausible that Uls1 plays important roles in turning over and/or regulating sumoylated proteins at the rDNA by ubiquitinating them and targeting them for degradation [179, 180]. Loss of Uls1 then, would lead to an increase in sumoylated DNA repair proteins which could be potentially beneficial when the primary mode of defense (i.e. repair *via* Sgs1 and STR complex activities) is abolished. By slowing removal of sumoylated proteins, this could provide additional time for less efficient mechanisms to effect repair. Whether Top3 is one of

these Uls1- targeted sumolyated proteins would be of considerable interest. Our lab has preliminary data indicating that Uls1 does not affect overall levels of Top3 on chromatin in the absence of Sgs1, but whether it affects the sumoylation status of Top3 on chromatin could be the more relevant question.

The rescue observed in *sgs1Δ* mutants by deletion of *ULS1* is also dependent on Smc5/6 and cohesin as well (data not shown), so the full mechanism by which this rescue occurs is likely to be multifaceted, and not simply the consequence of heightened enrichment of one sumoylated protein. Although our previous studies led us to believe Top3 is not sumoylated, more recent studies indicate that it can be sumoylated in an Mms21-dependent manner, and sumoylation of Sgs1, as well as its interaction with Smc5 has been shown to be required for MMS-induced X-structure resolution [81-83]. Top3 interacts indirectly with the Smc5/6 complex through Sgs1, and although MMS-induced sumoylation of Top3 also seems to be heavily reliant on a direct interaction of Sgs1 with the Smc5/6 complex, it is unclear whether this interaction is entirely necessary for this posttranslational modification, particularly in the context of other types of DNA damage [82, 83]. Importantly, we have shown that Top3 is capable of resolving MMS-induced X-structures in *sgs1Δ* mutants in an Smc5/6-dependent manner, suggesting that Top3 is still capable of communicating with the Smc5/6 complex independently of physical binding through Sgs1, and might be able to function in a nonsumoylated fashion (Figure 2.5 & Appendix Figure 1). Further investigation into how this Sgs1-independent association influences sumoylation and activities of Top3 will need to be explored.

With these thoughts in mind, a distinction must be made regarding Top3 independent rescuing activities in the absence of Sgs1, and Top3 independent rescuing activities of *sgs1* mutants in the absence of Uls1. As previously stated, the ability of Top3 to provide rescue to *sgs1Δ* mutants on MMS is through resolution of Rec-Xs, and this activity requires the Smc5/6 complex; however, deletion of Uls1 does not decrease X-structure levels in *sgs1Δ top3Δ smc6-9* mutants expressing Top3 from a plasmid, but rather increases "large forks," suggesting that deletion of Uls1 promotes rescue of *sgs1Δ* mutants by Top3 only through a D-loop mediated fork restart mechanism but is not able to promote rescue through Top3-mediated Rec-X resolution (Appendix Figure 2D-E). This suggests that whereas sumoylation of Sgs1 is important for X-structure resolution, sumoylation of Top3 could be more important for mediating fork restart within the rDNA.

Consistent with this idea, neither sumoylation of Sgs1 nor its interactions with Smc5, through its SIM domains, are required for resistance to HU, and so while loss of these functions greatly compromise MMS-induced X-structure resolution, they might be dispensable for replication fork restart [83]. This distinction could explain how deletion of Uls1 provides rescue to *sgs1Δ* mutants on HU but very little rescue to *sgs1Δ* mutants on MMS. If, in the absence of Sgs1, Uls1 can bind the Smc5/6 complex and Top3 through its SIM domains, it could ubiquitinate this complex, thus promoting rapid degradation. However, deletion of Uls1 would prevent this turnover, allowing sumoylated Top3 and Smc5/6 to perform beneficial functions which do not rely on Sgs1 sumoylation or its physical interaction with Smc5. We do note that deletion of Uls1 had

no effect on total or sumoylated Smc5 levels (unpublished data), and so Top3 is likely to be a more important Uls1 target in this scenario. To date, Top3 has only been shown to be sumoylated in response to MMS, so it remains to be tested whether Top3 can be sumoylated in response to HU and if this sumoylation is dependent on the presence of Sgs1. As previously stated, it is likely that non-sumoylated Top3 is capable of resolving MMS-induced X-structures, given that Top3 requires the presence of Sgs1 to be sumoylated by Mms21, but can still resolve MMS-induced X-structures in the absence of Sgs1; consequently, further deleting Uls1 would provide no added benefit in this context. However, if sumoylated Top3 is required for replication fork restart following HU-induced damage, and can occur in the absence of Sgs1, then deletion of Uls1 could be beneficial *via* a Top3 sumoylation-dependent mechanism. Further investigation into how Top3 is regulated by Uls1 following HU-induced damage will provide a better understanding of how this topoisomerase can contribute to replication restart independent of its complex members, and whether these activities are distinct from its known roles in X-structure and dHJ dissolution.

To date, only one STUbL, RNF4, has been identified in mammals. RNF4 has recently been proposed to remove sumoylated replisome components from stalled forks in mammalian cells, to allow DNA repair machinery to restart the fork following aphidicolin treatment [181]. Unlike what we have observed in yeast, knock-down of RNF4 results in fewer DSBs following fork stalling. RNF4 has also been implicated in DSB repair processes, where it is involved in turning over RPA on single-stranded DNA to allow Brca2 and Rad51 to bind. In this setting, depletion of RNF4 leads to persistent

DSBs [174, 182]. These seemingly contradictory roles of RNF4 and Uls1 are expected because RNF4 appears to have more functional homology to another yeast STUbL, Slx5-Slx8, whose relationship to Uls1 is partially antagonistic [174]. Indeed, expression of human RNF4 in fission yeast has been shown to complement the loss of Slx8-Rfp, the orthologs of *S. cerevisiae* Slx8-Slx5 [183]. Uls1 was only recently identified in yeast and thus the possibility of a secondary STUbL, orthologous to Uls1, existing in mammals is not out of the question. Should one be found, it could serve as a novel therapeutic target in individuals with Bloom and Werner syndromes, who lack BLM and WRN RecQ helicases, the human orthologs of Sgs1, and consequently have defects in maintenance during DNA replication and repair processes.

4.3 DNA HR Repair Pathway Choice

There has been considerable effort over the last decade to understand which of various DNA repair pathways are utilized in response to different types of DNA damage in yeast. The work described in this thesis provides insight to the HR pathways utilized in response to MMS- and HU-induced damage, and supports the predominance of GR-TSR in response to MMS-induced damage, and DSB repair pathways in response to HU-induced fork stalling. Furthermore, whereas the occurrence of overlapping HR mechanisms in response to a single lesion type has been previously suggested, this work provides evidence that indeed there is a decision made in regard to which repair pathway is utilized at a given lesion, and indicates that activities of the STR complex members can strongly influence this choice.

This is not the first example of repair pathway choice in the context of DNA damage. A relevant and very well studied scenario involves the competition between NHEJ and HR at a DSB. Whereas NHEJ often wins the tug-of-war *vs*. HR in G1, HR-based DSB repair dominates at all other stages of the cell cycle, by promoting end resection to both inhibit NHEJ and facilitate in HR repair [172]. The degree to which ends are resected can further influence the type of HR repair; when extensive end resection is inhibited (e.g. in the absence of Sgs1 and/or Exo1), BIR predominates over classical GC [37, 38]. Here we have demonstrated that the actions of the Swi2/Snf2-related STUbL, Uls1, can also regulate repair pathway choice at a stalled replication fork, specifically in the absence of Sgs1. We find that deletion of Uls1 in a *sgs1Δ* mutant exposed to HU leads to an increase in breaks and subsequent Rad51-dependent D-loop formation at the replication fork block within the rDNA, which is distinct from the Rad51-independent D-loops formed in *sgs1Δ* mutants exposed to HU. We hypothesize that this transition from a Rad51-independent pathway to a Rad51-dependent pathway in *sgs1Δ* mutants could be a switch from a BIR type of HR repair to a GC type of HR repair, which could provide rescue in the absence of Sgs1 by inhibiting BIR-induced mutagenesis that could otherwise compromise rDNA copy number. Indeed, deletion of *ULS1* has been shown to restore rDNA copy number stability in *sgs1Δ* mutants [169]. Exactly how deletion of Uls1 leads to this pathway switch is not fully worked out, but data reported here points to a role for sumoylation and Top3 in regulating this transition. We can envision two mechanism by which Rad51 could be recruited in the absence of Uls1: 1) Top3 could facilitate rewinding of ssDNA at a stalled fork, producing a recognizable substrate for enzymatic cleavage and subsequent binding by Rad51, or 2)

Rad51 has been shown to have SIM domains that interact with sumoylated Rad52, and thus a similar interaction between Rad51 and sumoylated Top3, or any other sumoylated repair protein could facilitate Rad51 recruitment to a stalled fork[184].

In addition to its presumed STUbL activity, Uls1 is part of the Swi2/Snf2 family of ATPases, and thus may have the capacity to translocate along DNA [168]. Similar to full *ULS1* knockouts, a point mutation in the Uls1 ATPase domain also provides rescue to *sgs1Δ* mutants on HU, suggesting that Uls1 could be altering DNA topology deleteriously in the absence of Sgs1 [169]. There are currently a number of examples of DNA topology modifiers influencing DNA repair, including another Snf2 ATPase Fun30, which promotes end resection, and the high mobility group box protein, Hmo1, dubbed the "DNA bender," which promotes template switch recombination over translesion synthesis by altering DNA topology and aiding in sister chromatid junction formation [51, 185]. Whether Uls1 could be altering DNA topology in the absence of Sgs1, and whether this alteration influences Rad51 recruitment and DNA repair (or both) is certainly worth exploring.

It will be interesting in the future to determine how Rad51 recruitment and activation is affected by *ULS1* deletion—either through direct association with other repair factors or through the recognition of processed ends or alternative structures—and whether this is an rDNA-specific effect or if it has implications for DNA repair genome wide. Intriguingly, wild type cells have an increase in HU-induced large Y-structures (i.e. unidirectional replication forks) compared to *sgs1Δ* mutants, suggesting that deletion of *ULS1* could restore repair pathway fate back to wild type conditions [65]. Whether this is

the case, or whether it represents a third pathway alternative could provide interesting clues regarding what dictates normal repair mechanisms.

While further investigation is certainly warranted to understand the mechanism by which the various HR pathways compensate for each other, our observations illuminate the nature of complex DNA repair pathways involved and reveal the different scenarios in which particular DNA repair pathways are favored over others.

4.4 Compensatory Functions of Mus81-Mms4 and the STR Complex

This work has focused primarily on how the activities of the STR complex stabilize and direct the processing of stalled forks, and resolve X-structures, but another repair complex, Mus81-Mms4 has also been shown to play critical roles in these settings. Like the STR complex, Mus81-Mms4 has been shown to be important for resolving MMS-induced X-structures, and has the capacity to process *in vitro* four way junctions. Furthermore, mutations in the genes encoding both the STR and Mus81-Mms4 complexes together result in synthetic lethality suggesting that the two complexes serve parallel, compensatory X-structure processing functions [105, 162]. However, whether these two complexes act on the same substrates is still debated. The STR complex has known roles in dHJ resolution, and the work presented here provides evidence that the STR complex also acts on a similar, but distinct joint molecule that we refer to as a Rec-X. In contrast, Mus81-Mms4 has been shown to act preferentially, at least *in vitro,* on nicked HJs and forked structures, while having poor cleavage efficiency on a classic HJ. We note that Rec-Xs and D-loops bear a striking resemblance to nicked HJs, and thus the MMS-induced X-structures resolved by Mus81-Mms4 in the absence of Sgs1 are more

likely to be one of the two former structures rather than a HJ. Regardless of the structure recognized by Mus81-Mms4, evidence points to the STR complex working in parallel to Mus81-Mms4 during X-structure resolution. Thus, determining whether Mus81-Mms4 can recognize and process a mature Rec-X or whether it recognizes the earlier D-loop structure could provide insight into which enzyme acts as first responder to joint molecule resolution, and which one acts as a backup mechanism.

Intriguingly, Mus81-Mms4 has also been implicated in replication fork restart as well. Mus81 is known to cleave stalled replication forks in mammalian and fission yeast cells exposed to HU, and thus the question of whether the STR complex works collaboratively with Mus81 to restart forks or whether these complexes work in separate parallel pathways is worth exploring[186, 187]. It has been shown previously that deletion of *ULS1* has opposite effects on *sgs1* and *mus81* mutants, with deletion of *ULS1* rescuing *sgs1* mutants, but enhancing sensitivity of *mus81* mutants [168, 169]. Data reported here indicates that deletion of *ULS1* provides rescue to *sgs1Δ* mutants through fork restart mechanisms not through X-structure resolution, thus, we hypothesize that the STR complex and Mus81-Mms4 do not function identically, but rather, work in competing pathways for mediating fork restart. We would predict that the STR complex primarily responds to stalled replication forks and only when this complex is compromised and Uls1 activity is abolished is Mus81-Mms4 recruited to mediate replication fork restart. Therefore, in the absence of both Uls1 and Mus81, stalled forks cannot be processed and replication is thus inhibited. In support of this model, previous PFGE (pulse-field gel electrophoresis) studies have shown that *uls1Δ mus81Δ* double

mutants are unable to complete S-phase in the presence of MMS [169]. It will be interesting to determine if cooperativity exists between Top3 and Mus81-Mms4 independent of Sgs1 to restart stalled forks. Investigation into this process will provide more insight into the multilevel DNA repair functions of these two proteins, and will help further define the roles for these proteins both upstream and downstream of HR.

4.5 Concluding Remarks

HR repair is undeniably complex, but the great strides that have been made to reveal its multilevel compensatory pathways have real applications in the cancer therapeutic field. The discovery that PARP-inhibition was particularly effective in BRCA1/2-deficient tumors is just one example of how such understanding can be applied for therapeutic benefit -[188, 189]. As whole exome sequencing and transcriptome mapping of tumors becomes more common, knowing which repair pathways are favored under different conditions of DNA damage and replication stress can help better predict how any one particular tumor will respond to treatment. DNA damaging agents have already been employed for decades as successful chemotherapeutics, and efforts to enhance their effectiveness through combined treatment with inhibitors of particular DNA repair pathways will undoubtedly provide a beneficial path into the future. The work presented here contributes to our understanding of the complexity of DNA repair and provides evidence for distinct mechanisms of HR repair, dependent on the DNA damage type. Further insights into these pathways should reveal even more key targets that could potentially be utilized for more effective chemotherapeutic treatments, as well

as suggest how DNA repair may be enhanced to ameliorate additional age-related diseases.

APPENDIX I

Rescue of *sgs1Δ* mutants *via* Top3-mediated Rec-X resolution requires the Smc5/6 complex

Similarly to STR deficient strains, a mutation in any one of the Smc5/6 complex members results in increased sensitivity to DNA damaging agents as well as an increase in X-structure accumulation [44, 81, 175, 190]. We wondered if the Smc5/6 complex could be aiding Top3 in providing rescue to *sgs1Δ* mutants on MMS. To this end, we tested the ability of Top3 overexpression to provide rescue to *sgs1Δ* mutants in the absence of a fully functional Smc5/6 complex. While Top3 overexpression provided increased damage tolerance to *sgs1Δ* mutants on MMS, it was unable to provide rescue to *sgs1Δ smc5/6* double mutants on MMS, indicating that Top3 requires the Smc5/6 complex to provide damage tolerance in the absence of Sgs1 (Appendix Figure 1A and [50]).

We next wanted to investigate the mechanism by which the Smc5/6 complex aids Top3 in rescuing *sgs1Δ* mutants on DNA damaging agents. We previously reported that rescue of *sgs1Δ* mutants by Top3 overexpression was correlated with a decrease in X-structure levels, and so we sought to determine whether the inability of Top3 overexpression to provide rescue to *sgs1Δ smc6-9* mutants was due to a failure to resolve X-structures. Indeed Top3 overexpression was not able to resolve X-structures in *sgs1Δ top3Δ smc6-9* mutants, (Appendix Figure 1B-C) suggesting that the Smc5/6 complex is necessary to aide Top3 in the resolution of X-structures in the absence of Sgs1.

Deficiencies in the Smc5/6 complex allow rescue of *sgs1Δ via* Top3-mediated Fork Restart in the absence of *ULS1* on MMS

Mms21-dependent sumoylation is also required for Top3-mediated replication fork restart in *sgs1Δ* mutants in the absence of Uls1. Given the dependence of Top3 on other Smc5/6 complex members for Rec-X resolution, we asked whether other Smc5/6 complex members were required for Top3-mediated fork restart. Interestingly, while deletion of *ULS1* was not able to confer damage tolerance to *sgs1Δ smc5-6* and *sgs1Δ mms21-sp* mutants on HU or MMS, it was able to confer damage tolerance to *sgs1Δ smc6-9* mutants on HU, and was able to provide even more rescue to these double mutants than to *sgs1Δ* single mutants on MMS, suggesting that deletion of *ULS1* might be altering repair choice in the context of MMS as a result of specific Smc5/6 deficiencies (Figure 3.6 and Appendix Figure 2A-B). In support of this, we found that while Top3 overexpression was not able to provide rescue to *sgs1Δ top3Δ smc6-9* mutants on MMS, it was able to provide benefit, in *sgs1Δ top3Δ smc6-9 uls1Δ* mutants (Appendix Figure 2C). Intriguingly, while we observed no changes in X-structure levels in *sgs1Δ top3Δ smc6-9* mutants in the absence of Uls1, we did observed an increase in MMS-induced "large stalled forks" in *sgs1Δ top3Δ smc6-9 uls1Δ* mutants following 1 hour in MMS, but only when Top3 was overexpressed, lending support that the rescue observed by deleting *ULS1* in *sgs1Δ* mutants occurs through a universal, Top3-dependent fork restart mechanism, and suggesting that certain deficiencies in Smc5/6 might promote this pathway in the context of MMS (Appendix Figure 2D-E).

Figure Legends

Appendix Figure 1: The Smc5/6 complex is required for rescue of *sgs1Δ* mutants *via* Top3-mediated Rec-X resolution. (**A**) Spot assay comparing the effects of MMS on growth of *sgs1Δ, smc6-9 sgs1Δ, smc5-6 sgs1Δ,* and *mms21-sp sgs1Δ* with or without a Top3 overexpression plasmid. **B**) Representative 2DGE-SB examining replication intermediates in *sgs1Δ top3Δ smc6-9* mutants with or without a Top3 overexpression plasmid at 60, 120, and 180 min following release from G2 arrest into YPAD + 0.03% MMS. (**C**) Quantification of **B**.

Appendix Figure 2: Deletion of Uls1 allows Top3 OE to provide rescue to *sgs1Δ top3Δ smc6-9* mutants on MMS. (**A-C**) Spot assays comparing the effects of MMS and HU on growth of (**A**) *sgs1Δ smc5-6* and *sgs1Δ smc5-6 uls1Δ*, (**B**) *sgs1Δ smc6-9* and *sgs1Δ smc6-9 uls1Δ,* and (**C**) *sgs1Δ top3Δ smc6-9* and *sgs1Δ top3Δ smc6-9 uls1Δ* with or without a Top3 overexpression plasmid. (**D**) Representative 2DGE-SB examining replication intermediates at the rDNA in a fragment containing the RFB in *sgs1Δ top3Δ smc6-9* and *sgs1Δ top3Δ smc6-9 uls1Δ* with or without a Top3 overexpression plasmid. Samples were taken 1 hour following treatment with 0.016% MMS, and 2 and 3 hours following release of MMS treated samples into fresh YPAD. (**E**) Quantification of X-spike:arc (*top*) and RFB:arc (*bottom*) seen in (**D**).

Appendix Figure 1A-C

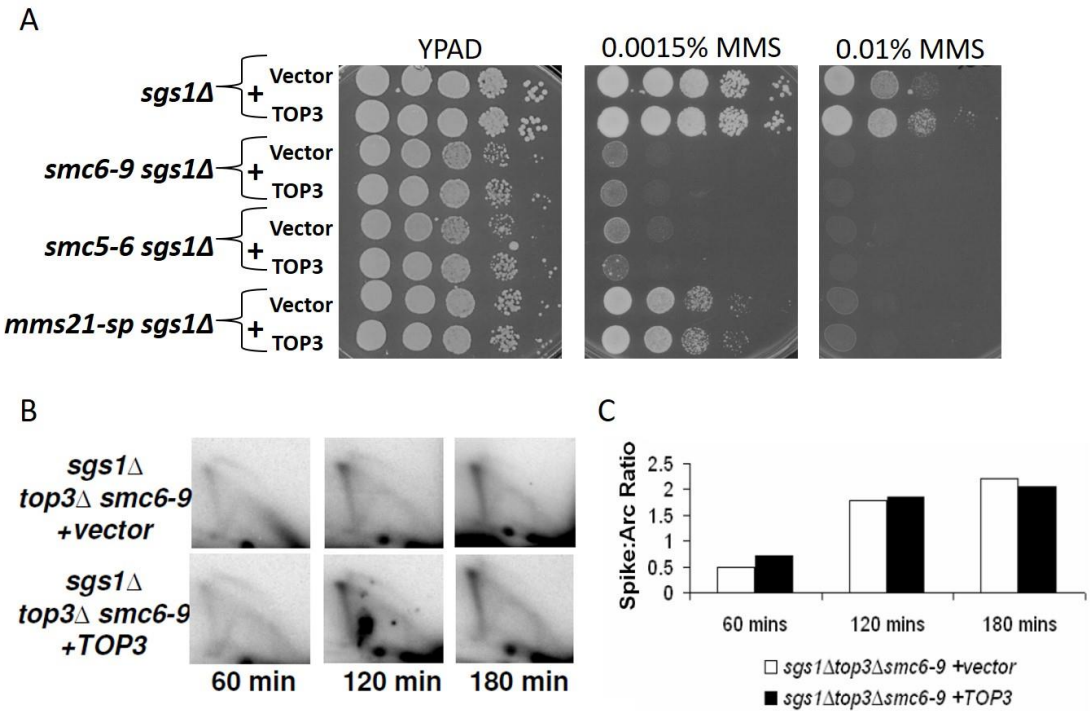

Appendix Figure 2A-E

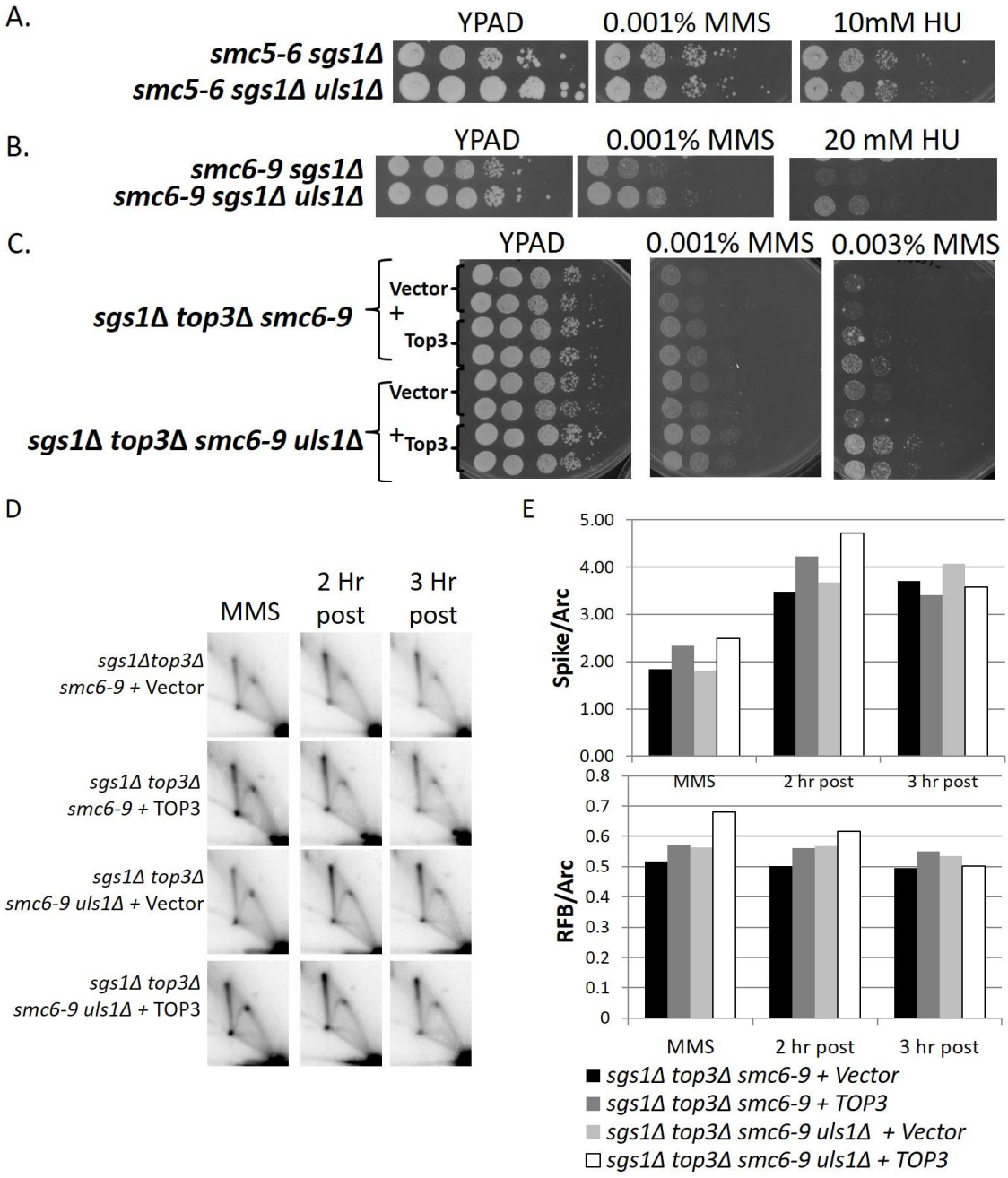

BIBLIOGRAPHY

1. Zellweger, R., et al., *Rad51-mediated replication fork reversal is a global response to genotoxic treatments in human cells.* J Cell Biol, 2015. **208**(5): p. 563-79.
2. Hashimoto, Y., et al., *Rad51 protects nascent DNA from Mre11-dependent degradation and promotes continuous DNA synthesis.* Nat Struct Mol Biol, 2010. **17**(11): p. 1305-11.
3. Lopes, M., M. Foiani, and J.M. Sogo, *Multiple mechanisms control chromosome integrity after replication fork uncoupling and restart at irreparable UV lesions.* Mol Cell, 2006. **21**(1): p. 15-27.
4. Hoege, C., et al., *RAD6-dependent DNA repair is linked to modification of PCNA by ubiquitin and SUMO.* Nature, 2002. **419**(6903): p. 135-41.
5. Branzei, D., F. Vanoli, and M. Foiani, *SUMOylation regulates Rad18-mediated template switch.* Nature, 2008. **456**(7224): p. 915-20.
6. Le Breton, C., et al., *Srs2 removes deadly recombination intermediates independently of its interaction with SUMO-modified PCNA.* Nucleic Acids Res, 2008. **36**(15): p. 4964-74.
7. Karras, G.I. and S. Jentsch, *The RAD6 DNA damage tolerance pathway operates uncoupled from the replication fork and is functional beyond S phase.* Cell, 2010. **141**(2): p. 255-67.
8. Fabre, F., et al., *Alternate pathways involving Sgs1/Top3, Mus81/ Mms4, and Srs2 prevent formation of toxic recombination intermediates from single-stranded gaps created by DNA replication.* Proc Natl Acad Sci U S A, 2002. **99**(26): p. 16887-92.
9. Hanada, K., et al., *The structure-specific endonuclease Mus81 contributes to replication restart by generating double-strand DNA breaks.* Nat Struct Mol Biol, 2007. **14**(11): p. 1096-104.
10. Doe, C.L., et al., *Mus81-Eme1 and Rqh1 involvement in processing stalled and collapsed replication forks.* J Biol Chem, 2002. **277**(36): p. 32753-9.
11. Hanada, K. and I.D. Hickson, *Molecular genetics of RecQ helicase disorders.* Cell Mol Life Sci, 2007. **64**(17): p. 2306-22.
12. Ii, M., et al., *Epistasis analysis between homologous recombination genes in Saccharomyces cerevisiae identifies multiple repair pathways for Sgs1, Mus81-Mms4 and RNase H2.* Mutat Res, 2011. **714**(1-2): p. 33-43.
13. Lundin, C., et al., *Methyl methanesulfonate (MMS) produces heat-labile DNA damage but no detectable in vivo DNA double-strand breaks.* Nucleic Acids Res, 2005. **33**(12): p. 3799-811.
14. Liberi, G., et al., *Rad51-dependent DNA structures accumulate at damaged replication forks in sgs1 mutants defective in the yeast ortholog of BLM RecQ helicase.* Genes Dev, 2005. **19**(3): p. 339-50.
15. Mimitou, E.P. and L.S. Symington, *DNA end resection: many nucleases make light work.* DNA Repair (Amst), 2009. **8**(9): p. 983-95.
16. Niu, H., et al., *Mechanism of the ATP-dependent DNA end-resection machinery from Saccharomyces cerevisiae.* Nature, 2010. **467**(7311): p. 108-11.
17. Sugiyama, T. and N. Kantake, *Dynamic regulatory interactions of rad51, rad52, and replication protein-a in recombination intermediates.* J Mol Biol, 2009. **390**(1): p. 45-55.
18. Wu, Y., et al., *Rad51 protein controls Rad52-mediated DNA annealing.* J Biol Chem, 2008. **283**(21): p. 14883-92.
19. Nimonkar, A.V., R.A. Sica, and S.C. Kowalczykowski, *Rad52 promotes second-end DNA capture in double-stranded break repair to form complement-stabilized joint molecules.* Proc Natl Acad Sci U S A, 2009. **106**(9): p. 3077-82.

20. Miura, T., et al., *Homologous recombination via synthesis-dependent strand annealing in yeast requires the Irc20 and Srs2 DNA helicases.* Genetics, 2012. **191**(1): p. 65-78.
21. Bachrati, C.Z. and I.D. Hickson, *Dissolution of double Holliday junctions by the concerted action of BLM and topoisomerase IIIalpha.* Methods Mol Biol, 2009. **582**: p. 91-102.
22. Ip, S.C., et al., *Identification of Holliday junction resolvases from humans and yeast.* Nature, 2008. **456**(7220): p. 357-61.
23. Malkova, A., E.L. Ivanov, and J.E. Haber, *Double-strand break repair in the absence of RAD51 in yeast: a possible role for break-induced DNA replication.* Proc Natl Acad Sci U S A, 1996. **93**(14): p. 7131-6.
24. Saini, N., et al., *Migrating bubble during break-induced replication drives conservative DNA synthesis.* Nature, 2013. **502**(7471): p. 389-92.
25. Moriel-Carretero, M. and A. Aguilera, *A postincision-deficient TFIIH causes replication fork breakage and uncovers alternative Rad51- or Pol32-mediated restart mechanisms.* Mol Cell, 2010. **37**(5): p. 690-701.
26. Lydeard, J.R., et al., *Break-induced replication and telomerase-independent telomere maintenance require Pol32.* Nature, 2007. **448**(7155): p. 820-3.
27. Signon, L., et al., *Genetic requirements for RAD51- and RAD54-independent break-induced replication repair of a chromosomal double-strand break.* Mol Cell Biol, 2001. **21**(6): p. 2048-56.
28. Jain, S., et al., *A recombination execution checkpoint regulates the choice of homologous recombination pathway during DNA double-strand break repair.* Genes Dev, 2009. **23**(3): p. 291-303.
29. Sugawara, N., G. Ira, and J.E. Haber, *DNA length dependence of the single-strand annealing pathway and the role of Saccharomyces cerevisiae RAD59 in double-strand break repair.* Mol Cell Biol, 2000. **20**(14): p. 5300-9.
30. Fishman-Lobell, J. and J.E. Haber, *Removal of nonhomologous DNA ends in double-strand break recombination: the role of the yeast ultraviolet repair gene RAD1.* Science, 1992. **258**(5081): p. 480-4.
31. Ozenberger, B.A. and G.S. Roeder, *A unique pathway of double-strand break repair operates in tandemly repeated genes.* Mol Cell Biol, 1991. **11**(3): p. 1222-31.
32. Ruiz, J.F., B. Gomez-Gonzalez, and A. Aguilera, *Chromosomal translocations caused by either pol32-dependent or pol32-independent triparental break-induced replication.* Mol Cell Biol, 2009. **29**(20): p. 5441-54.
33. Payen, C., et al., *Segmental duplications arise from Pol32-dependent repair of broken forks through two alternative replication-based mechanisms.* PLoS Genet, 2008. **4**(9): p. e1000175.
34. Mayle, R., et al., *DNA REPAIR. Mus81 and converging forks limit the mutagenicity of replication fork breakage.* Science, 2015. **349**(6249): p. 742-7.
35. Symington, L.S. and J. Gautier, *Double-strand break end resection and repair pathway choice.* Annu Rev Genet, 2011. **45**: p. 247-71.
36. Ira, G. and J.E. Haber, *Characterization of RAD51-independent break-induced replication that acts preferentially with short homologous sequences.* Mol Cell Biol, 2002. **22**(18): p. 6384-92.
37. Marrero, V.A. and L.S. Symington, *Extensive DNA end processing by exo1 and sgs1 inhibits break-induced replication.* PLoS Genet, 2010. **6**(7): p. e1001007.
38. Jain, S., et al., *Sgs1 and Mph1 Helicases Enforce the Recombination Execution Checkpoint During DNA Double-Strand Break Repair in Saccharomyces cerevisiae.* Genetics, 2016. **203**(2): p. 667-75.

39. Sakofsky, C.J., et al., *Translesion Polymerases Drive Microhomology-Mediated Break-Induced Replication Leading to Complex Chromosomal Rearrangements.* Mol Cell, 2015. **60**(6): p. 860-72.
40. Whitby, M.C., F. Osman, and J. Dixon, *Cleavage of model replication forks by fission yeast Mus81-Eme1 and budding yeast Mus81-Mms4.* J Biol Chem, 2003. **278**(9): p. 6928-35.
41. Neelsen, K.J. and M. Lopes, *Replication fork reversal in eukaryotes: from dead end to dynamic response.* Nat Rev Mol Cell Biol, 2015. **16**(4): p. 207-20.
42. Higgins, N.P., K. Kato, and B. Strauss, *A model for replication repair in mammalian cells.* J Mol Biol, 1976. **101**(3): p. 417-25.
43. Berti, M., et al., *Human RECQ1 promotes restart of replication forks reversed by DNA topoisomerase I inhibition.* Nat Struct Mol Biol, 2013. **20**(3): p. 347-54.
44. Chavez, A., V. Agrawal, and F.B. Johnson, *Homologous recombination-dependent rescue of deficiency in the structural maintenance of chromosomes (Smc) 5/6 complex.* J Biol Chem, 2011. **286**(7): p. 5119-25.
45. Thangavel, S., et al., *DNA2 drives processing and restart of reversed replication forks in human cells.* J Cell Biol, 2015. **208**(5): p. 545-62.
46. Sogo, J.M., M. Lopes, and M. Foiani, *Fork reversal and ssDNA accumulation at stalled replication forks owing to checkpoint defects.* Science, 2002. **297**(5581): p. 599-602.
47. Ray Chaudhuri, A., et al., *Topoisomerase I poisoning results in PARP-mediated replication fork reversal.* Nat Struct Mol Biol, 2012. **19**(4): p. 417-23.
48. Vanoli, F., et al., *Replication and recombination factors contributing to recombination-dependent bypass of DNA lesions by template switch.* PLoS Genet, 2010. **6**(11): p. e1001205.
49. Giannattasio, M., et al., *Visualization of recombination-mediated damage bypass by template switching.* Nat Struct Mol Biol, 2014. **21**(10): p. 884-92.
50. Glineburg, M.R., et al., *Resolution by unassisted Top3 points to template switch recombination intermediates during DNA replication.* J Biol Chem, 2013. **288**(46): p. 33193-204.
51. Gonzalez-Huici, V., et al., *DNA bending facilitates the error-free DNA damage tolerance pathway and upholds genome integrity.* EMBO J, 2014. **33**(4): p. 327-40.
52. Rupp, W.D. and P. Howard-Flanders, *Discontinuities in the DNA synthesized in an excision-defective strain of Escherichia coli following ultraviolet irradiation.* J Mol Biol, 1968. **31**(2): p. 291-304.
53. Rupp, W.D., et al., *Exchanges between DNA strands in ultraviolet-irradiated Escherichia coli.* J Mol Biol, 1971. **61**(1): p. 25-44.
54. Heller, R.C. and K.J. Marians, *Replisome assembly and the direct restart of stalled replication forks.* Nat Rev Mol Cell Biol, 2006. **7**(12): p. 932-43.
55. McInerney, P. and M. O'Donnell, *Functional uncoupling of twin polymerases: mechanism of polymerase dissociation from a lagging-strand block.* J Biol Chem, 2004. **279**(20): p. 21543-51.
56. Ira, G., et al., *Srs2 and Sgs1-Top3 suppress crossovers during double-strand break repair in yeast.* Cell, 2003. **115**(4): p. 401-11.
57. Bzymek, M., et al., *Double Holliday junctions are intermediates of DNA break repair.* Nature, 2010. **464**(7290): p. 937-41.
58. Schwacha, A. and N. Kleckner, *Identification of double Holliday junctions as intermediates in meiotic recombination.* Cell, 1995. **83**(5): p. 783-91.
59. Liu, Y. and S.C. West, *Happy Hollidays: 40th anniversary of the Holliday junction.* Nat Rev Mol Cell Biol, 2004. **5**(11): p. 937-44.

60. Panyutin, I.G. and P. Hsieh, *The kinetics of spontaneous DNA branch migration.* Proc Natl Acad Sci U S A, 1994. **91**(6): p. 2021-5.
61. Lee, J., et al., *Evidence that a RecQ helicase slows senescence by resolving recombining telomeres.* PLOS Biology, 2007. **5**(6): p. e160.
62. Branzei, D., M. Seki, and T. Enomoto, *Rad18/Rad5/Mms2-mediated polyubiquitination of PCNA is implicated in replication completion during replication stress.* Genes Cells, 2004. **9**(11): p. 1031-42.
63. Lambert, S., et al., *Homologous recombination restarts blocked replication forks at the expense of genome rearrangements by template exchange.* Mol Cell, 2010. **39**(3): p. 346-59.
64. Liberi, G., et al., *Methods to study replication fork collapse in budding yeast.* Methods Enzymol, 2006. **409**: p. 442-62.
65. Mankouri, H.W., T.M. Ashton, and I.D. Hickson, *Holliday junction-containing DNA structures persist in cells lacking Sgs1 or Top3 following exposure to DNA damage.* Proc Natl Acad Sci U S A, 2011. **108**(12): p. 4944-9.
66. Mueller, J.E., et al., *T4 endonuclease VII cleaves the crossover strands of Holliday junction analogs.* Proc Natl Acad Sci U S A, 1988. **85**(24): p. 9441-5.
67. Picksley, S.M., et al., *Cleavage specificity of bacteriophage T4 endonuclease VII and bacteriophage T7 endonuclease I on synthetic branch migratable Holliday junctions.* J Mol Biol, 1990. **212**(4): p. 723-35.
68. Biertumpfel, C., et al., *Structure and mechanism of human DNA polymerase eta.* Nature, 2010. **465**(7301): p. 1044-8.
69. Garcia-Luis, J. and F. Machin, *Mus81-Mms4 and Yen1 resolve a novel anaphase bridge formed by noncanonical Holliday junctions.* Nat Commun, 2014. **5**: p. 5652.
70. Yu, C.E., et al., *Positional cloning of the Werner's syndrome gene.* Science, 1996. **272**(5259): p. 258-62.
71. Bartram, C.R., T. Koske-Westphal, and E. Passarge, *Chromatid exchanges in ataxia telangiectasia, Bloom syndrome, Werner syndrome, and xeroderma pigmentosum.* Ann Hum Genet, 1976. **40**(1): p. 79-86.
72. Watt, P.M. and I.D. Hickson, *Structure and function of type II DNA topoisomerases.* Biochem J, 1994. **303 (Pt 3)**: p. 681-95.
73. Bennett, R.J., J.L. Keck, and J.C. Wang, *Binding specificity determines polarity of DNA unwinding by the Sgs1 protein of S. cerevisiae.* J Mol Biol, 1999. **289**(2): p. 235-48.
74. Mohaghegh, P., et al., *The Bloom's and Werner's syndrome proteins are DNA structure-specific helicases.* Nucleic Acids Res, 2001. **29**(13): p. 2843-9.
75. Gangloff, S., C. Soustelle, and F. Fabre, *Homologous recombination is responsible for cell death in the absence of the Sgs1 and Srs2 helicases.* Nat Genet, 2000. **25**(2): p. 192-4.
76. Yang, J., et al., *Human topoisomerase IIIalpha is a single-stranded DNA decatenase that is stimulated by BLM and RMI1.* J Biol Chem, 2010. **285**(28): p. 21426-36.
77. Wu, L., et al., *The HRDC domain of BLM is required for the dissolution of double Holliday junctions.* Embo J, 2005. **24**(14): p. 2679-87.
78. Cejka, P., et al., *Rmi1 stimulates decatenation of double Holliday junctions during dissolution by Sgs1-Top3.* Nat Struct Mol Biol, 2010. **17**(11): p. 1377-82.
79. Plank, J.L., J. Wu, and T.S. Hsieh, *Topoisomerase IIIalpha and Bloom's helicase can resolve a mobile double Holliday junction substrate through convergent branch migration.* Proc Natl Acad Sci U S A, 2006. **103**(30): p. 11118-23.
80. Bermudez-Lopez, M., et al., *The Smc5/6 complex is required for dissolution of DNA-mediated sister chromatid linkages.* Nucleic Acids Res, 2010. **38**(19): p. 6502-12.

81. Chavez, A., et al., *Sumoylation and the structural maintenance of chromosomes (Smc) 5/6 complex slow senescence through recombination intermediate resolution.* J Biol Chem, 2010. **285**(16): p. 11922-30.
82. Bermudez-Lopez, M., et al., *Sgs1's roles in DNA end resection, HJ dissolution, and crossover suppression require a two-step SUMO regulation dependent on Smc5/6.* Genes Dev, 2016. **30**(11): p. 1339-56.
83. Bonner, J.N., et al., *Smc5/6 Mediated Sumoylation of the Sgs1-Top3-Rmi1 Complex Promotes Removal of Recombination Intermediates.* Cell Rep, 2016. **16**(2): p. 368-78.
84. Ralf, C., I.D. Hickson, and L. Wu, *The Bloom's syndrome helicase can promote the regression of a model replication fork.* J Biol Chem, 2006. **281**(32): p. 22839-46.
85. Machwe, A., et al., *The Werner and Bloom syndrome proteins catalyze regression of a model replication fork.* Biochemistry, 2006. **45**(47): p. 13939-46.
86. Bolterstein, E., et al., *The Drosophila Werner exonuclease participates in an exonuclease-independent response to replication stress.* Genetics, 2014. **197**(2): p. 643-52.
87. Cobb, J.A., et al., *DNA polymerase stabilization at stalled replication forks requires Mec1 and the RecQ helicase Sgs1.* Embo J, 2003. **22**(16): p. 4325-36.
88. Bjergbaek, L., et al., *Mechanistically distinct roles for Sgs1p in checkpoint activation and replication fork maintenance.* Embo J, 2005. **24**(2): p. 405-17.
89. Hegnauer, A.M., et al., *An N-terminal acidic region of Sgs1 interacts with Rpa70 and recruits Rad53 kinase to stalled forks.* EMBO J, 2012. **31**(18): p. 3768-83.
90. Lydeard, J.R., et al., *Sgs1 and exo1 redundantly inhibit break-induced replication and de novo telomere addition at broken chromosome ends.* PLoS Genet, 2010. **6**(5): p. e1000973.
91. Mizuuchi, K., et al., *T4 endonuclease VII cleaves holliday structures.* Cell, 1982. **29**(2): p. 357-65.
92. de Massy, B., R.A. Weisberg, and F.W. Studier, *Gene 3 endonuclease of bacteriophage T7 resolves conformationally branched structures in double-stranded DNA.* J Mol Biol, 1987. **193**(2): p. 359-76.
93. Duckett, D.R., M.J. Panis, and D.M. Lilley, *Binding of the junction-resolving enzyme bacteriophage T7 endonuclease I to DNA: separation of binding and catalysis by mutation.* J Mol Biol, 1995. **246**(1): p. 95-107.
94. Seigneur, M., et al., *RuvAB acts at arrested replication forks.* Cell, 1998. **95**(3): p. 419-30.
95. Flores, M.J., et al., *Protection provided by exogenous DNA ligase in G0 human lymphocytes treated with restriction enzyme MspI or bleomycin as shown by the comet assay.* Environ Mol Mutagen, 1998. **32**(4): p. 336-43.
96. Chan, S.N., et al., *Sequence specificity and biochemical characterization of the RusA Holliday junction resolvase of Escherichia coli.* J Biol Chem, 1997. **272**(23): p. 14873-82.
97. McGlynn, P., R.G. Lloyd, and K.J. Marians, *Formation of Holliday junctions by regression of nascent DNA in intermediates containing stalled replication forks: RecG stimulates regression even when the DNA is negatively supercoiled.* Proc Natl Acad Sci U S A, 2001. **98**(15): p. 8235-40.
98. Mandal, T.N., et al., *Resolution of Holliday intermediates in recombination and DNA repair: indirect suppression of ruvA, ruvB, and ruvC mutations.* J Bacteriol, 1993. **175**(14): p. 4325-34.
99. Rass, U., et al., *Mechanism of Holliday junction resolution by the human GEN1 protein.* Genes Dev, 2010. **24**(14): p. 1559-69.

100. Blanco, M.G., et al., *Functional overlap between the structure-specific nucleases Yen1 and Mus81-Mms4 for DNA-damage repair in S. cerevisiae.* DNA Repair (Amst), 2010. **9**(4): p. 394-402.
101. Ho, C.K., et al., *Mus81 and Yen1 promote reciprocal exchange during mitotic recombination to maintain genome integrity in budding yeast.* Mol Cell, 2010. **40**(6): p. 988-1000.
102. Chan, Y.W. and S.C. West, *Spatial control of the GEN1 Holliday junction resolvase ensures genome stability.* Nat Commun, 2014. **5**: p. 4844.
103. Mullen, J.R., et al., *Requirement for three novel protein complexes in the absence of the Sgs1 DNA helicase in Saccharomyces cerevisiae.* Genetics, 2001. **157**(1): p. 103-18.
104. Kaliraman, V., et al., *Functional overlap between Sgs1-Top3 and the Mms4-Mus81 endonuclease.* Genes Dev, 2001. **15**(20): p. 2730-40.
105. Ashton, T.M., et al., *Pathways for Holliday junction processing during homologous recombination in Saccharomyces cerevisiae.* Mol Cell Biol, 2011. **31**(9): p. 1921-33.
106. Wechsler, T., S. Newman, and S.C. West, *Aberrant chromosome morphology in human cells defective for Holliday junction resolution.* Nature, 2011. **471**(7340): p. 642-6.
107. Wyatt, H.D., et al., *Coordinated actions of SLX1-SLX4 and MUS81-EME1 for Holliday junction resolution in human cells.* Mol Cell, 2013. **52**(2): p. 234-47.
108. Bastin-Shanower, S.A., et al., *The mechanism of mus81-mms4 cleavage site selection distinguishes it from the homologous endonuclease rad1-rad10.* Mol Cell Biol, 2003. **23**(10): p. 3487-96.
109. Chen, X.B., et al., *Human Mus81-associated endonuclease cleaves Holliday junctions in vitro.* Mol Cell, 2001. **8**(5): p. 1117-27.
110. Munoz-Galvan, S., et al., *Distinct roles of Mus81, Yen1, Slx1-Slx4, and Rad1 nucleases in the repair of replication-born double-strand breaks by sister chromatid exchange.* Mol Cell Biol, 2012. **32**(9): p. 1592-603.
111. Fricke, W.M. and S.J. Brill, *Slx1-Slx4 is a second structure-specific endonuclease functionally redundant with Sgs1-Top3.* Genes Dev, 2003. **17**(14): p. 1768-78.
112. Castor, D., et al., *Cooperative control of holliday junction resolution and DNA repair by the SLX1 and MUS81-EME1 nucleases.* Mol Cell, 2013. **52**(2): p. 221-33.
113. Prakash, S. and L. Prakash, *Nucleotide excision repair in yeast.* Mutat Res, 2000. **451**(1-2): p. 13-24.
114. Habraken, Y., et al., *Holliday junction cleavage by yeast Rad1 protein.* Nature, 1994. **371**(6497): p. 531-4.
115. Davies, A.A., et al., *Role of the Rad1 and Rad10 proteins in nucleotide excision repair and recombination.* J Biol Chem, 1995. **270**(42): p. 24638-41.
116. Bardwell, A.J., et al., *Specific cleavage of model recombination and repair intermediates by the yeast Rad1-Rad10 DNA endonuclease.* Science, 1994. **265**(5181): p. 2082-5.
117. Karlin, J. and P.L. Fischhaber, *Rad51 ATP binding but not hydrolysis is required to recruit Rad10 in synthesis-dependent strand annealing sites in S. cerevisiae.* Adv Biol Chem, 2013. **3**(3): p. 295-303.
118. Larsen, N.B. and I.D. Hickson, *RecQ Helicases: Conserved Guardians of Genomic Integrity.* Adv Exp Med Biol, 2013. **767**: p. 161-84.
119. Chang, M., et al., *RMI1/NCE4, a suppressor of genome instability, encodes a member of the RecQ helicase/Topo III complex.* EMBO J, 2005. **24**(11): p. 2024-33.
120. Mullen, J.R., et al., *Yeast Rmi1/Nce4 controls genome stability as a subunit of the Sgs1-Top3 complex.* Mol Cell Biol, 2005. **25**(11): p. 4476-87.

121. Myung, K., et al., *SGS1, the Saccharomyces cerevisiae homologue of BLM and WRN, suppresses genome instability and homeologous recombination.* Nat Genet, 2001. **27**(1): p. 113-6.
122. Wallis, J.W., et al., *A hyper-recombination mutation in S. cerevisiae identifies a novel eukaryotic topoisomerase.* Cell, 1989. **58**(2): p. 409-19.
123. Watt, P.M., et al., *Sgs1: a eukaryotic homolog of E. coli RecQ that interacts with topoisomerase II in vivo and is required for faithful chromosome segregation.* Cell, 1995. **81**(2): p. 253-60.
124. Bohr, V.A., *Rising from the RecQ-age: the role of human RecQ helicases in genome maintenance.* Trends Biochem Sci, 2008. **33**(12): p. 609-20.
125. Monnat, R.J., Jr., *Human RECQ helicases: roles in DNA metabolism, mutagenesis and cancer biology.* Semin Cancer Biol, 2010. **20**(5): p. 329-39.
126. Ashton, T.M. and I.D. Hickson, *Yeast as a model system to study RecQ helicase function.* DNA Repair (Amst), 2010. **9**(3): p. 303-14.
127. Oh, S.D., et al., *BLM ortholog, Sgs1, prevents aberrant crossing-over by suppressing formation of multichromatid joint molecules.* Cell, 2007. **130**(2): p. 259-72.
128. Wu, L. and I.D. Hickson, *The Bloom's syndrome helicase suppresses crossing over during homologous recombination.* Nature, 2003. **426**(6968): p. 870-4.
129. Kass, E.M. and M. Jasin, *Collaboration and competition between DNA double-strand break repair pathways.* FEBS Lett, 2010. **584**(17): p. 3703-8.
130. Branzei, D., *Ubiquitin family modifications and template switching.* FEBS Lett, 2011. **585**(18): p. 2810-7.
131. Mankouri, H.W. and I.D. Hickson, *Top3 processes recombination intermediates and modulates checkpoint activity after DNA damage.* Mol Biol Cell, 2006. **17**(10): p. 4473-83.
132. Mankouri, H.W., H.P. Ngo, and I.D. Hickson, *Shu proteins promote the formation of homologous recombination intermediates that are processed by Sgs1-Rmi1-Top3.* Mol Biol Cell, 2007. **18**(10): p. 4062-73.
133. Koster, D.A., et al., *Cellular strategies for regulating DNA supercoiling: a single-molecule perspective.* Cell, 2010. **142**(4): p. 519-30.
134. Bennett, R.J. and J.C. Wang, *Association of yeast DNA topoisomerase III and Sgs1 DNA helicase: studies of fusion proteins.* Proc Natl Acad Sci U S A, 2001. **98**(20): p. 11108-13.
135. Kim, R.A. and J.C. Wang, *Identification of the yeast TOP3 gene product as a single strand-specific DNA topoisomerase.* J Biol Chem, 1992. **267**(24): p. 17178-85.
136. Wang, J.C., *Cellular roles of DNA topoisomerases: a molecular perspective.* Nat Rev Mol Cell Biol, 2002. **3**(6): p. 430-40.
137. Cejka, P., et al., *Decatenation of DNA by the S. cerevisiae Sgs1-Top3-Rmi1 and RPA Complex: A Mechanism for Disentangling Chromosomes.* Mol Cell, 2012. **47**: p. 1-11.
138. Chakraverty, R.K., et al., *Topoisomerase III acts upstream of Rad53p in the S-phase DNA damage checkpoint.* Mol Cell Biol, 2001. **21**(21): p. 7150-62.
139. Gangloff, S., et al., *The essential role of yeast topoisomerase III in meiosis depends on recombination.* Embo J, 1999. **18**(6): p. 1701-11.
140. Bennett, R.J., M.F. Noirot-Gros, and J.C. Wang, *Interaction between yeast sgs1 helicase and DNA topoisomerase III.* J Biol Chem, 2000. **275**(35): p. 26898-905.
141. Bennett, R.J. and J.C. Wang, *Association of yeast DNA topoisomerase III and Sgs1 DNA helicase: Studies of fusion proteins.* Proc Natl Acad Sci U S A, 2001. **98**(20): p. 11108-13.

142. Gangloff, S., et al., *The yeast type I topoisomerase Top3 interacts with Sgs1, a DNA helicase homolog: a potential eukaryotic reverse gyrase.* Mol Cell Biol, 1994. **14**(12): p. 8391-8.
143. Ui, A., et al., *The N-terminal region of Sgs1, which interacts with Top3, is required for complementation of MMS sensitivity and suppression of hyper- recombination in sgs1 disruptants.* Mol Genet Genomics, 2001. **265**(5): p. 837-50.
144. Fricke, W.M., V. Kaliraman, and S.J. Brill, *Mapping the DNA topoisomerase III binding domain of the Sgs1 DNA helicase.* J Biol Chem, 2001. **276**(12): p. 8848-55.
145. Onodera, R., et al., *Functional and physical interaction between Sgs1 and Top3 and Sgs1- independent function of Top3 in DNA recombination repair.* Genes Genet Syst, 2002. **77**(1): p. 11-21.
146. Wagner, M., G. Price, and R. Rothstein, *The absence of Top3 reveals an interaction between the Sgs1 and Pif1 DNA helicases in Saccharomyces cerevisiae.* Genetics, 2006. **174**(2): p. 555-73.
147. Alberti, S., A.D. Gitler, and S. Lindquist, *A suite of Gateway cloning vectors for high-throughput genetic analysis in Saccharomyces cerevisiae.* Yeast, 2007. **24**(10): p. 913-9.
148. Fritsch, O., et al., *DNA ligase 4 stabilizes the ribosomal DNA array upon fork collapse at the replication fork barrier.* DNA Repair (Amst), 2010. **9**(8): p. 879-88.
149. Whitby, M.C., et al., *Interactions between RuvA and RuvC at Holliday junctions: inhibition of junction cleavage and formation of a RuvA-RuvC-DNA complex.* J Mol Biol, 1996. **264**(5): p. 878-90.
150. Fu, T.J., B. Kemper, and N.C. Seeman, *Cleavage of double-crossover molecules by T4 endonuclease VII.* Biochemistry, 1994. **33**(13): p. 3896-905.
151. Chen, C.F. and S.J. Brill, *Binding and activation of DNA topoisomerase III by the Rmi1 subunit.* J Biol Chem, 2007. **282**(39): p. 28971-9.
152. Tay, Y.D., J.M. Sidebotham, and L. Wu, *Mph1 requires mismatch repair-independent and -dependent functions of MutSalpha to regulate crossover formation during homologous recombination repair.* Nucleic Acids Res, 2010. **38**(6): p. 1889-901.
153. Hanai, R., P.R. Caron, and J.C. Wang, *Human TOP3: a single-copy gene encoding DNA topoisomerase III.* Proc Natl Acad Sci U S A, 1996. **93**(8): p. 3653-7.
154. Lopes, M., et al., *Branch migrating sister chromatid junctions form at replication origins through Rad51/Rad52-independent mechanisms.* Mol Cell, 2003. **12**(6): p. 1499-510.
155. Chen, Y.H., et al., *Interplay between the Smc5/6 complex and the Mph1 helicase in recombinational repair.* Proc Natl Acad Sci U S A, 2009. **106**(50): p. 21252-7.
156. Choi, K., et al., *The Smc5/6 complex and Esc2 influence multiple replication-associated recombination processes in Saccharomyces cerevisiae.* Mol Biol Cell, 2010. **21**(13): p. 2306-14.
157. Robert, T., et al., *Mrc1 and Srs2 are major actors in the regulation of spontaneous crossover.* EMBO J, 2006. **25**(12): p. 2837-46.
158. Wilson, T.M., A.D. Chen, and T. Hsieh, *Cloning and characterization of Drosophila topoisomerase IIIbeta. Relaxation of hypernegatively supercoiled DNA.* J Biol Chem, 2000. **275**(3): p. 1533-40.
159. Liberi, G. and M. Foiani, *The double life of Holliday junctions.* Cell Res, 2010. **20**(6): p. 611-3.
160. Boddy, M.N., et al., *Mus81-Eme1 are essential components of a Holliday junction resolvase.* Cell, 2001. **107**(4): p. 537-48.
161. Bolt, E.L. and R.G. Lloyd, *Substrate specificity of RusA resolvase reveals the DNA structures targeted by RuvAB and RecG in vivo.* Molecular Cell, 2002. **10**(1): p. 187-98.

162. Kaliraman, V., et al., *Functional overlap between Sgs1-Top3 and the Mms4-Mus81 endonuclease.* Genes Dev, 2001. **15**(20): p. 2730-40.
163. Fricke, W.M., S.A. Bastin-Shanower, and S.J. Brill, *Substrate specificity of the Saccharomyces cerevisiae Mus81-Mms4 endonuclease.* DNA Repair (Amst), 2005. **4**(2): p. 243-51.
164. Szakal, B. and D. Branzei, *Premature Cdk1/Cdc5/Mus81 pathway activation induces aberrant replication and deleterious crossover.* EMBO J, 2013. **32**(8): p. 1155-67.
165. Lopes, M., et al., *The DNA replication checkpoint response stabilizes stalled replication forks.* Nature, 2001. **412**(6846): p. 557-61.
166. Cotta-Ramusino, C., et al., *Exo1 processes stalled replication forks and counteracts fork reversal in checkpoint-defective cells.* Mol Cell, 2005. **17**(1): p. 153-9.
167. Fumasoni, M., et al., *Error-free DNA damage tolerance and sister chromatid proximity during DNA replication rely on the Polalpha/Primase/Ctf4 Complex.* Mol Cell, 2015. **57**(5): p. 812-23.
168. Cal-Bakowska, M., et al., *The Swi2-Snf2-like protein Uls1 is involved in replication stress response.* Nucleic Acids Res, 2011. **39**(20): p. 8765-77.
169. Kramarz, K., et al., *Swi2/Snf2-like protein Uls1 functions in the Sgs1-dependent pathway of maintenance of rDNA stability and alleviation of replication stress.* DNA Repair (Amst), 2014. **21**: p. 24-35.
170. Jiang, Y.W. and C.M. Kang, *Induction of S. cerevisiae filamentous differentiation by slowed DNA synthesis involves Mec1, Rad53 and Swe1 checkpoint proteins.* Mol Biol Cell, 2003. **14**(12): p. 5116-24.
171. Weitao, T., et al., *Dna2 helicase/nuclease causes replicative fork stalling and double-strand breaks in the ribosomal DNA of Saccharomyces cerevisiae.* J Biol Chem, 2003. **278**(25): p. 22513-22.
172. Ira, G., et al., *DNA end resection, homologous recombination and DNA damage checkpoint activation require CDK1.* Nature, 2004. **431**(7011): p. 1011-7.
173. Malkova, A., et al., *RAD51-independent break-induced replication to repair a broken chromosome depends on a distant enhancer site.* Genes Dev, 2001. **15**(9): p. 1055-60.
174. Tan, W., Z. Wang, and G. Prelich, *Physical and Genetic Interactions Between Uls1 and the Slx5-Slx8 SUMO-Targeted Ubiquitin Ligase.* G3 (Bethesda), 2013.
175. Sollier, J., et al., *The Saccharomyces cerevisiae Esc2 and Smc5-6 proteins promote sister chromatid junction-mediated intra-S repair.* Mol Biol Cell, 2009. **20**(6): p. 1671-82.
176. Oakley, T.J., et al., *Inactivation of homologous recombination suppresses defects in topoisomerase III-deficient mutants.* DNA Repair (Amst), 2002. **1**(6): p. 463-82.
177. Irmisch, A., et al., *Smc5/6 maintains stalled replication forks in a recombination-competent conformation.* EMBO J, 2009. **28**(2): p. 144-55.
178. Torres-Rosell, J., et al., *SMC5 and SMC6 genes are required for the segregation of repetitive chromosome regions.* Nat Cell Biol, 2005. **7**(4): p. 412-9.
179. Takahashi, Y. and A. Strunnikov, *In vivo modeling of polysumoylation uncovers targeting of Topoisomerase II to the nucleolus via optimal level of SUMO modification.* Chromosoma, 2008. **117**(2): p. 189-98.
180. Takahashi, Y., et al., *Cooperation of sumoylated chromosomal proteins in rDNA maintenance.* PLoS Genet, 2008. **4**(10): p. e1000215.
181. Ragland, R.L., et al., *RNF4 and PLK1 are required for replication fork collapse in ATR-deficient cells.* Genes Dev, 2013. **27**(20): p. 2259-73.
182. Galanty, Y., et al., *RNF4, a SUMO-targeted ubiquitin E3 ligase, promotes DNA double-strand break repair.* Genes Dev, 2012. **26**(11): p. 1179-95.

183. Prudden, J., et al., *SUMO-targeted ubiquitin ligases in genome stability.* EMBO J, 2007. **26**(18): p. 4089-101.
184. Bergink, S., et al., *Role of Cdc48/p97 as a SUMO-targeted segregase curbing Rad51-Rad52 interaction.* Nat Cell Biol, 2013. **15**(5): p. 526-32.
185. Costelloe, T., et al., *The yeast Fun30 and human SMARCAD1 chromatin remodellers promote DNA end resection.* Nature, 2012. **489**(7417): p. 581-4.
186. Froget, B., et al., *Cleavage of stalled forks by fission yeast Mus81/Eme1 in absence of DNA replication checkpoint.* Mol Biol Cell, 2008. **19**(2): p. 445-56.
187. Forment, J.V., et al., *Structure-specific DNA endonuclease Mus81/Eme1 generates DNA damage caused by Chk1 inactivation.* PLoS One, 2011. **6**(8): p. e23517.
188. Helleday, T., *The underlying mechanism for the PARP and BRCA synthetic lethality: clearing up the misunderstandings.* Mol Oncol, 2011. **5**(4): p. 387-93.
189. McCabe, N., et al., *Deficiency in the repair of DNA damage by homologous recombination and sensitivity to poly(ADP-ribose) polymerase inhibition.* Cancer Res, 2006. **66**(16): p. 8109-15.
190. Branzei, D., et al., *Ubc9- and mms21-mediated sumoylation counteracts recombinogenic events at damaged replication forks.* Cell, 2006. **127**(3): p. 509-22.